MÄLARDALEN UNIVERSITY
SWEDEN

School of Innovation, Design and Engineering

ABB

ABB Corporate Research Center

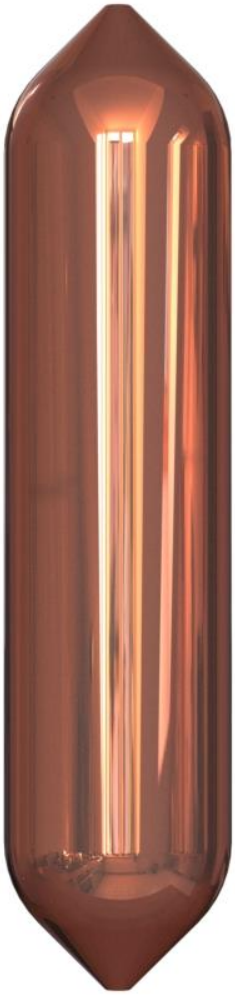

Ultra light-weight design through Additive Manufacturing

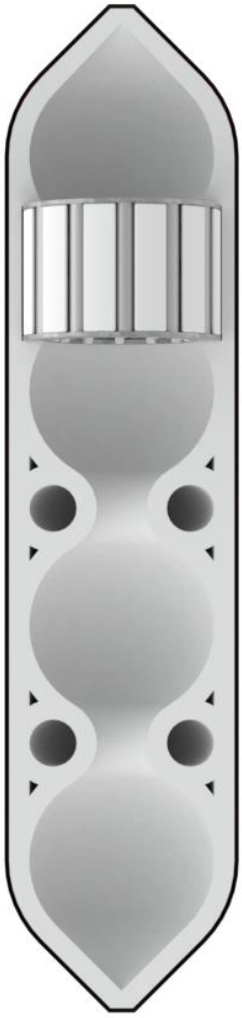

Master thesis work
Advanced level, 30 credits

Product and process development

Barrett Sauter

Mälardalen University, Academy for Innovation, Design and Engineering
Presentation day: June 7th, 2019
Supervisor, company: Fredric Tholence & Eric Johansson
Supervisor, university: Bengt Gustafsson
Examiner: Sten Grahn

ABSTRACT

ABB Corporate Research was looking to redevelop one product to be manufactured via polymer additive manufacturing (AM), as opposed to its previously traditionally manufacturing method. The current product is cylindrical in shape and must withstand a certain amount of hydrostatic pressure. Due to the pressure and the current design, the cannister is prone to buckling failure. The cannister is currently produced from two cylindrical tube parts and two spherical end sections produced from solid blocks of the same material. For assembly, an inner assembly is inserted into one of the tube parts and then all parts are welded together. This product is also custom dimensioned for each purchase order. The purpose of investigating this redevelopment for AM is to analyse if an updated inner design unique to additive manufacturing is able to increase the performance of the product by increasing the pressure it can withstand from both a material failure standpoint and a buckling failure. The redevelopment also aims to see if the component count and process count can be decreased. Ultimately, two product solutions are suggested, one for low pressure ranges constructed in ABS and one for high pressure ranges constructed in Ultem 1010.

To accomplish this, relevant literature was referred to gain insight into how to reinforce cylindrical shell structures against buckling. Design aspects unique to AM were also explored. Iterations of these two areas were designed and analysed, which led to a final design choice being decided upon. The final design is ultimately based on the theory of strengthening cylindrical structures against buckling through the use of ring stiffeners while also incorporating AM unique design aspects in the form of hollow network structures. By utilizing finite element analysis, the design was further developed until it held the pressure required. Simulation results suggest that the ABS product can withstand 3 times higher pressure than the original design while being protected against failure due to buckling. The Ultem simulation results suggest that the product can withstand 12 times higher pressure than the current design while also being protected against failure due to buckling. Part count and manufacturing processes are also found to have decreased by half.

Post-processing treatments were also explored, such as the performance of sealants under pressure and the effects of sealants on material mechanical properties. Results show that one sealant in particular, an acrylic spray, is most suitable to sealing the ABS product. It withstood a pressure of 8 bar during tests. The flexural tests showed that the sealant did indeed increase certain mechanical properties, the yield strength, however did not affect the flexural modulus significantly.

This work gives a clear indication that the performance of this product is feasibly increased significantly from redeveloping it specifically to AM.

(Keywords:) additive manufacturing, AM, fused deposition modeling, FDM, polymer, buckling, post-processing treatments

ACKNOWLEDGEMENTS

I would like to thank everyone who supported me in this endeavour. First and foremost, I would like to thank my university supervisor, Bengt Gustafsson, not only for the help in simulations and manufacturing test equipment, but for being a source of strength and encouragement in certain times. I would like to thank my supervisors from ABB CRC, Fredric Tholence, Eric Johansson and Saeed Maleksaeedi. You gave me direction and further insight into areas which were interesting to explore and what was expected from this work. I would like to thank Fredrik Finnberg and Digital Mechanics for advising on manufacturing questions as well as manufacturing the test specimens. I thank personnel in the MDH IDT prototype lab for helping me with getting all the gear in order to carry out certain experiments. I would like to thank the IT department at ABB CRC, as they were always available to help with getting necessary software up and running quickly as well as going through the trouble of connecting my computer to the 3D printer multiple times. I would like to thank Santanu Singha for accepting me for this thesis work and allowing me to experience working within ABB CRC. Lastly, I would like to thank my significant other, Nathan Zimmerman for always being supportive and encouraging, and being there for me through both the good and the hard times.

Contents

List of Figures

List of Tables

ABBREVIATIONS

ABB CRC	ABB Corporate Research Center
AM	Additive Manufacturing
ASTM	ASTM International
BU	Business Unit
CAD	Computer Aided Design
DFA	Design for Assembly
DFAM	Design for Additive Manufacturing
DFM	Design for Manufacturing
FDM	Fused Deposition Modeling
FEA	Finite Element Analysis
FOS	Factor of Safety
FEM	Finite Element Method
IDT	School of Innovation, Design and Engineering
ISO	International Organization for Standardization
MDH	Mälardalen University
PEI	Polyethylenimine

1. INTRODUCTION

Additive manufacturing (AM) is a manufacturing process which has been around for a few decades, however it now seems to be experiencing a boom. Many companies are interested in AM as it allows them to innovate in ways that were not possible before and therefore produce certain products more efficiently. One strategy the companies are taking is to look into their existing product group and determine which products would be best suited to be manufactured using AM opposed to the current manufacturing method. The reasons for doing so can be numerous, from minimizing weight to reducing lead times. Whatever the case, once a product has been chosen to be analysed, it must then be reanalysed in various ways in order to fully take advantage of AM.

1.1. Background

ABB AB Corporate Research Center (ABB CRC) is a segment of ABB which provides research within a variety of areas. One of these areas is that of materials, where "novel materials for future products are investigated and cutting-edge manufacturing processes are identified/deployed". In this endeavor to explore cutting-edge manufacturing processes, ABB CRC has analyzed their product listing and has determined that one of their products shall be investigated for AM. The product is cylindrically shaped with spherical end sections, is immersed in a fluid and must withstand some hydrostatic pressure. Due to its overall shape and how it is pressurized, the product is susceptible to failure via buckling. The product is manufactured from two sections of cylindrical tubing while the end sections are milled from a solid block of the same material. During assembly, an inner assembly is inserted in to one tube section and then all parts are welded together. This product is seen as a good candidate for AM as it is a product which is customized to fit each customer's needs, and therefore requires a change in design per product, and even slight change in manufacturing process. By implementing the AM process, the intention is to decrease the processing steps and part count while optimizing the overall performance of the product.

1.2. Problem Formulation

AM has a variety of techniques that can be considered when optimizing a part. However, finding the appropriate combination of techniques can be a challenge, especially when a multitude of variables must be accounted for. The function of the product must not be altered even with a change in design and manufacturing method. Furthermore, the product is susceptible to many environmental factors including various temperatures, high pressure loads and being in contact with a fluid, all of which must be taken in to account in the redesign for AM. Currently, there exists two types of the product overall, one manufactured in polymer and one in metal. Therefore, the problem will be to find a design which can be implemented for the low pressure, low temperature range product, and a design which withstands high pressure and high temperature ranges, while decreasing the manufacturing steps and part count as much as possible and ultimately keeping its initial function.

1.3. Aim and Research Questions

The aim of this project is to translate the design of a current product into two designs which can be manufactured through AM in a polymer with the purpose of increasing the performance of the part, such as overall pressure allowance and improved buckling behaviour, while also decreasing processing steps and the parts required. The aim is to also incorporate post-processing techniques which seal the product from its outside environment.

The following research questions are the basis for this study:

> *RQ1: What AM specific design aspects are available to increase the performance of a structure when redeveloping a traditionally manufactured[1] product to one for AM?*
>
> *RQ2: What factors should be taken in to account when manufacturing an end-use part through AM?*

The following lists the goals for the results of the study in regard to the amount at which the overall performance of the part is increased (pressure allowance and safety against buckling) as well as the amount at which processing steps and parts required are decreased.

> *Goal 1: To increase the performance in reference to both pressure allowance and safety against buckling by 30%*
>
> *Goal 2: To decrease the overall amount of processing steps and parts required by 20%*

1.4. Project Limitations

This study is undertaken during spring 2019 and it accounts for 30 university credits, which translates to a 20 week time period.

The current product is a typically a customized, made to order product. However, this study will focus on one specific version from the low pressure/temperature range. Therefore, the AM designs will correspond dimensionally when necessary to the current design, such as in diameter, and will utilize the same inner components.

This study will test two materials, ABSPlus-M430 and Ultem 1010, printed through the Fused Deposition Modeling (FDM) technique. The ABSPlus-M430 test pieces and prototypes will be printed on the Stratasys uPrint SE printer, as this is what is currently available at ABB CRC. Ultem-1010 test pieces and protoypes will be printed at a nearby AM company, Digital Mechanics, on a Stratasys Fortus 450. Due to the above, printing parameters such as layer height and raster angle of all test pieces and final prototypes are limited to a specific setting as set by the machine (uPrint) or will be printed in the recommended settings set by the company (Digital Mechanics).

[1] Traditional manufacturing refers to various subtractive manufacturing methods such as CNC milling and lathing or plastic injection molding. These processes are considered to be more limited when designing for, as one must take in to account uni-directional cutting possibilities as with the case of the CNC milling. Machinery required for injection molding becomes easily complicated and expensive especially when the design includes multi-directional through holes.

The amount of experiments conducted in this study will be limited due to time constraints. The experiments that are carried out will focus on the ABS material, while those carried out on the Ultem material will not be included. This limitation relates directly to the types of sealants being tested as well. The ABS sealants will be tested while the copper plating will not be tested. Lastly, pressurized testing of an entire structure will not occur due to limited testing equipment, and therefore the final results are limited to simulated results.

2. METHODOLOGY

The methodology section describes how all information pertaining to the study was gathered as well as the specific methods followed when carrying out the study. Sections include *Information Gathering, Material Data* and *Product Development Method.*

2.1. Information Gathering

The method in which non-material data was gathered is described here. Data includes information gathered from research literature, experts within the company, manufacturers, the company business unit, product drawings, and utilized software.

2.1.1 Literature study

A literature study was conducted via online databases, where scientific articles and journals were referenced. Databases included DiVA, Emerald Insight, Research Gate and Science Direct. Searches were conducted for a variety of topics necessary to explore a range of variables. Search words pertaining to material properties and the manufacturing process included "fused deposition modelling", "ABS", "Ultem 1010", "FDM polymer mechanical properties", "anisotropy", "FDM polymer porosity", FDM polymer ageing", "FDM polymer temperature, working temperature", "FDM sealing methods", "Vapor polishing", and "Metal plating on polymer FDM". Search words pertaining to the design of the product included "buckling of thin shelled structures", "strengthening thin shelled structures", "hydrostatic pressure", "design for additive manufacturing", and "DFAM".

2.1.2 Group discussion

This study was conducted at ABB CRC where a large amount of experience through those who worked there was available. Furthermore, weekly meetings were held in the form of informal gates with a team who were highly experienced within AM and therefore were available to discuss ideas and possibilities for the project to pursue. These meetings were used as opportunities to generate ideas in terms of inner structure designs and experiments to carry out.

2.1.3 Study visit

Digital Mechanics, the AM company used to manufacture the Ultem test specimens and prototypes were consulted to gain their insight. This pertained to the recommended print parameters, tolerances and the manufacturing strategies of the test specimens and the design for additive manufacturing aspect of the final design.

2.1.4 Conference calls

Two conference calls occurred in the form of informal interviews, one with ABB business unit and one with Polymertal. Some questions were prepared beforehand while other questions arose from the discussion taking place with the purpose of gathering information in regard to design specifications (ABB business unit) or design recommendations (Polymertal).

ABB business unit
The business unit was consulted to acquire information regarding the environments of the current cannisters and current production processes.

Polymertal
The company which applied the copper plating to the test specimens and prototypes were consulted regarding plating layer thickness and design recommendations for plating.

2.1.5 ABB Documents

Documents include a product drawing of a specific cannister order, a polymer, low range pressure/temperature cannister (Appendix A).

2.1.6 Software

SolidWorks was the CAD software utilized to create the designs and to perform the FEM-analysis.

2.2. Material Data

This section describes how information relating to material data was gathered. This includes why and how test specimens were produced as well as why experimental methods were chosen and how they were setup.

2.2.1 Production of test specimens

The ABS test specimens and prototypes were printed on the Stratasys uPrint SE located at ABB CRC and the Ultem 1010 test specimens and prototypes were printed on the Stratasys Fortus 450 at Digital Mechanics located in Västerås. The uPrinte SE is limited to two layer heights (0,254mm and 0,3302mm). The remaining print parameters such as support structure placement or layer direction were unable to be changed due to that they are simply not function choices that are provided by the uPrint model. The recommended settings set by Digital Mechanics were used to print the Ultem 1010 test specimens and prototypes. Post-processing methods including spray sealants, vapors and metal plating were conducted according to relevant literature where similar tests were conducted. International Organization for Standization (ISO) standards were adhered, in this case ISO 291:2008- Plastics- Standard atmospheres for conditioning and testing, when preparing all test specimens for experiments.

2.2.2 Experimental choice and setup

Material properties wanted in the study included flexural properties of the ABS material. This is due to the fact that the structure in question experiences flexural characteristics when being pressurized. Flexural properties were found from conducting flexural tests on the Zwick\Roell Z100 using a 1kN load cell at ABB CRC. The software used to gather the data from the machine was the testXpert II- V3.6. All tests followed International Organization for Standardization (ISO) 178:2019- Flexural test standards when available. ABSPlus-M430 flexural specimens were limited to 5 per test.

The porosity, or the amount that a material absorbs an outside fluid, was tested on the ABS material. This was done to find an adequate post-process treatment to fully seal the ABS structure

from its outside environment as specified under the construction specifications. To examine this, porosity tests were conducted by following steps described by similar literature on the subject, such as by Miguel, M. et. al (2018). Three specimens were tested per post-processing treatment. Results were determined by following ISO 62:2008- Plastics- Determination of water absorption

The performance of post-processing treatments in a pressurized environment were tested. The purpose of this was to analyse the treatments in an environment which resembled that of the real-life environment as closely as possible, and therefore produce the most applicable results. To carry out, pressure tests were conducted by following steps described by similar literature, such as by Mireles et. al (2011). One specimen was tested per post-process treatment.

2.2.3 ISO Standards

"ISO creates documents that provide requirements, specifications, guidelines or characteristics that can be used consistently to ensure that materials, products, processes and services are fit for their purpose." (ISO)

Standards, or in this case ISO standards, ensure that tests or data are carried out in a way so that they are repeatable and will give the same result time after time. Standards are used to ensure outside variables do not interfere with the searched for data, and therefore the final results can accurately be compared to one another, even if they are found in different places of the world.

Three ISO standards are used in this work:

ISO 291:2008- Plastics- Standard atmospheres for conditioning and testing: The standard describes the environments and conditions that plastic specimens should be kept in if they will undergo testing.

ISO 178:2019- Flexural test: Standard when carrying out flexural tests. Describes how the machine and jig should be set up. Also describes how the results are calculated and how to interpret the graphs. States the recommended specimen dimensions.

ISO 62:2008- Plastics- Determination of water absorption: this standard specifies the method for determining if and how much a plastic absorbs water.

2.3. Product Development Method

"Design methodology is about how to design with logical consequential phases where the task is completed to develop product specifications." (Tomiyama et. Al, 2009)

Design methodologies have continuously been developed and coincided with product development within conventional manufacturing for a substantial amount of time. One such methodology is the DFXs, or design for, which are design subdivisions intended to aid the designer in the development process. Two of such are design for assembly (DFA) and design for manufacturing (DFM). One such recommendation which falls under DFA is part consolidation, or consolidating many parts in to one with the purpose of reducing processing time and cost. Yang and Zhao (2015) point out that part consolidation is negatively affected by DFM, as parts need to be designed for a specific manufacturing process, which limits the freedom of the overall design. Even though these methodologies should exist to aid the designer in the development process, Yang and Zhao argue that they cause limitations when used together.

The surge in AM techniques has arguably lifted many limitations imposed on part design due to manufacturing, thus allowing the designer to focus on other criteria that the customer sees as having value, such as performance and assembly. This surge in techniques and popularity has led to the rise and importance of design for additive manufacturing (DFAM), or the design methodology suited specifically for AM, to aid in maximizing product performance. The DFAM methodology give general practices that designers within AM should adhere to for designing structures for optimized manufacturability. DFAM compromises of a plethora of variables, however simplified versions of DFAM are presented by Yang and Zhao (2015) and expanded upon by Kumke et. al (2016). Bousquet (2017) presents a culmination of these methods which can be seen below in Figure 1. The presented method is followed in this study.

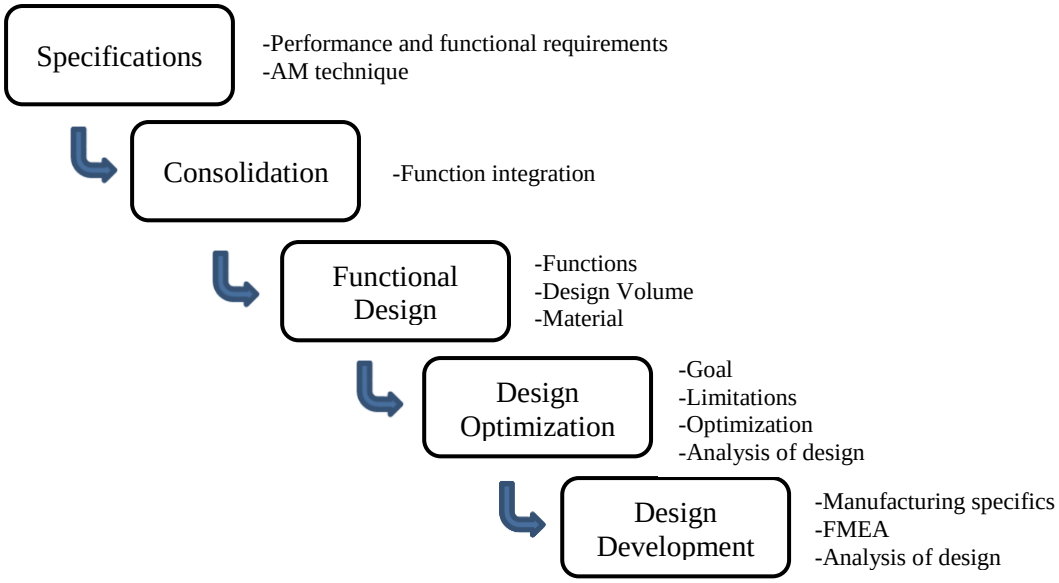

Figure 1: DFAM Method (Bousquet, 2017)

During the Specification stage, all necessary performance and functional requirements should be determined. The next stage, Consolidation, is where as many parts as possible should be integrated in to one and is considered a stage where AM can be taken advantage of to carry out. The Functional Design stage is where functional aspects should be designed for in consideration to the available volume and materials. During Design Optimization, the performance and functional requirements stated in Specifications should be fully realized. Lastly, in Design Development, variables related specifically to the manufacturing process should be incorporated and an analysis of the design should be conducted.

2.4. Reliability and Validity

Reliability and validity are terms which relate to how trustworthy the work is in relation to experimental design and analysis.

Reliability refers to the consistency of results from experiments, and thereby the trustworthiness of the results. Higher reliability can be incorporated in the work by following certain standardized experimental setup and specimen manufacturing procedures such as those described in *ISO Standards* above. The results obtained from the experiments are deemed more reliable by following these standards because the standards ensure that the results are reproduceable and therefore more trustworthy. Validity asks the questions: do the results measure what was

intended to be measured? In other words, when not specified by a given standard, has an experiment or methodology been set up in a way which will produce results that have a direct relation to what is being searched for. Validity also extends to asking if the conclusions drawn from the method are valid, as in are the conclusions based on a direct relationship between initial variables and the observed outcome. (Center for Innovation in Research and Teaching)

In this work, reliability of test results has been ensured by following ISO standardized experimental setups when available. All experiments and experimental setup is described in detail in chapter *5: Production of Material Data.* It should be noted the ISO standards for additively manufactured specimens and processes are still being developed, which leads to the fact that there simply doesn't exist an exact standard for all types of AM specimen manufacturing. In these cases, the expertise of the manufacturers was relied upon to provide test specimens with the highest quality possible and with consistent characteristics, such as in the case of the copper plated Ultem specimens.

Validity has also been taken in to account in this work. When standards for experimental setups were unavailable, other similar setups found in literature were used as a guide to follow with the purpose of producing legitimate results to the question at hand. The product development methodology which is adhered to in the work is based on research and is specific to AM. This ensures that the process followed will generate a compatible result for the limitations and specifications placed upon it. Throughout the product development process, each decision has also been detailed as to why a direction was chosen to move forward with, how it would be accomplished and what the results entail.

3. CURRENT SITUATION ASSESSMENT

This chapter describes useful information pertaining to the function of the current cannister, an FEA analysis and a manufacturing overview of the cannister. The information is categorized under *Product Overview, FEA of Current Design* and *Manufacturing of Current Design.*

3.1. Product Overview

The cannisters are used in measuring applications. They are cylindrical in shape and contain an inner assembly. A section view as well as the inner assembly can be seen in Figure 2. A full description of the function can be found in Appendix B.

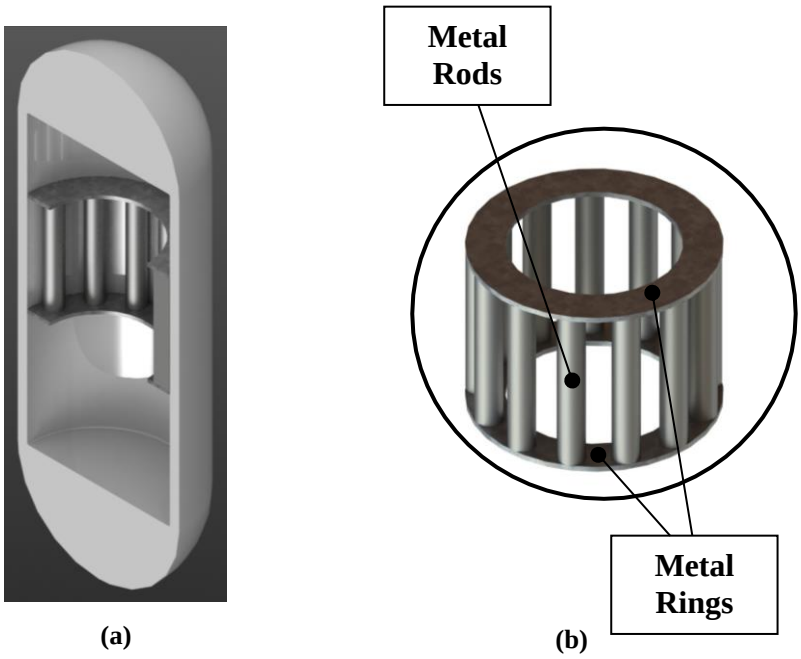

Figure 2: **(a) Inside view of cannister**
(b) Inner assembly contains metal rods and rings

3.1.1 Current Dimensioning and Construction of Cannister

The cannisters are partially standardized, all having the same diameter. The cannisters are designed custom for their specific environment as certain variables which affect the function and mechanical failure due to buckling are subject to change. According ABB business unit (BU) these cannisters are dimensioned off of test records from roughly 20 years ago. The records contain basic cannister construction details and the pressure at which they collapsed at under a hydrostatic pressure test. Current cannister designs are dimensioned from extrapolations based on this data. ABB US also stated that the max design rating for their polymer cannisters is that of *P* MPa (used as nominal value here forth, value seen in Appendix B). (BU)

3.1.2 Current Material of Cannister

The current polymer cannister is manufactured in polyvinylidene fluoride, better known as Kynar. Kynar mechanical properties are displayed in Table 1.

Table 1: Kynar mechanical properties (Quadrant Engineering Plastic Products)

	Tensile Strength, Yield (MPa)	*Tensile Modulus (MPa)*	*Flexural Strength (MPa)*	*Flexural Modulus (MPa)*
Kynar	60	2300	Not available	Not available

3.2. FEA of Current Design

The drawing of the cannister in which this study is based upon can be seen in Appendix A. The cannister was 3D modeled and analyzed. The cannister was first simulated without the inner assembly with an outside pressure of *P* MPa. An eighth of the cannister was simulated, and fixtures of 0mm movement normal to the cut faces were added. A static and buckling analysis were conducted on the part, the results shown below in Figure 3.

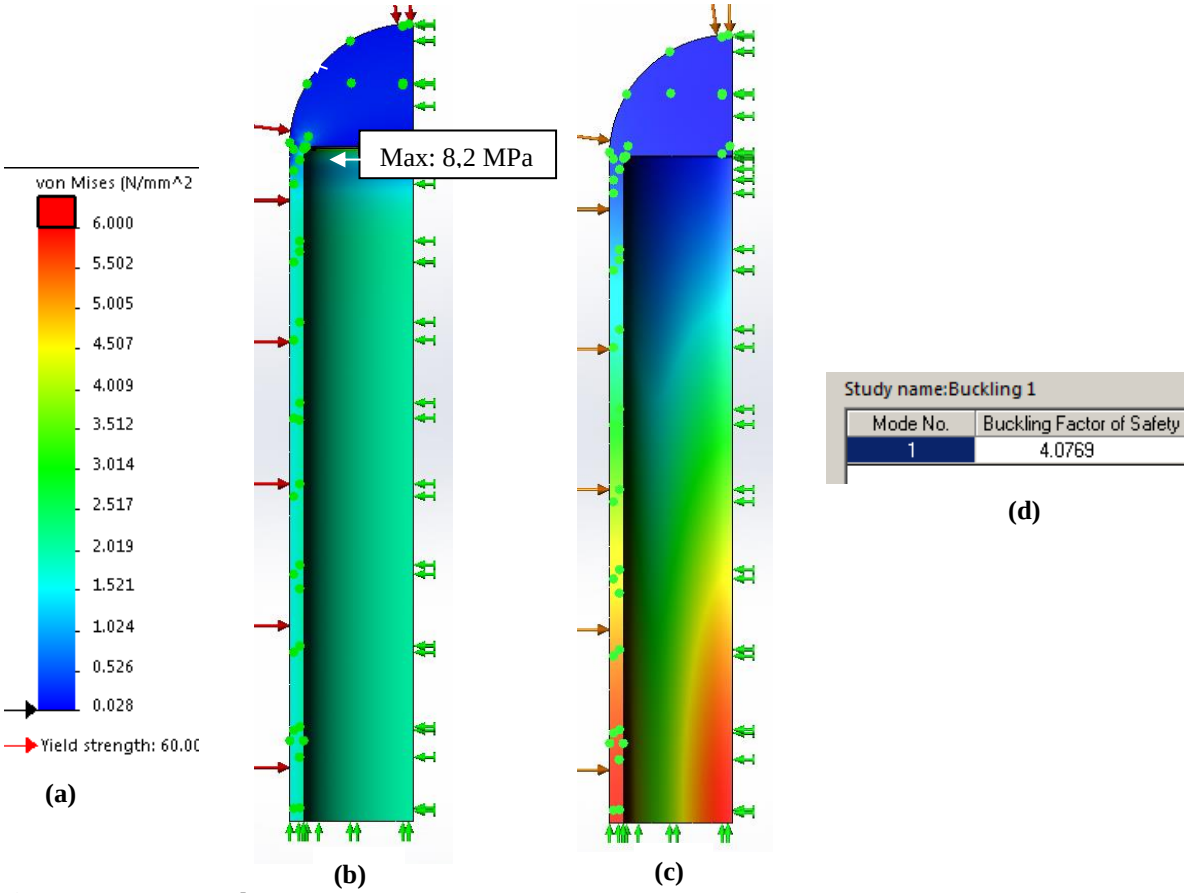

(a) **(b)** **(c)** **(d)**

Figure 3 **a: Scale**
b: Results from static study, stress
c: Results from buckling study, displays buckling mode as an overall column buckling
d: Results from buckling study, buckling FOS

As can be seen in Figure 3b, the max stress is 8,2 MPa and is located in the corner of the cannister where the solid spherical top (end cap) meets the hollow cylinder. The end cap has relatively low stress within it. Figure 3c shows that the buckling mode would be an overall buckling, and the part has a buckling FOS of 4. This suggests that the structure ultimately fails to buckling at approximately 1,5 MPa.

3.3. Manufacturing of Current Design

The manufacturing process of the current product can be assumed when referencing the drawing (see *Appendix A*). The canister is constructed from two cut sections of an extruded Kynar tube. The two end caps are milled from a solid block of the same material. During assembly, the inner assembly is inserted in to the shorter tube part. The four pieces are then welded together. A sub-total of the part count (excluding metal rods and rings) and processes is seen below:

	Tube cut sections	2
	End caps	2
Total Part Count	=	4 Parts

	Cut tube	1
	Mill end caps x2	2
	Inner part insertion	1
	Weld	1
Total Process Count	=	5 Processes

4. THEORETICAL FRAMEWORK

This section describes the information utilized in the work which was gathered from relevant literature. The categories include *AM and Performance, Polymer FDM Process, Polymer FDM Material Characteristics, Quality and Accuracy, Stratasys, Post Processing, Polymer Mechanical Properties, Buckling of Cylindrical Shells* and *Finite Element Analysis.*

4.1. AM and Performance

AM provides the ability to include AM specific design features, all of which can increase the performance of a structure in several ways. Hällgren (2017) breaks down increased performance opportunities into Product Common, Product Specific, Customer Specific and Company Specific. Figure 4 displays how these are further categorized. Product Common breaks down into lower mass and improved efficiency while Customer Specific breaks down further to individuality. A selection of these performance increasing variables such as decreasing mass and improving efficiency are described further below.

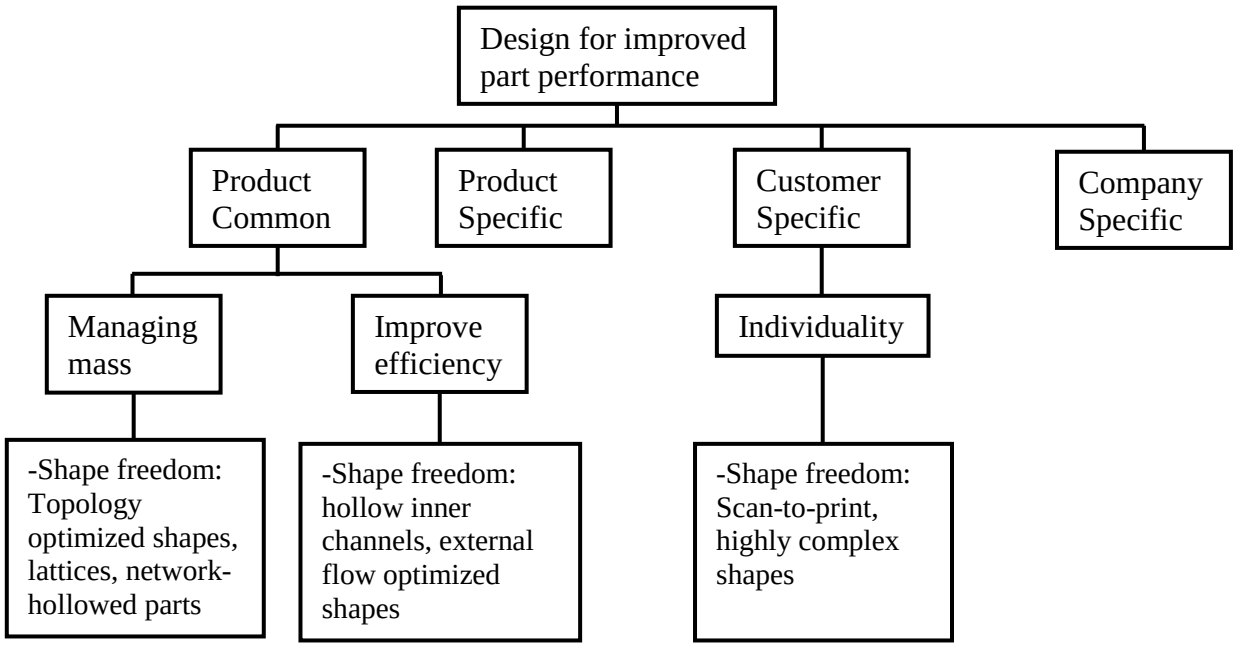

Figure 4: Design variables for improving part performance (Hällgren)

4.1.1 Managing and decreasing mass

The ability to tightly control the mass of an object is seen as improved part performance, especially when the mass is paramount to the function of the design. AM provides several unique design aspects which aid in decreasing the mass, such as topology optimization, lattice structures, and internal hollowed sections. Due to the FDM process, mass can more easily be subtracted from the design compared to traditional manufacturing processes, which may not even be able to reach those areas in the part effectively.

4.1.2 Lattice structures

One way to control and lower mass, as described above, is by incorporating lattice structures in the design. When doing so, the outer shell of the structure is commonly kept while the inside is exchanged for lattices, mesh or cellular structures. These inner structures can be homogenous throughout or be of varying density. Specialized software is typically needed to incorporate these types of structures.

4.1.3 Hollow inner channels

Traditional manufacturing methods can typically only produce straight-lined channels. With AM, internal channels can be conformed and optimized for the function instead of the manufacturing process. The function of these inner networks or channels can be to either lower the mass or to improve fluid efficiency. Whatever the case, AM allows for the integration of these types of structures, unlike traditional machining processes.

4.2. Polymer FDM Process

AM refers to a wide range of manufacturing techniques, where the commonality is they build the component layer by layer, until the component is completely printed. Also, a large variety of materials exist for these various manufacturing methods, including polymers in powder, liquid and solid forms. Layers can be deposited in a melted string such as in material extrusion, the powder can be swept over the build plate and adhered with a liquid binding agent such as in binder jetting or melted together by a laser or electron beam in powder bed fusion. In material jetting, liquid photopolymer droplets are deposited and are hardened by an ultraviolet light. (Wohlers et. al, 2017) The current full list of AM processes according to ASTM[2] International (ASTM) are the following:

- Powder Bed Fusion
- Vat Photopolymerization
- Binder Jetting
- Material Extrusion
- Directed Energy Deposition
- Material Jetting
- Sheet Lamination (GE Additive)

Material extrusion, or FDM (the name patented by Stratasys), operates by feeding the solid polymer material (part filament) through the extrusion head, which heats the polymer to a viscous state. The extruder then deposits the material on the build platform. Once one layer is complete, the build platform moves downward, and the nozzle deposits the next layers on top of the previous. Support structures may be necessary when printing objects with overhangs or wide, unsupported surfaces. Support structures may either be dissolved in post processing (if the support material is dissolvable) or removed by hand. (Wohlers et. al, 2017) Figure 5 below displays a typical FDM setup.

[2] ASTM, similar to ISO, is a set of standards which defines how a range of methods should be carried out. This extends to defining key concepts, and how they should be interpreted.

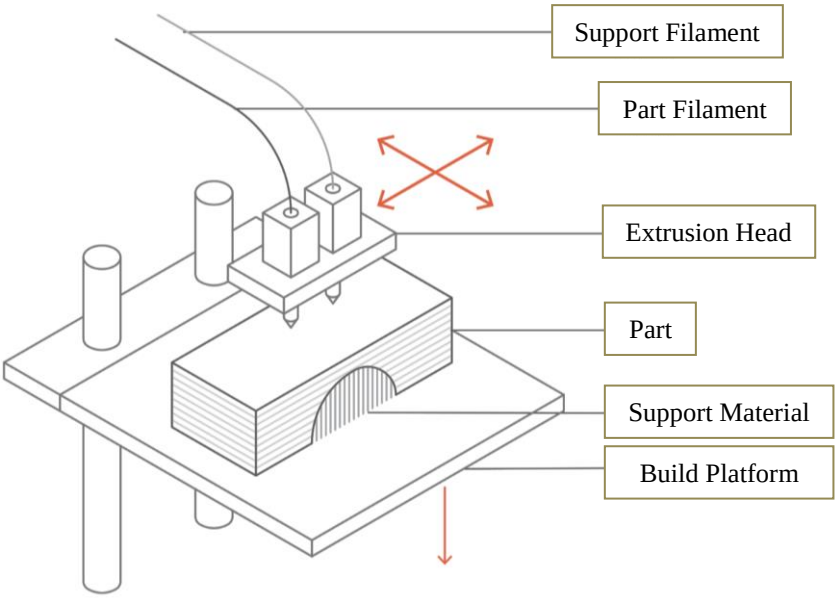

Figure 5: Schematic of FDM setup (Varotsis)

FDM currently represents the largest percentage of machines used both by industry standards and personal use and is the least expensive when compared to other AM processes (Wohlers et. al, 2017).

4.2.1 Build Orientation

FDM naturally produces parts with anisotropic characteristics. This anisotropy is directly related to the direction that the melted polymer is deposited. Therefore, the orientation in which the part is built will directly influence characteristics such as mechanical properties in the part as well as surface roughness, stepping, and required support structures. Several other print parameters, including layer height, infill, raster angle, build temperature, and more also have an effect on the parts' mechanical properties, however the build orientation has the greatest overall effect. Figure 6 displays this.

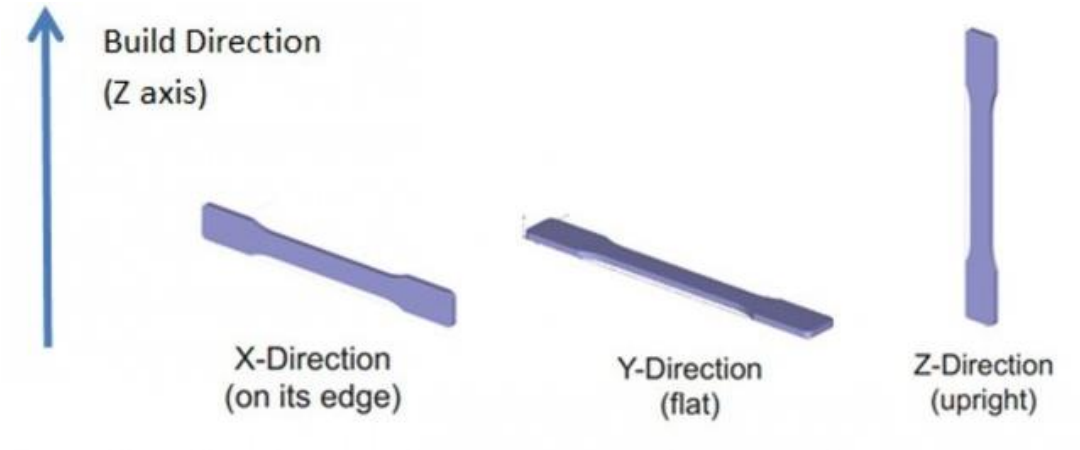

Figure 6: Build orientation, labeled as X, Y and Z directions (Lambert)

Many studies, including those by Bagsik et. al (2010) (2012), show that there is a direct relation between build orientation and mechanical properties, and all conclude that a part exhibits the highest E-modulus, tensile strength, flexural modulus and flexural strength in the X and Y

direction compared to the Z direction. Therefore, a part's build orientation should be taken in to account before printing.

4.2.2 Support Structures

Due to the nature of the FDM process, extra material, i.e. support structures, may also need to be printed. Each layer printed needs an underlying layer to support the extruded viscous material. In the case of overhangs and large, unsupported surfaces, support material will be required for the part to print successfully. FDM design recommendations suggest that overhangs with an angle greater than 45° degrees should be printed with support material. This is displayed in Figure 7 below. Holes and channels can be considered self-supporting up to a certain diameter and do not require support material.

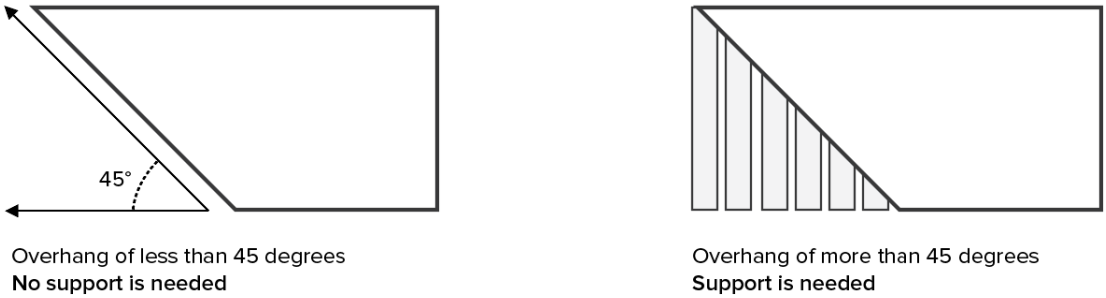

Figure 7: General rule of thumb for when support structure is needed (Cain)

Support material may be printed in a dissolvable material, as with the uPrint SE Plus. Once printed, the part along with the support material is submerged in a bath solution. The bath is run for approximately 12 hours. The part is then removed from the bath and the support has been removed. The part is left with little to no surface distortions from the support.

Support material for the Ultem 1010 are printed in the same material. The support must be removed by hand or machine in post-processing. Removal of support may leave a rough surface texture on the part. Due to this, consideration should also be taken when designing and orienting the part to minimize support material if the surface texture is of concern.

4.2.3 Hardware Embedding

Many FDM machines come with the function to be paused mid print, allowing for an opportunity to embed hardware into the part. A cavity for the part must be incorporated in to the CAD design. While printing, the printer is then paused at the correct height, the hardware is inserted, and the print is resumed. Stratasys suggests entering the machine from the top of the system so as to not lose heat in the build chamber (Stratasys, 2014) as a loss in heat could lead to poor layer adhesion. Embedded sensors, magnets, bolts, and optical devices are among the hardware that has been tested for embedding. Stark et. al (2014) embedded sensors in unmanned aerial systems to acquire unique information and monitor certain variables more accurately. Yuen (2016) examined embedding fluidic and optical devices into FDM parts, finding the ability to integrate and embed other objects as highly useful and stated it could lead to new functionalities and opportunities in FDM parts.

4.3. Polymer FDM Material Characteristics

Polymer FDM materials are mostly all thermoplastics, with the most common being acrylonitrile butadiene styrene (ABS), polycarbonate (PC), nylon and polyactic acid (PLA). Ultem is a thermoplastic produced by Stratasys with a high strength-to-weight ratio and the ability to withstand high temperatures.

Temperature has a significant impact on the mechanical properties of thermoplastics, with the lowest tested temperature of -60°C exhibiting the highest tensile strength, tensile modulus and flexural modulus for ABS and Ultem (Stratasys, 2013 & Bagsik et. al, 2012). These same mechanical properties decrease as temperature increases. The aforementioned studies pertaining to thermoplastics and temperature also analysed these properties after up to 52 weeks of exposure time. Both studies found that their materials maintained the properties, with little affect from exposure time.

ABS is among the most commonly used material in FDM. Stratasys produces a range of ABS thermoplastics, many of which are promoted as production-grade thermoplastics. ABSplus-P430 is a part of this family and is utilized for concept models and prototypes. Its mechanical and thermal properties closely resemble those of ABS-M30, which is used for parts requiring low bearing loads such as functional prototyping, manufacturing tools and productions parts.

Ultem, otherwise known as polyethylenimine (PEI), is a high-performance FDM thermoplastic and is used in many applications where strength and thermal stability are required and is certified for aerospace. Ultem is ideal for aerospace and automotive applications due its flame, smoke and toxicity rating and high strength to weight ratio. It is currently used in noncritical interior components in aerospace such as brackets and wall panelling (Stratasys Direct Manufacturing) . Within automotive, Ultem is utilized for producing 1-off prototypes for heating, ventilation and air conditioning systems for on- and off-highway vehicles which are robust enough to undergo serious testing compared to other rapid prototyping processes (Stratasys). Ultem 1010 offers the highest heat resistance, chemical resistance, tensile strength, and lowest coefficient of thermal expansion of any FDM thermoplastic. Certain grades are even certified for food processing and medical devices. Applications include semi-structural components and housings in aerospace, heat lamp reflectors and electrical connectors in automotive, medical devices in healthcare, and temperature resistant dies, patterns and fixtures for food productions. Applications also include those requiring high heat and flame resistance such as reflectors, connectors and housing in lighting and electronics. Ultem also maintains its mechanical properties under high temperatures and has a relatively low coefficient of thermal exapansion.

Table 2 Published mechanical properties for ABSplus-P430 and Ultem 1010 (Stratasys)

	Tensile Strength, Yield (MPa)	*Tensile Modulus (MPa)*	*Flexural Strength (MPa)*	*Flexural Modulus (MPa)*	*Co-efficient of Thermal Expansion (μm/(m·℃))*
Ultem 1010	X: 64 Z: 41	2 770, 2 200	144 77	2 820 2 230	47
ABSPlus-P430	X: 31 Z: Not available	2,200 Not available	58 35	2 100, 1 650	88

4.4. Quality and Accuracy

Parts manufactured through FDM tend to have a rougher surface than those produced through other processes such as injection moulding (Rama Krishna & Gundeti, 2017). This is due to the nature of the FDM process as it deposits material layer by layer, depositing cylindrical strings in the form of the specific layer. These cylindrical strings produce an uneven, semi-wavy surface on the outer surfaces of the printed part, while producing slightly smoother finishes on horizontal flat surfaces. This is demonstrated in Figure 8 below:

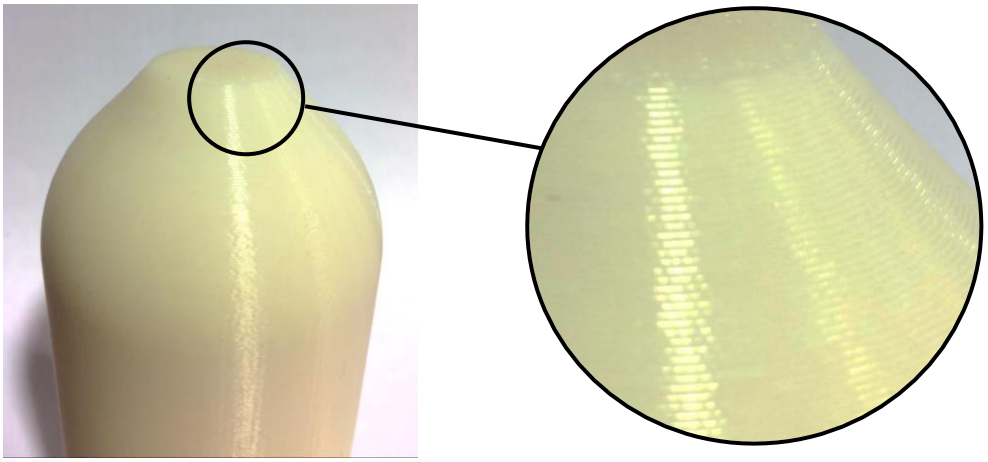

Figure 8: FDM process produces parts with visible layers

Several parameters affect the surface quality, including layer thickness, orientation of part, road width, air gap between roads and print temperature (Gaydos et. al, n.d.). This surface roughness affects the function of the part including mechanical properties and porosity due to air gaps and voids.

Dimensional accuracy of FDM parts was also found to be slightly lower than that of plastic injected parts of the same material, such as found by Rama Krishna & Gundeti (2017) and Dawould et. al (2016) when examining ABS parts. However, both studies noted that the amount of dimensional deviation in FDM ABS parts still lies within the standards' acceptable range of ±0,2mm

The published accuracy of the Stratasys Fortus 450 machine is ±0,127mm or ±0,0015mm/mm (whichever is greater) (Stratasys). No published information regarding the uPrint SE Plus could be found.

4.5. FDM Machinery

Stratasys is a company which produces AM printers and materials. They sold their first AM FDM printer in 1991 and are now the largest manufacturers of FDM systems (Wohlers, 2017). Stratasys collaborates with companies in a range of industries including Airbus, Boeing Ford, McLaren Racing and Siemens. Within the FDM technology, Stratasys offer a range of 3D printers, including the uPrint SE Plus and the Fortus 450mc (Figure 10) and F900 (Figure 9). The uPrint SE Plus has the capability to print in ABS with dissolvable support material while the Fortus 450mc and F900 machines have the capability to print high performance, heat-resistant Ultem materials.

Figure 10: Stratasys Fortus 450mc FDM printer (Stratasys, 2019)

Figure 9: Stratasys F900 FDM printer (Stratasys, 2019)

4.6. Post Processing

The use of polymers is becoming more widespread in many industries for several purposes such as design freedom, weight reduction, improved performance properties, and lower costs. To extend the range of polymer usage, post-processes such as surface smoothing and sealing the product whether through acetone vaporization, applying a sealant coating or metal plating the product has become standard to improve variables such as reducing porosity, increasing overall strength, and improving heat deflection, chemical resistance and corrosion resistance, while maintaining relatively low weight and cost (Mittal, 1991).

Now that AM is gaining popularity in a range of industries for its relatively limitless design capabilities, a large interest resides in studying the effects of coating and plating AM components for the same reasons as stated above (Stratasys Direct Manufacturing).

4.6.1 Vaporization and Spray Sealants

Several methods have been researched regarding smoothing or sealing polymer FDM parts for various reasons. ABS parts were smoothed by acetone vapor by Neff et al. (2016) to determine if and how it would affect surface roughness and thereby affect mechanical properties. The acetone vapor was found to decrease surface roughness, however needed to be controlled as to not change dimensional characteristics too much. Elongation to break increased in the vapor smoothed specimens compared to non-smoothed specimens. Mireles et. al (2011) compared 11 different sealants on ABS parts through three applications methods (spraying, brushing and vacuum infiltration) under various pressures. Noteworthy results showed that the two polyurethane sealants withheld to approximately 0,15 MPa while a penetrating epoxy withheld to 0,325 MPa. Mireles et. al suggested that more coating layers would increase overall strength of sealants, while also noting that when used industrially, ease-of-use and drying/working times should be taken in to consideration. Miguel et. al (2018) compared the porosity of non-coated Nylon specimens to polyurethane coated specimen and found that the coating led to a major reduction in water absorption by the test specimens.

4.6.2 Metal Plating

Polymer FDM parts can be plated by metal, which can greatly improve thermal and mechanical properties. Many studies have been done on the plating processes themselves on various test specimens produced through AM, such as by Ajibola (2016), Equbal and Sood (2015) and Olivera (2016), all concluding that successful plating (i.e. good adhesion performance between plating and substrate) result in increased tensile modulus and impact strength. Studies on the effects of plating thickness have been carried out by Saleh (2004) and (Kannan) on components from various AM processes, both leading to the conclusion that an increase in plating thickness results in increase in strength and lesser surface roughness. However, Saleh had further concluded that the plating thickness did not relate accordingly to composite theory from comparing predictions and test results. As a consequence, predicting results using composite theory prove to be inaccurate. Kannan studied copper plating on ABS with thicknesses ranging between 0-80 μm, and concluded that the thickness on the lower range (less than 60 μm) displayed brittle characteristics, while greater thicknesses proved to be more ductile. The findings showed that a plating thickness of 80 μm lead to a 49.3% increase in strength. McCarthy (2012) examined complex hollow structures produced through AM which were then plated. This resulted in an even more complex metal structure, leading to conclusions that the results provided a new hybrid approach to AM.

4.7. Polymer Mechanical Properties under Flexure

Materials are typically classified using specific properties. The material properties that are important are dependent on how the object made with that material is being used and what is acting upon it. If the object is used to hold a hanging object to the ceiling causing the object to be under tension, then its tensile properties would be used. If the object is situated between two points and is used to hold something along it causing it to bend, it's flexural properties would then be used. Figure 11 displays these basic stresses. A material's mechanical properties include it's yield strength, max strength, breaking strength, tensile/flex modulus, elongation, and more.

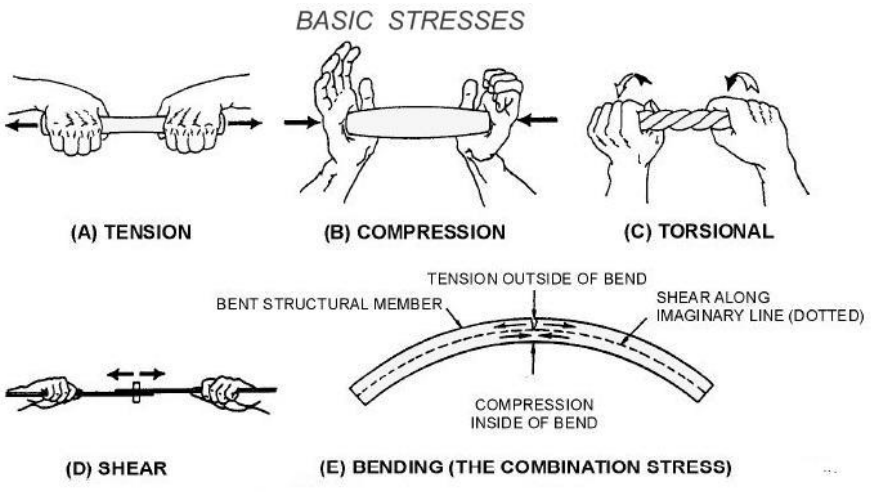

Figure 11: Displays basic stresses (Waters)

Flexure is a culmination of tension (such as on the outside of the bend) and compression (as on the inside of the bend). The flexure upon the specimen causes stress. When the load on the object causes the stress to surpass a specific point, the yield, the material has entered the plastic state,

or the state at which it deformed enough that it cannot morph back to its original state. Typically, objects are designed to not surpass this yield point, as doing so may cause the object to become mechanically unstable and eventually fail.

To find these specific mechanical properties, test specimens are produced and tested under certain conditions. A flexural test is conducted on a tensile test machine. A rectangular test specimen is placed between two points at a specific distance and a load is then applied which causes the specimen to bend. A software used in conjunction with the machine records the amount of force that is applied as well as the distance that the specimen is displaced at the loaded point. From this data, a graphical curve is produced from which material properties such as the flexural modulus and flexural yield strength are calculated from. The stress in the specimen at the load point can be measured using the following equation (1), where F is the load (at a specific point), L is the length of the support span, w is the width of the specimen and h is the thickness of the specimen (see Figure 12):

$$\sigma = \frac{3FL}{2wh^2} \quad (1)$$

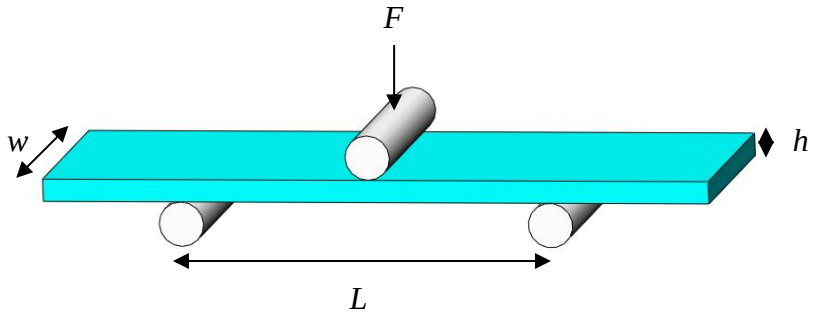

Figure 12: Depicts 3-point flexural test

Furthermore, specific standards are adhered to find these properties. In the case of determining flexural properties, the standard ISO 178:2019 is used.

4.8. Buckling of Cylindrical Shells

Buckling may occur in structures which are under compressive stress. It is a result of instability in a structure which can result in structural failure. Buckling in columns occurs when the ratio of length to diameter becomes so large that the column becomes unstable, and the column will deform laterally. Once this lateral deformation occurs, the column loses stiffness and partial vertical strength. Therefore, the forces acting upon it will cause even greater stresses, ultimately causing the column to fail entirely.

Cylindrical shells are another structure prone to buckling and at the same time are important elements in many designs. The structure is considered to have a shell when the thickness of the shell is much smaller compared to the diameter of the structure. These structures are used in a wide range of applications, including underwater vessels such as submarines and pipelines, and on land such as chimneys, tanks and silos. They may undergo outward pressures, inward pressures, vertical loads, etc. Cylindrical shell structures which reside underwater are affected by hydrostatic pressure, or evenly distributed pressure from all directions. This can be seen in the Figure 13 below.

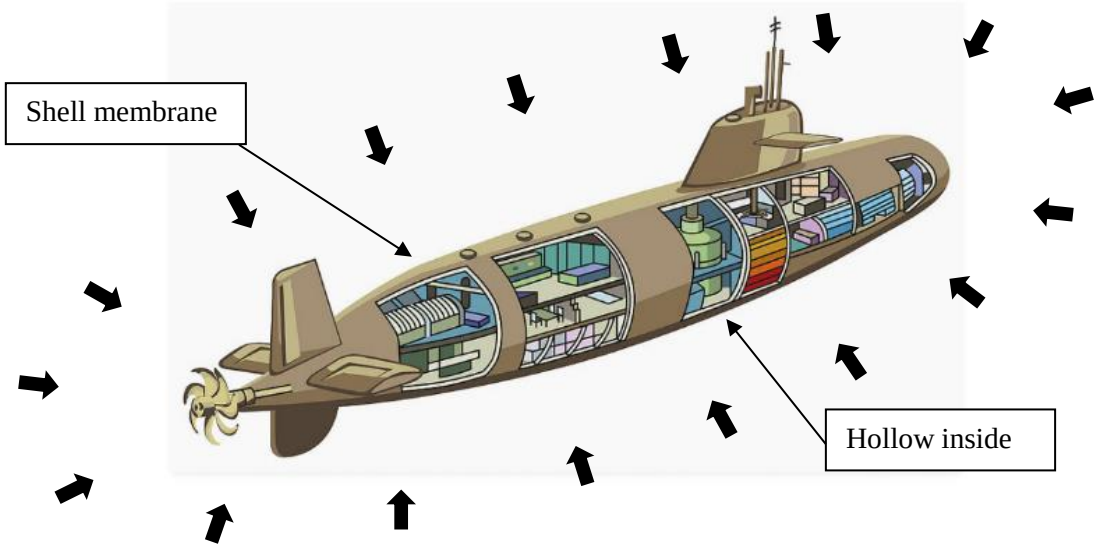

Figure 13: A cylindrical shell structure, a submarine, under hydrostatic pressure (Kindersley, 2019)

4.8.1 Designing for Buckling in Cylindrical Shells

There are various methods to reinforce a cylindrical shell against buckling, including adding longitudinal, ring and spiral stiffeners (such as in Figure 14) or by incorporating a composite sandwich structure into the shell itself. Amdahl (2005) describes the geometrical parameters of a cylindrical shell, various stiffener arrangements including longitudinal and ring stiffeners, and the various possible buckling modes that the stiffener arrangements are susceptible to. The buckling modes include shell buckling, panel buckling, general buckling, local buckling of stiffeners and frames, and overall buckling of the cylinder. Table 3 below displays various stiffeners and what type of buckling they are prone to. It should also be noted that small imperfections in the shell can lead to an even earlier buckling.

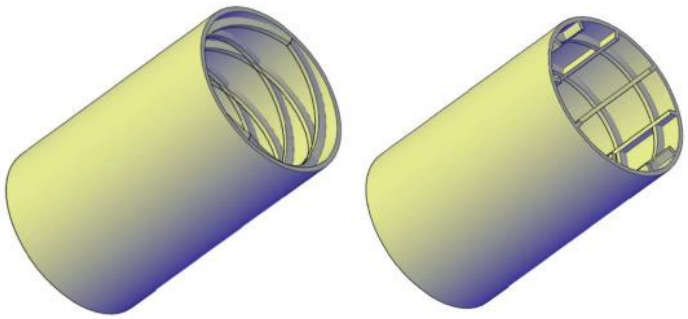

Figure 14: Spiral, longitudinal and ring stiffened cylindrical shells (Nam)

Table 3: Buckling modes in cylinders with various stiffener arrangements (Amdahl, 2005)

Buckling Mode	Geometry	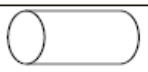			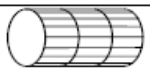
SHELL BUCKLING	Unstiffened cylinder	X	X		
	Unstiffened curved panel			X	X
PANEL BUCKLING	Stringer stiffened cylinder			X	X
GENERAL BUCKLING	Ring stiffened cylinder		X		
	Ring / Stringer stiffened cylinder				X
OVERALL BUCKLING	Column	X	X	X	X
LOCAL STIFFENER BUCKLING	Ring		X		X
	Stringer			X	X

A range of strategies are used to find the optimal dimensions of a cylindrical shell structure to hold against buckling including linear analysis calculations, stability calculations of ideal structures and non-linear calculations with structural imperfections. Amdahl (2005) presents the equations necessary to calculate for the various buckling modes which arise from the different stiffener arrangements and suggests ways to account for imperfections. Hajmohammad (2013) calculated the buckling due to the distance between ring stiffeners using a simplified formula while D. Lemák (2005) utilized parametric studies and the Finite Element Analysis (FEA) to determine the optimal stiffness of the ring stiffeners and the distance between them. Spiral stiffeners were analyzed by Nam et al. (2018) through linear calculations utilizing the Galerkin method while Lopatin and Morozov (2017) incorporated a sandwich structure into the shell wall and analyzed buckling through both calculations utilizing the Galerkin method and FEM results.

4.9. Finite Element Analysis

FEM is a method in which a component is divided into many smaller parts called finite elements. These elements are then calculated using a large system of equations resulting in an approximate solution. FEM is used in order to perform Finite Element Analysis (FEA), or simply an analysis of the solution, which produces a simulated result. FEA is used in various ways including structural analysis, heat transfer, fluid flow, mass transport and electromagnetism.

To utilize this method the computer aided designed (CAD) component must be subdivided, or meshed. The areas which are of most interest should be subdivided even more, or meshed more finely, to obtain a more accurate result. Various variables and parameters are established in the simulation such as how the model is fixed, what forces are acting upon the model, material, etc. The simulation is then run, resulting in a coloured image showing the variation in the output. Figure 15 displays the steps of CAD model, mesh, finer mesh and FEA analysis.

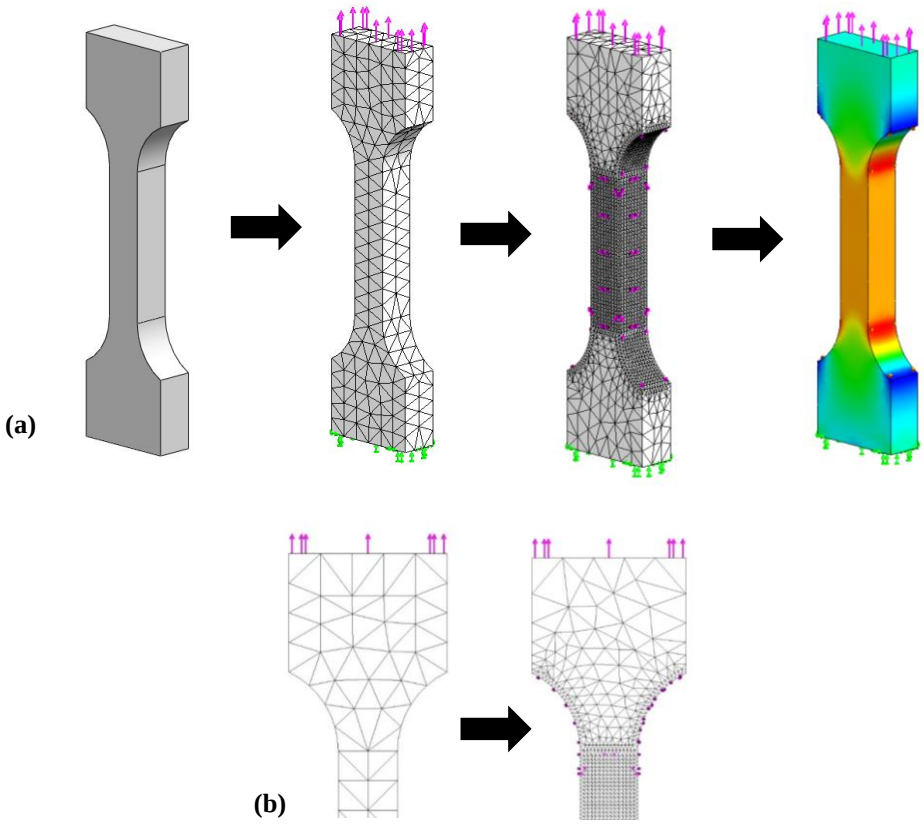

Figure 15 **(a) FEA analysis from CAD model, simple mesh, refined mesh, and final result**
(b) Mesh refinement

5. PRODUCTION OF MATERIAL DATA

This section describes how all test specimens were designed, manufactured and tested. It also includes the findings of these tests and analysis. This information is found among the following sub-categories: *Design of Test Pieces, Manufacturing of Test Pieces, Material Tests, Results of Material Tests* and *Analysis of Test Results.*

Although a part of empirics, this information is collected in its own chapter to make it easier for the reader to see all of it at once.

Certain limitations were imposed on the subjects in this section. Porosity, Ultem sealant specimens and Ultem flexural specimens are limited to three specimens per test due to the cost of the Ultem specimens and post processing treatment.

5.1. Design of Test Pieces

5.1.1 Porosity Test Specimens

The porosity specimens were dimensioned similarly to those found in a recent porosity study (Miguel, M. et. Al, 2018).

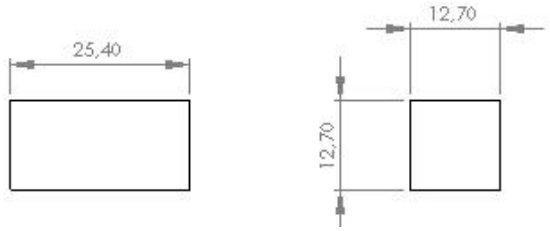

Figure 16: Porosity test specimen dimensions

5.1.2 Performance of Sealant Under Pressure Test Specimens

Specimen 1

A full description of the design of this initial specimen can be found in chapter *6.1.4: Design Development.*

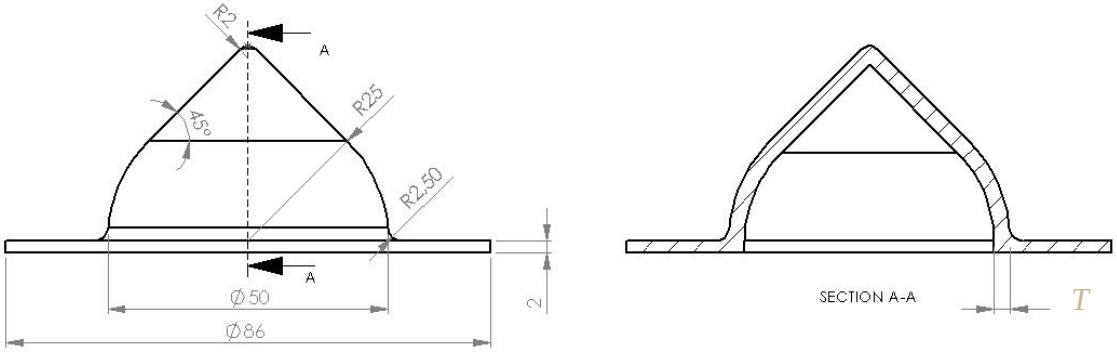

Figure 17: Initial sealant under pressure test specimen dimensions

Specimen 2

An explanation of the change in design can be found in chapter *5.5.2: Performance of Sealants Under Pressure*.

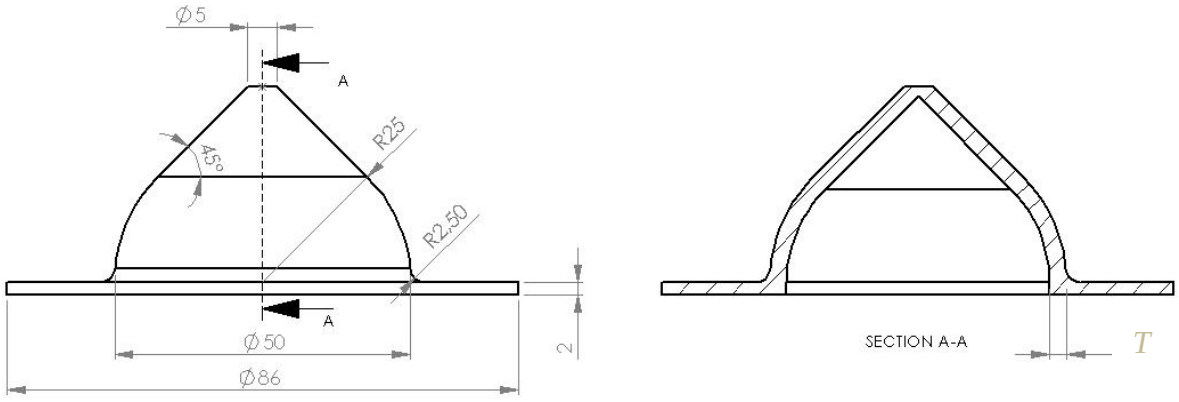

Figure 18: Second specimen design with altered tip

5.1.3 Flexural Test Specimens

The flexural test specimens for ABSplus-P430 and Ultem 1010 have been designed in accordance with ISO178:2019 standards. The dimensions are as follows:

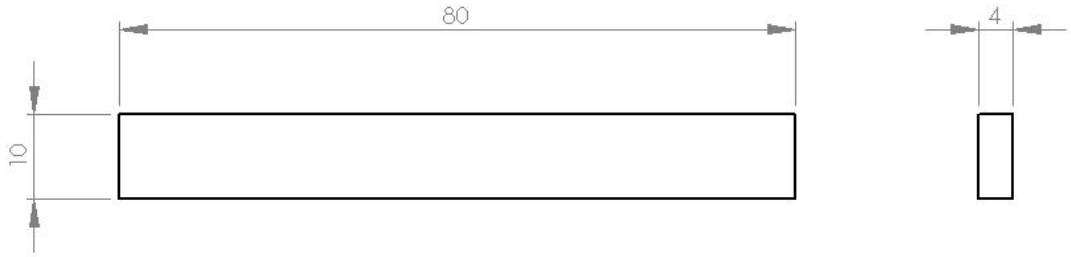

Figure 19: Flexural test specimen dimensions

5.2. Manufacturing of Test Pieces

5.2.1 ABSplus-P430

The ABS porosity, sealant under pressure and flexural test specimens were manufactured in the Stratasys uPrint SE Plus FDM printer. The printing parameters were set using CatalystEX and can be seen below. Porosity specimens were printed in the X direction and the sealant under pressure specimens were printed flat with the conical shape point upwards and no support material. Flexural specimens were all printed in the same direction to ensure sameness. Half of the flexural specimens were printed in the Y direction while the other half were printed in the Z direction. Figure 20 below displays a pre-picture of how the Y direction specimens will be printed, and as seen, they are all printed in the same direction.

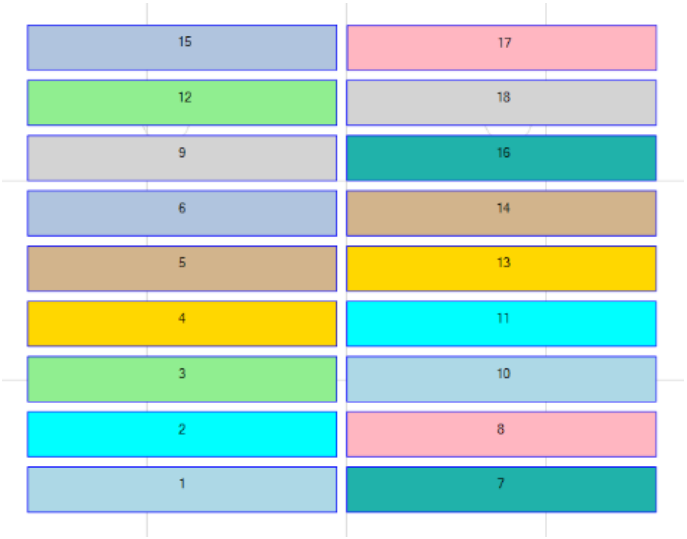

Figure 20: Flexural specimen print layout

The porosity specimens and sealant under pressure specimens were then subjected to various forms of sealants, including acetone vaporization, two spray sealants, and a combination of acetone vaporization and sealant.

The acetone vaporization procedure followed those of a similar test (Neff et. al, 2016). A napkin was soaked with 10 ml of acetone and was placed around the perimeter of a glass vessel. Specimens were placed so that they did not touch each other and that the maximum amount of surface area would be affected. The glass vessel was sealed and the specimens were left for 1 hour. After, the specimens were taken out and were left to dry for 3 whole days to ensure any remaining acetone had evaporated before testing or applying the next post-process.

The two sealants used were a URC200D (Electrolube), a high perfomance urethane coating and HPA 200 H (Electrolube), a high performance acrylic coating. Both sealants are commonly used as electronic protective sprays against abrasion, corrosion and humidity. The sealants were used as instructed by the supplier. Two spray treatments were applied to the test specimens, on the entire porosity specimen while only on the top side of the sealant under pressure specimen. The sealant under pressure specimen's flat edge was sprayed a third time to ensure that it was not the weak point. The treatment which proved to be most effective was then applied in the same manner to flexural test specimens.

All specimens were then dried for the alloted 88h at 23°C at 50% humidity in accordance with ISO 291:2008 before testing.

5.2.2 Ultem 1010

Ultem 1010 test specimens, including 'sealing under pressure' and flexural, were manufactured in the Stratasys Fortus 450 FDM printer at 0,25 build height. Certain specimens were then sent to Polymertal to be plated. Plating was carried out based on Polymertal's expertise on the subject. All specimens were plated with copper at 60 µm thick.

All specimens were then dried for the alloted 88h at 23°C at 50% humidity in accordance with ISO 291:2008 before testing.

5.3. Material Tests

5.3.1 Porosity Test

Porosity test procedures of the vaporized and sprayed specimens followed the ISO 62 standard for water absorption. The specimens were weighed and then immersed in distilled water at room temperature for 1 hour. Afterwards, the specimens were dried off using a dry cloth and immediately weighed again. The percentage change in mass is then calculated *c* by using the following formula, where m_1 is mass before immersion and m_2 is mass after immersion:

$$c = \frac{m_2 - m_1}{m_1} \times 100\%$$

5.3.2 Performance of Sealants and Plating Under Pressure Test

The sealant under pressure test followed procedures of a similar test (Mireles et. Al, 2011). A test pressure vessel was manufactured from a polyurethane block, BM 5173, with a flexural strength of 80 MPa using a Brother TC-S2A CNC milling machine. Once the test specimen was fitted in the vessel, they were both submerged in water. The vessel was connected to a compressed air source. The vessel was then filled at a rate of approximately 1 bar/min up to the max pressure of 8 bar (0,8 Mpa) and was then held constant for 5 minutes if the specimen passed initial pressures. The pressure at which air bubbles formed on the visible side of the test specimen was noted. 1 specimen was tested per sealant. Figure 21 displays the test vessel and setup.

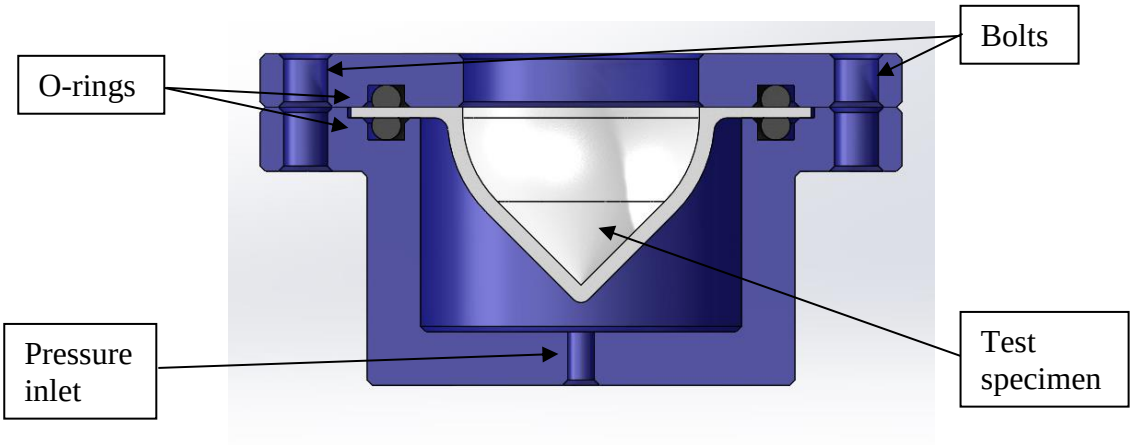

(a)

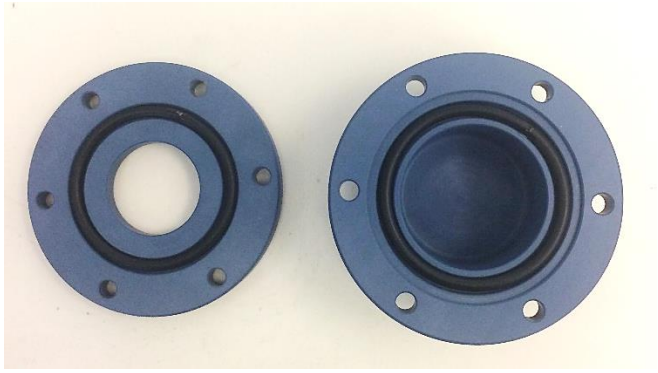

(b)

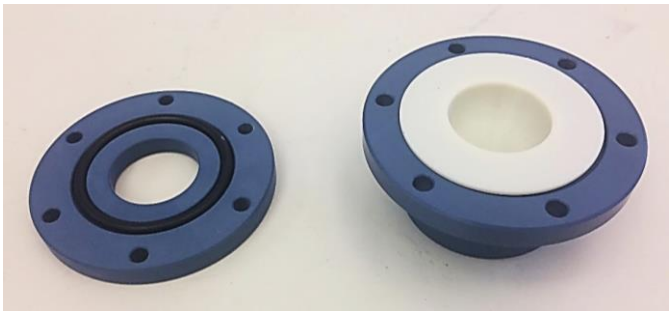

(c)

Figure 21 **(a) Cross section of sealant specimen inside pressure vessel**
(b) Top view of pressure vessel with o-rings
(c) Angles view of pressure vessel with test specimen inserted

5.3.3 Flexural Test

The flexural test followed the ISO 178:2019 standard for such tests. ABS-P430 (Y) and (Z) specimens as well as ABS-P430 (Y) and (Z) post-processed specimens were tested. 5 specimens were tested for each, resulting in 20 tests. Ultem 1010 (Y) and (Z) specimens as well as Ultem 1010 (Y) and (Z) specimens with additional copper plating were not tested due to delays in post-processing.

5.4. Results of Material Tests

5.4.1 Porosity Test

The table below displays the results of the porosity test. See chapter *4.6.1: Vaporization and Spray Sealants* for further description of exposure environment and/or sealants used on test specimens. See chapter *5.3.1: Porosity Test* for test method and result calculation.

Table 4: Results of ABS-450 Porosity test

	Exposed to					*Test Results*		
Sp.	None	Acetone Vapor	Urethane Spray	Acrylic Spray	Polishing	Initial Weight	Final Weight	*c* (%)
01	✓					3,93	3,93	0
02	✓					3,91	3,92	+0,3
03	✓					3,94	3,94	0
1		✓				3,89	3,90	+0,3
2		✓				3,9	3,91	+0,3
3		✓				3,9	3,91	+0,3
4		✓	✓			3,95	3,95	0
5		✓	✓			3,91	3,92	+0,3
6		✓	✓			3,94	3,95	+0,3
7		✓		✓		3,94	3,94	0
8		✓		✓		3,93	3,93	0
9		✓		✓		3,93	3,93	0
10			✓			3,93	3,94	+0,3
11			✓			3,93	3,94	+0,3
12			✓			3,94	3,95	+0,3
13				✓		3,92	3,92	0
14				✓		3,92	3,92	0
15				✓		3,93	3,93	0
16					✓	2,05	2,05	0
17					✓	2,07	2,08	+0,5
18					✓	2,05	2,05	0

5.4.2 Performance of Sealants Under Pressure Test

The following table displays the results of the Sealant Under Pressure Test. See chapter *4.6.1: Vaporization and Spray Sealants* for further description of exposure environment and/or sealants used on test specimens. See chapter *5.3.2: Sealant Under Pressure Test* for test method.

Table 5: Results of Sealant Under Pressure Test

	Specimen	*Exposed to*				*Test Results*		
		None	Acetone Vapor	Urethane Spray	Acrylic Spray	Pressure Held (bar)	# Leaks	Place of Leakage
1	1	✓				0	5	Tip, 4 deformities
2	1		✓			0	3	3 deformities
3	1		✓	✓		0	2	2 deformities
4	1		✓		✓	7,5:8	1	Tip after 7,5 bar
5	1			✓		0	2	Tip, 1 deformity
6	1				✓	1,5:8	1	Tip after 1,5 bar
7	2				✓	8	0	None

5.4.3 Flexural Test

ABSPlus-M430

The follow table shows the results of the flexural test. A complete list of results and curves can be found in Appendix C.

Table 6: ABSPlus-M430 flexural test results. Compares unsealed and sealed specimens

	Rp0,2 (MPa)	*Flexural Modulus (MPa)*
Y, Unsealed	39	1650
Y, Sealed	45	1678
% Difference	(13%)	(2%)
Z, Unsealed	35	1668
Z, Sealed	37	1692
% Difference	(5%)	(1%)

5.5. Analysis of Test Results

5.5.1 Porosity Test

Table 4 displays the results of specimens exposed to acetone vaporization and/or various sealants, and then subjected to a porosity test. The change in weight was calculated, and presented as a percentage to show if the specimen had been fully sealed (zero change in weight), or if the sealant had failed to seal the specimen (positive change in weight). Untreated specimens 01-03 increased in weight on average 0,1%. This is not seen as a substantial amount, and is assumed that the material is not gaining any moisture. However, if the specimens had been left longer, more water may have entered them. Noteworthy results such as those exposed to just acetone or just sprayed with urethane increased in weight on average of 0,3%. This suggests that these post-processes are not optimal for sealing against water. Specimens that were exposed to acrylic spray and acrylic spray + acetone vaporization did not increase in weight at all. By regarding what was noted earlier about acetone vaporization results, it can be concluded that the acrylic spray alone provides a sufficient seal for the ABS-430 against water.

5.5.2Performance of Sealants Under Pressure Test

The results from this test are displayed in Table 5. Two stages were completed for the Sealant Under Pressure Test. The first stage consisted of testing the specimen seen in chapter *5.4.2: Sealant Under Pressure Test, Design 1*. Sealants were applied to the specimen and the specimen was pressurized to see if and where the sealants failed. See chapter *5.3.2: Sealant and Plating Under Pressure Test* for a full description of the test method. As shown in Table 4, the acrylic spray seems to hold under pressure the best, as seen in specimens 4 and 6. One common mode of failure for all tests is that the tip of the specimen leaks, as seen in 1, 4, 5 and 6. Even the specimens sprayed with acrylic sealant eventually failed at this location. This suggests a weak point in the design itself, and not necessarily the form of sealant. The weak point is likely due to the FDM AM layer slicing software and how it calculates sharp points. The software instructs to print in tight, ringlet circles, which is apparently prone to leaking (see Figure 22 below).

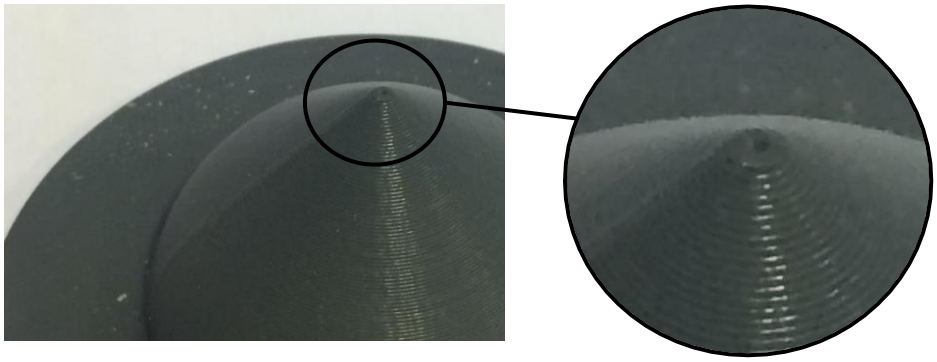

Figure 22: Weakness point located at tip of specimen

Therefore, a second design was tested with the acrylic spray (see chapter *5.1.2: Sealant Under Pressure Test Specimen, Design 2*). The second design held the 8 bar pressure for 5 minutes without leaking. The post-processed part also has a noticeably smoother surface finished compared to the non-post-processed part. This can be due to the sealant sliding from the peaks

of each layer and accumulating in the crevices which creates less deviation between the peaks and crevices.

5.5.3 Flexural Test

Specimens were printed along the Y (flat) and Z (upright) directions. See chapter *5.1.3: Flexural Test Specimens* for dimensions. Table 6 displays the results from the test, comparing the flexural yield strength and flexural modulus between unsealed and sealed specimens. The sealant had little effect on the flexural modulus, as the X and Z results only increased by 2% and 1% respectively. The sealant seemed to have a slightly larger effect on the yield strength of the specimens, as the X specimens increased by 13% and the Z specimens increased by 5%. Therefore, the sealant is seen as advantageous in terms of adding slight material strength to the component.

6. EMPIRICS

Two products should be developed which are designed to be manufactured by AM. Two product solutions are of interest, one manufactured in *ABSplus-P430* and one in *Ultem-1010*.

6.1. ABSplus-P430 Cannister

6.1.1 Construction Specifications

The first product is a structure which would cover the functions of the current polymer cannister, or withstand a lower pressure of at least *P* MPa. The printed structure needs to be coated with a sealant to protect the inner structure from its outside environment. The product should have minimal production processes including manufacturing and post-processing. The redeveloped product should function as before and therefore should contain the inner assembly and be sealed against outer fluids. These specifications decided upon by ABB and the developer are summarized below:

- Should withstand an outer pressure of *P* MPa
- Should have a buckling FOS of 1,5 or higher
- Should be sealed from its outer environment
- Should be manufactured with least amount of processes possible
- Inner assembly should be inserted as a single unit

6.1.2 Manufacturing Specifications

The low range product will be manufactured on the Stratasys uPrint SE Plus located at ABB CRC. The product will be made in ABSplus-P430. ABSplus-P430 is a valid material to test for the low range cannister as it is subject to very low pressures, which the ABS can withstand. ABSplus-P430 has similar mechanical properties to ABS-M30, which is a common industrial manufacturing material within AM, and can therefore easily be integrated into the process. The inner assembly should be assembled previously and be inserted in to the product as one piece.

6.1.3 Functional Design and Design Optimization

Step 0: Design Decisions

The construction specifications say that the product should be manufactured with the least amount of processes possible. Therefore, it was decided to design the product as one entire part, with the inner assembly embedded. To accomplish this, the product would be printed up to a certain height, at which point the assembly is inserted to the inner cavity. The print job would then be resumed, and the product finalized. This process is portrayed in Figure 23. The Stratasys uPrint SE printer was tested for this function and it was found that the printer could indeed perform this.

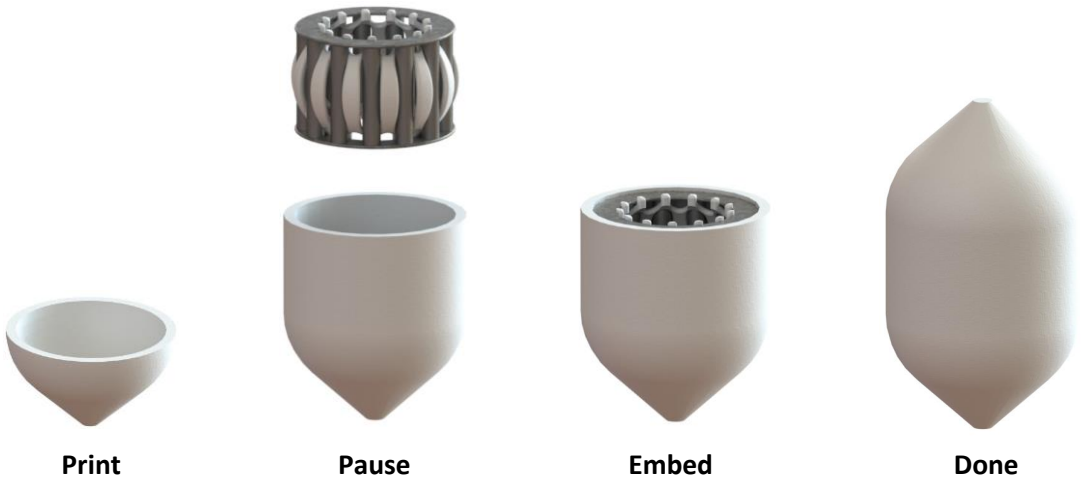

Figure 23: Process of embedding inner assembly

Step 1: Dimensioning for Function

The outer and inner diameter was chosen based on the original cannister design, which will enable the part to fit within current manufactured housings. Furthermore, this allows the original metal rings to fit inside. Looking back at the original cannister design (as seen in chapter *3.2: FEA of Current Design*), it is apparent that the top spherical caps contain extra material which is under relatively little stress, and so it was determined to design the new cannister with a continuous wall thickness by removing the extra material. An excel sheet (as seen in Appendix D) was used to calculate the resultant height of the cylinder based on the above parameters, as well as parameters seen in Appendix E, while maintaining the necessary volume to weight ratio needed. The resulting weight takes in to consideration the weight of the inner assembly as well. The resultant cylinder height was 30mm. This height also provides adequate space for the inner assembly to fit inside, as it has a height of 30 mm (inner assembly weight and height can be seen in Appendix A). The preliminary cannister dimensions are displayed below in Figure 24:

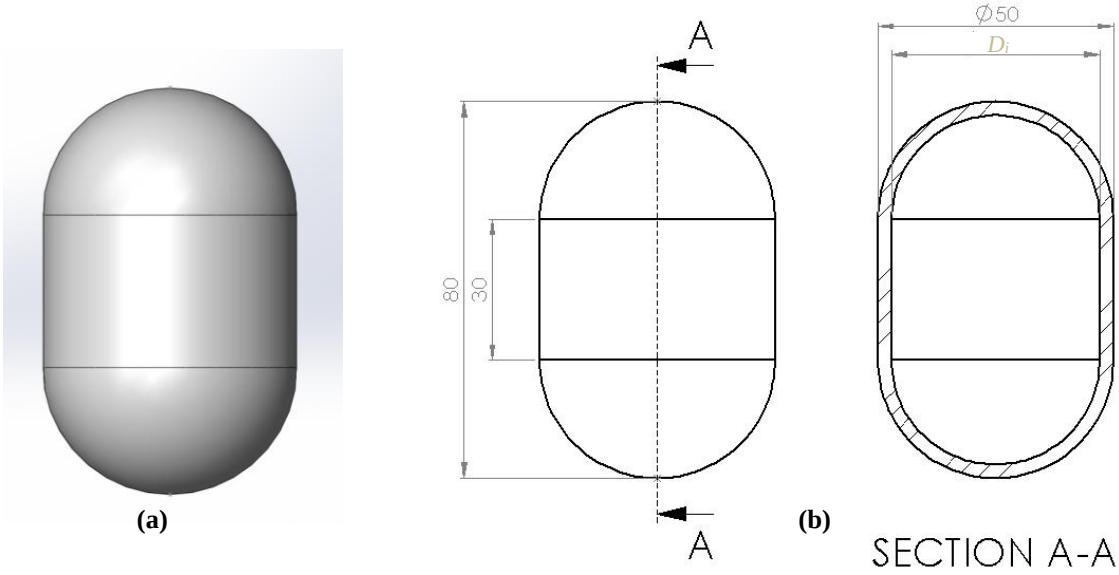

(a) (b)

Figure 24 (a) Front view of cannister exterior with 30mm cylinder height
(b) Cross-section drawing with cannister dimensions

Step 2: FEA

To perform a preliminary analysis, the required loaded pressure of *P* MPa was placed on the outer surface of the model.

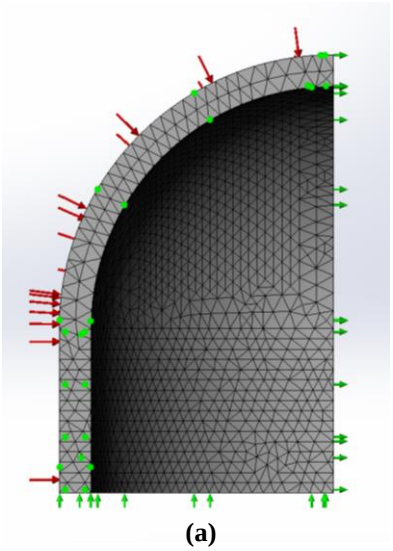

(a)

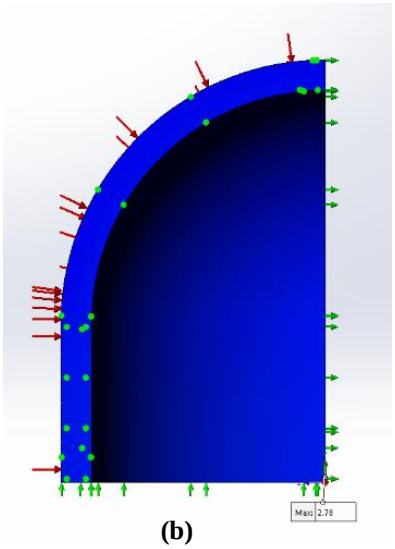

(b)

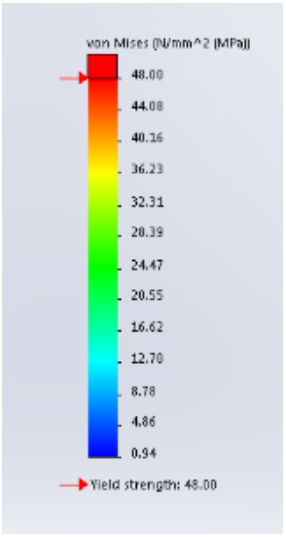

(c)

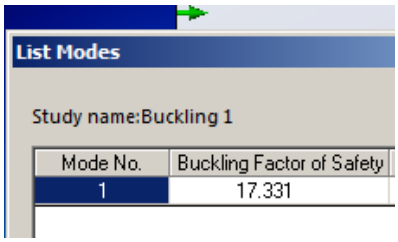

(d)

Figure 25 **(a) Mesh, size 1,3mm, applied on model**
(b) Results of static FEA analysis show max stress at 2,78 MPa
(c) Scale of results shows only low stresses reached compared to yield at 48 MPa
(d) Result of buckling FEA, suggests FOS of 17

Figure 25b displays that the construction reaches a max inner stress of 2,78 MPa, which results in a buckling FOS of 17,33. This suggests that the preliminary design adequately holds against a pressure of *P* MPa.

When the pressure was increased, as displayed in Figure 26, the FEA suggests that the construction can withstand 17,06(*P)* MPa before surpassing yield strength (reaches max stress of 47,36 MPa), and maintain a buckling FOS of 1.

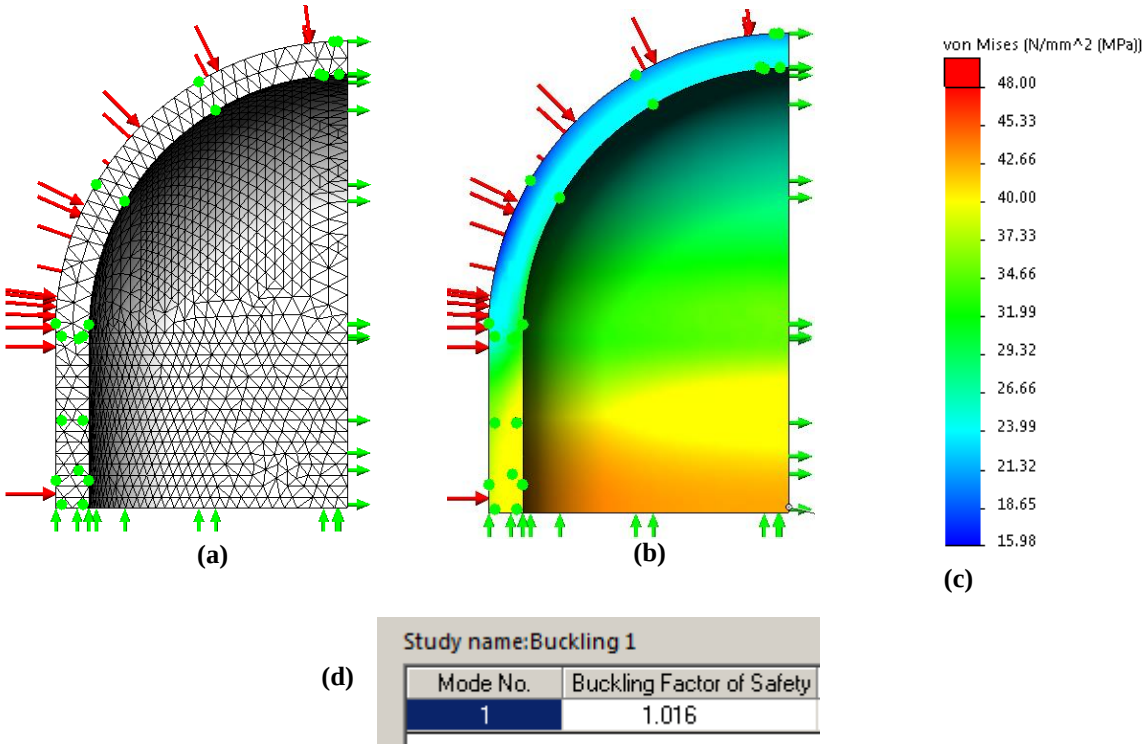

Figure 26 **(a) 1,3mm curvature based mesh**
(b) Static analysis results suggests design holds for 5,8 MPa
(c) Scale shows yield is not surpassed
(d) Results of buckling FEA, suggest FOS of 1

Step 3: Inner assembly

As it was determined previously to insert the inner assembly as a single unit, a holder needed to be constructed, which would keep the metal rods and rings in the correct position. The holder was modeled to be as light weight as possible while allowing easy assembly of all units. The holder designs were kept at as a single part to keep processes and part count to a minimum. The outermost diameter of the design is kept less than the diameter of the metal rings so as to not impede with the inner wall of the cannister. Various designs can be seen below in Figure 27. This part was not a crucial design element, so therefore analysis on the decision is minimal.

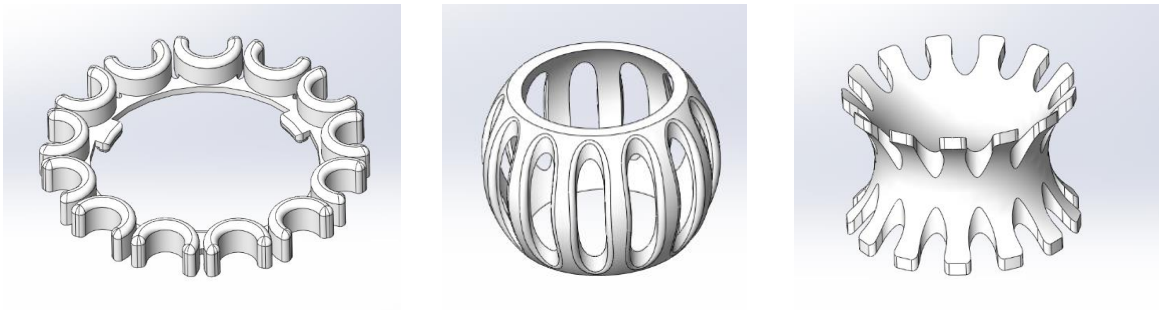

(a)

(b)

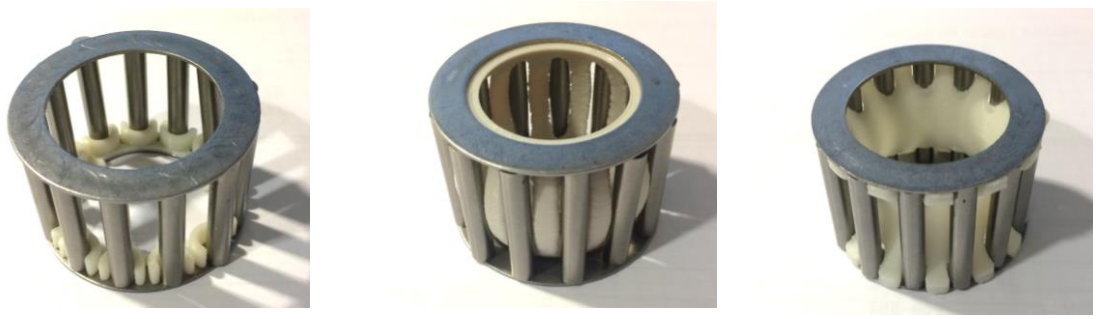

(c)

Figure 27 (a) 3 ideas for metal rods and rings holder
(b) Printed versions of (a)
(c) Printed versions of (a) with metal rods and metal rings inserted

Based on ease of assembly and possible additional structural strength, design (b) was chosen to move forward with. The design was altered for further weight reduction and additional points were added for easy metal ring placement. The design can be seen below:

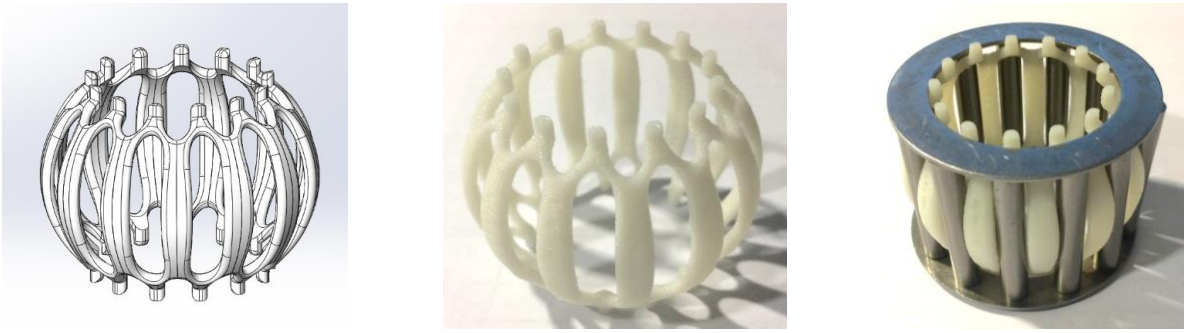

Figure 28: Optimized holder. Shows CAD design, printed version, and printed version with all parts

Step 4: Inner Assembly Ledge

A ledge was incorporated in the exact position that the inner assembly should rest and directly above the inner assembly to keep it in place. See Figure 29 below.

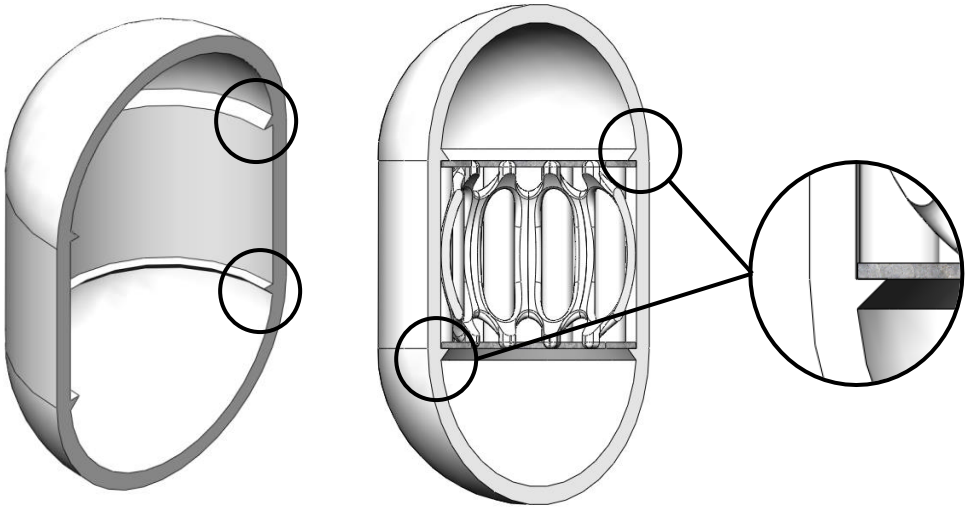

Figure 29: Ledge design to keep assembly in place

The structure with the ledges was analyzed. Instead of analyzing with the rigid body metal rings, lines were drawn on the inner surface of the column and limited to 0 radial movement. The FEA static results show stress concentrations directly near the ledges, surpassing yield strength. The stress reduces from the middle section, reaching only 45 MPa, while the buckling FOS increases (Figure 30).

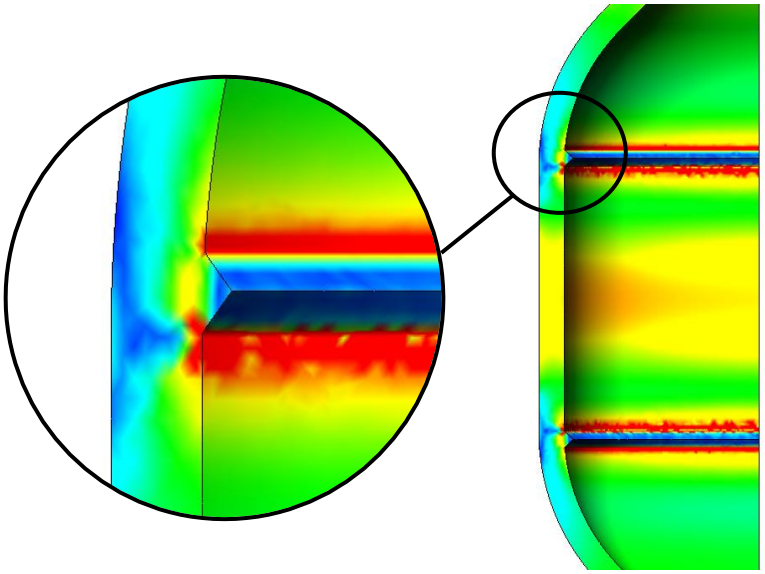

(a)

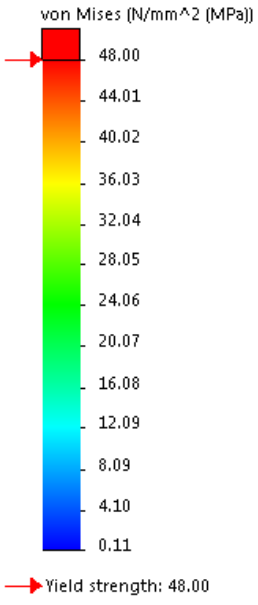

(b)

(c)

Study name:Buckling 1

Mode No.	Buckling Factor of Safety
1	1.5329

Figure 30: **(a) Stress concentration form at the ledge**
(b) Stress scale
(c) Ledges lead to increased buckling FOS

6.1.4 Design Development

Development in Relation to FDM Process

The design described above is not optimized for the FDM process as the spherical top section, with an inner diameter of D_i, is too large to print successfully due to the steep overhangs of the large sphere, and therefore cannot be manufactured without printing with support structures (See chapter *4.2.2: Support Structures*). Therefore, the top and bottom spherical end caps were exchanged for a 45° conical shape as seen in Figure 31. The end caps attach to the main cylinder with the same curvature as the spherical end cap as to maintain the same stress and buckling resultants. When simulated, the maximum inner stress and buckling FOS were relatively the same and can be seen in Table 7 below.

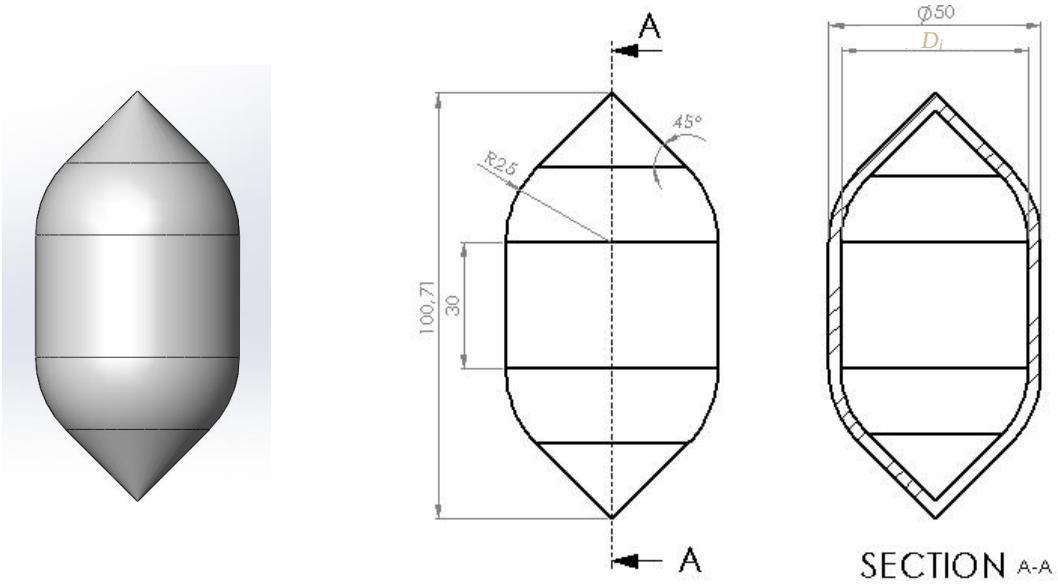

Figure 31 **(a) Front view of cannister exterior with 30mm cylinder height and cone end caps**
(b) Cross-section drawing with cannister dimensions

Table 7: Comparison between spherical and conical end caps

	Spherical end cap	*Conical end cap*	*Scale*
Max Stress (MPa)	47,36	47,34	
FEA Static Analysis	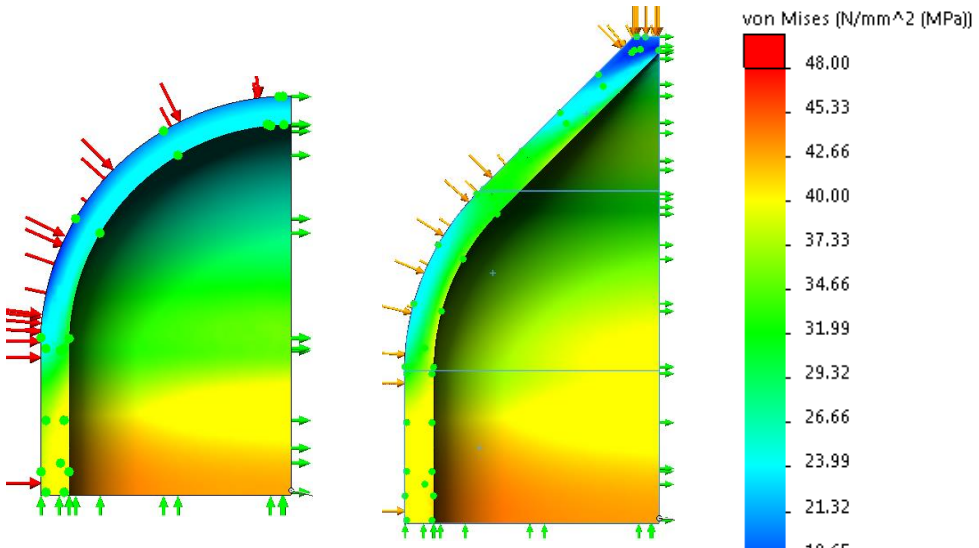		
Buckling FOS	Study name:Buckling 1 Mode No. | Buckling Factor of Safety 1 | 1.016	Study name:Buckling 1 Mode No. | Buckling Factor of Safety 1 | 1.0169	
Weight (g)	34,4	35,7	

Development in Relation to Sealing Against Outside Environment

The exchange in end cap design mentioned above was also carried out to aid in sealing the structure against the outside environment (see chapter *5.5.1: Porosity Test* for reasoning). The spherical design results in larger steps between layers causing weak points against fluids to enter. The conical shape results in smaller steps, or layer edges that are closer together, which aids in sealing the part.

Additional tests were conducted on various sealing methods that would be added post-process (see chapter *4.6.1: Vaporization and Spray Sealants* for post-process reasoning). Further information regarding the test specimen designs, manufacturing of test pieces, test methods, results and analysis can be found in chapter *5: Production of Material Data.* From the test results it was decided that the HPA 200 H (Electrolube), a high performance acrylic coating, would be used to seal the cannister as it was the top performing option in terms of sealing against porosity and performance under pressure.

Manufacturing Process Count

A sub-total of the part count (excluding metal rods and rings) and processes is seen below. The process ‘holder insertion’ is not counted as an additional process as it is carries out during the ‘print cannister’ process.

	Cannister	1
	Inner assembly holder	1
Total Part Count	=	2 Parts
	Print holder	1
	Print cannister	1
	Holder insertion	-
	Seal cannister	1
Total Process Count	=	3 Processes

6.2. Ultem 1010 Cannister

6.2.1 Construction Specifications

The second product is a structure which should withstand a higher pressure range up to 20 MPa and the highest temperature possible. The printed structure will be metal plated, also to protect the inner structure from its outside environment. The product should have minimal production processes including manufacturing and post-processing. The redeveloped product should function as before and therefore should contain the inner assembly as well as be sealed from the outside environment. The specifications are summarized below:

- Should withstand an outer pressure of 20 MPa
- Should withstand temperature of 150°C
- Should have a buckling FOS of 1,5 or higher
- Is metal plated
- Should be manufactured with least amount of process possible
- Inner assembly should be inserted as a single unit

6.2.2 Manufacturing Specifications

The high range product will be manufactured on the Stratasys Fortus 450cc located at Digital Mechanics, Västerås. The product will be manufactured using Ultem 1010. The high range product needs to withstand considerably more pressure and temperature and Ultem 1010 is suitable for both of these criteria as it is considered a high-performance industrial plastic which can withstand much higher working temperatures than typical polymers. The inner assembly should be assembled previously and be inserted in to the product as one piece, before the product is copper plated. The product will be copper plated by Polymertal, a metal plating company located in Israel.

6.2.3 Functional Design

Step 0: Design Decisions

As was the case with the ABSplus-P430 cannister, it was decided that this design should be designed as one overall part with an additional embedded inner assembly to minimize process steps. See chapter *6.1.3: Functional Design, Step:0* to see a further description of this process.

Step 1: Inner Structure

An initial study was done using FEM analysis to investigate various types of inner structures for the cannister. Both a static and buckling study were performed on all designs. The outer structure was kept the same as the original Kynar cannister, such as the height and the outer diameter and wall thickness, so that the cannister would fit within its current housing. The initial pressure of *P* MPa was kept the same as was the Kynar material. The designs were kept to a mass similar to the original and the resulting buckling FOS was used to compare the structures. Some structures can be seen below as well as a summary of the above mentioned variables. A more comprehensive list of initial tested structures can be seen in Appendix F.

Constant variables

- Outer dimensions: height, diameter, wall thickness
- Applied pressure of *P* MPa
- Material: Kynar
- Similar weight to Original cannister: 324,6 g

Compared variable

- Buckling FOS

The design process started by referring back to the original Kynar cannister. An FEA analysis (see chapter *3.2: FEA of Current Design*) of the cannister shows that the upper and lower end caps are filled solid with material, however these areas also undergo relatively no stress. Therefore, the material was removed, resulting in the cannister having a constant wall thickness. This result is the basis for the rest of the cannister designs. Furthermore, the buckling FEA analysis shows that the original cannister design will ultimately fail due to an overall buckling, which is also stated as the failure mode by Table 3 displayed in chapter *4.8.1: Designing for Buckling in Cylindrical Shells*.

Table 8 displays the three main designs that were then produced and compared. The designs included the following inner structures: Rings and Ribs, Lattices and Bridges. A more comprehensive description of how these designs came to be is described below.

Table 8: Original design and three new designs to compare

	Original Kynar cannister	*Rings and Ribs (Bricks 1)*	*Lattice (Vert Spring 4)*	*Bridge (Bubbles 1)*
Design	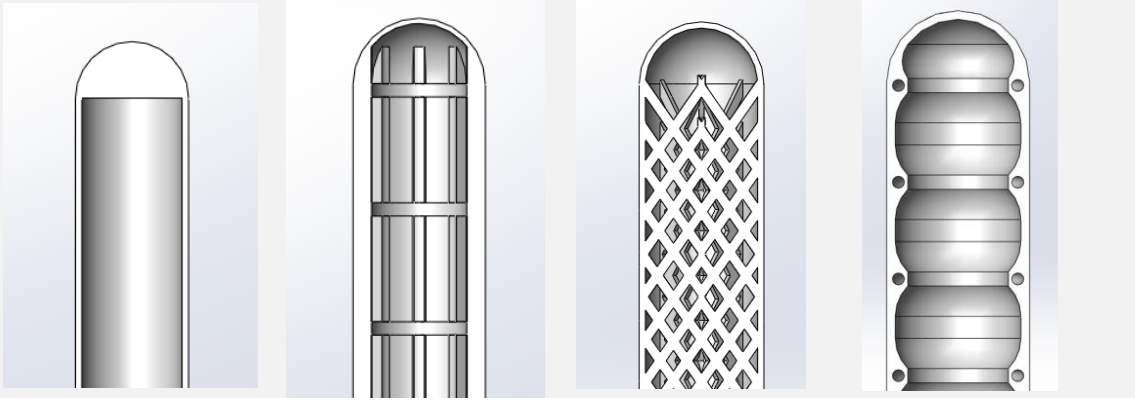			
Weight (g)	324,6	294	336	330

Rings and Ribs

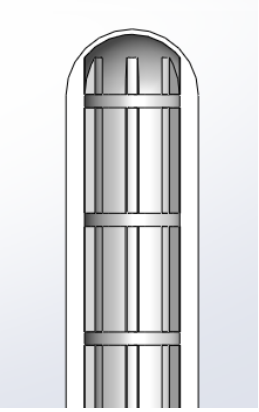

Figure 32: Rings and Ribs design

According to studies performed on buckling of cylindrical shells (see chapter *4.8 Buckling of Cylindrical Shells*), rings and ribs are a commonly used design tactic to reinforce structures against buckling. As can be seen in the Rings and Ribs CAD drawing, the structure mainly sits close to the wall leaving the core of the cylinder hollow. According to Table 3, this design will be prone to all of the buckling modes, including shell, panel, general, overall and local stiffener buckling. Many variables need to be taken in to consideration when optimizing this design, such as number of rings and stiffeners and their size and shape, as all of these greatly affect the type of buckling mode, which is why this design is prone to all of the different modes.

This design resulted in a buckling FOS of 11,6. Figure 33c shows how stresses are concentrated directly where the stiffeners join the shell as well as in areas where rings and stiffeners intersect. The buckling mode is mainly a local stiffener buckling, which would lead to the second buckling mode to occur in the nearby panels.

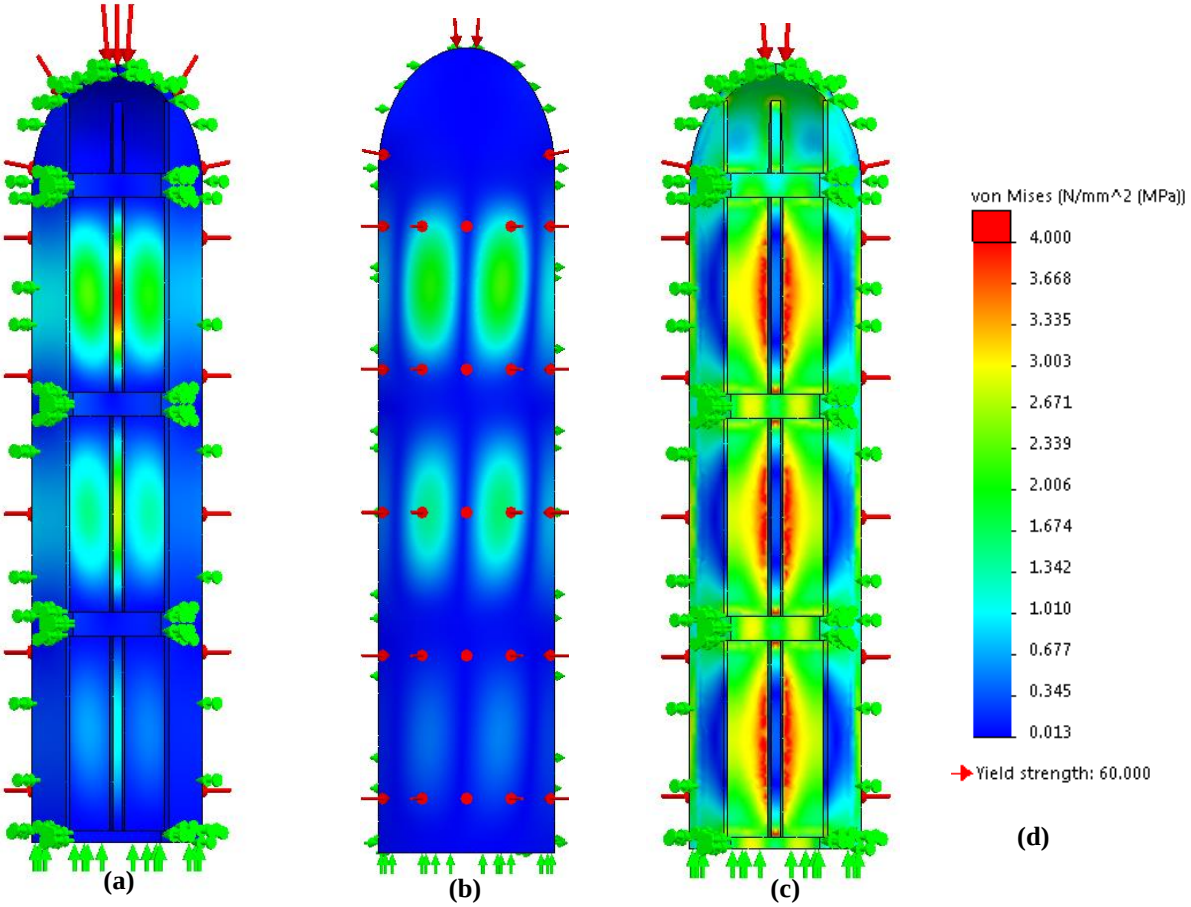

Figure 33: **(a) Results from buckling analysis show local stiffener buckling**
(b) Secondary buckling occurs in the outer shell
(c) Stress concentrations form near the stiffeners
(d) Stress scale

Many iterations of this design were tested, including varying numbers of stiffeners and rings as well as their cross-sectional size and shape. One design, Bricks 7, resulted in a buckling FOS of 34. However, the primary buckling modes varied throughout the designs, leading to the conclusion that this type of design would be especially difficult to optimize. One design, seen in Figure 34, even included fillets on all panel walls to reduce the stress concentrations, however the stresses then became concentrated in the panels themselves and changed the buckling mode to shell buckling.

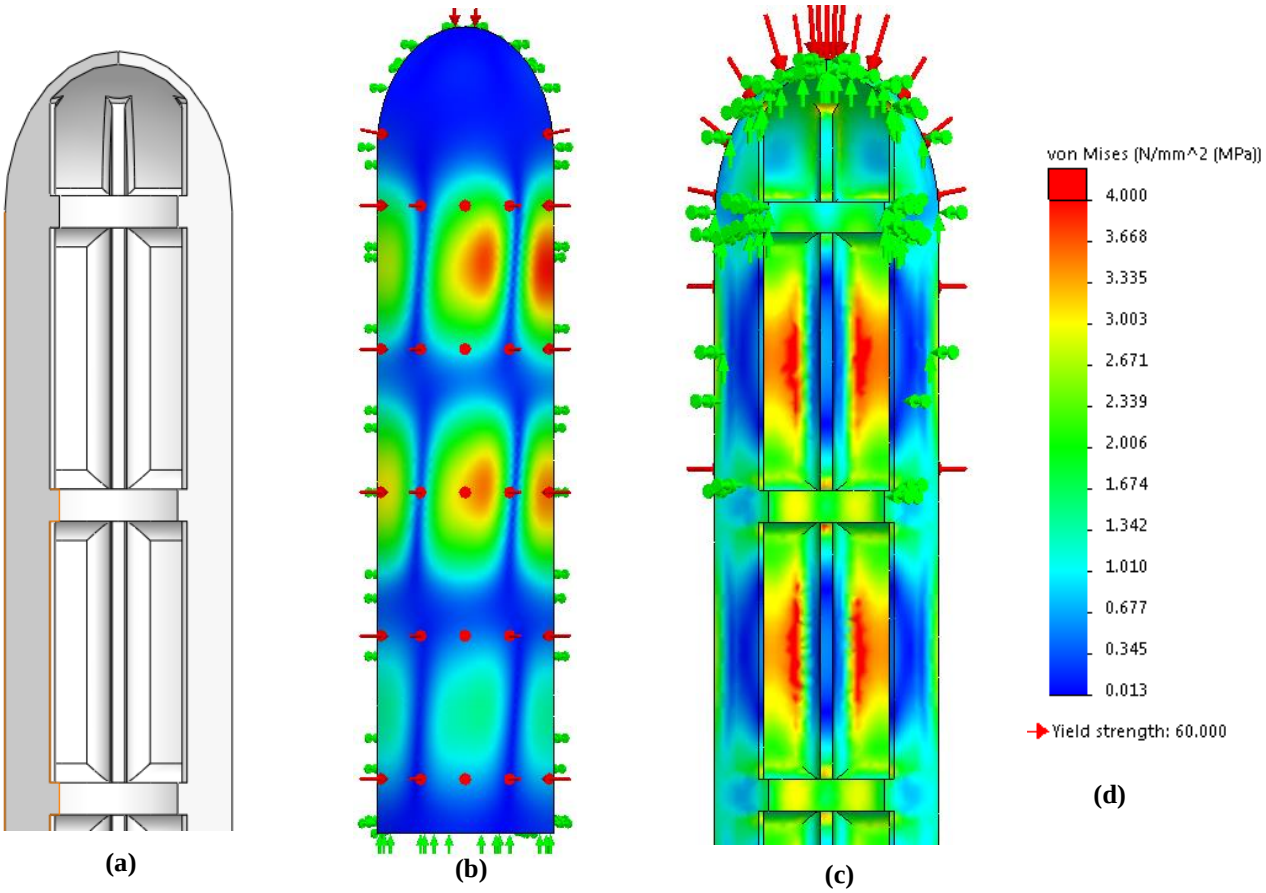

(a) **(b)** **(c)** **(d)**

Figure 34: **(a) Rings and ribs design with added fillets**
(b) Buckling occurs in the outer shell
(c) Stress concentration migrates to panels
(d) Stress scale

Lattices

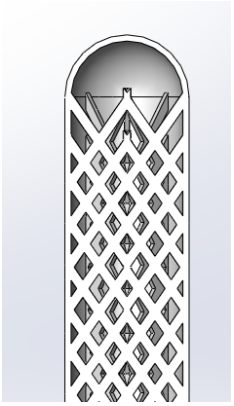

Figure 35: Lattice design

Incorporating lattice structures is a design tool available through additive manufacturing, and therefore it was tested as an inner structure as displayed in Figure 35.

This design resulted in a buckling FOS of 17,7. The lattice is modeled on one vertical plane and then circularly patterned (8 times), causing the lattice to act as longitudinal stiffeners. As a result of this, this design will be prone to local stiffener buckling (Figure 36b). As the lattice fills the cavity homogenously, the stress concentrates in the middle of the design, similarly to if the cannister had only a constant thick wall, as this point is the least supported compared to the rest (Figure 36c).

Iterations of this design included testing different shapes and size of lattices, changing the density and amount of revolutions (see Appendix F, Vertical Spring 1-4). A separate software was also tried to create lattice structures, however complications arose and it was not able to be used. In this case, this type of structure is limited by what the CAD software, SolidWorks, can relatively easily produce.

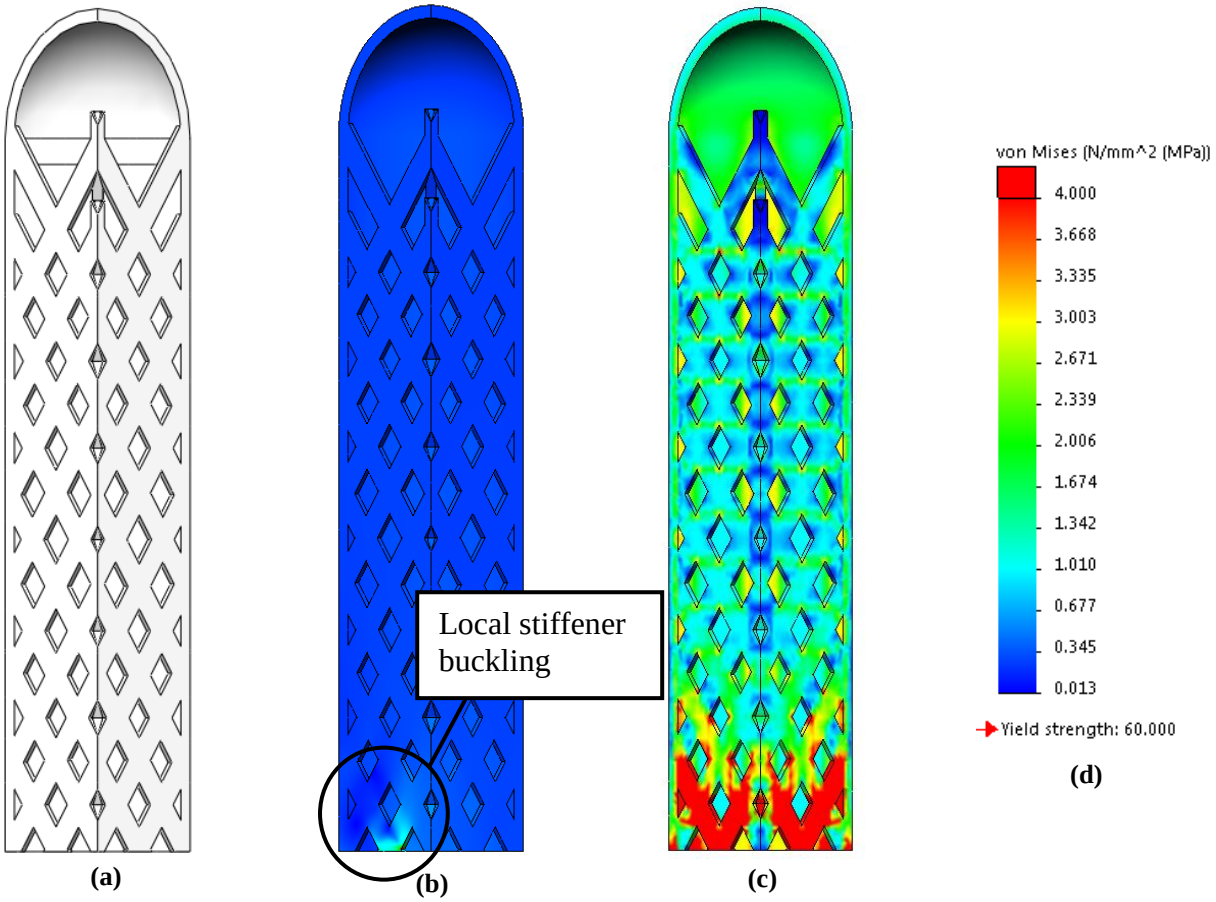

Figure 36: **(a) Lattice design, ¼ section**
(b) Buckling results show local stiffener buckling
(c) Stress concentrates in middle section of whole cannister
(d) Stress scale

Bridges

This design idea originated from taking a cross-section of the original cannister and likening the wall to a clamped beam under compression, which can be seen in Figure 38.

Figure 38: Clamped beam under pressure

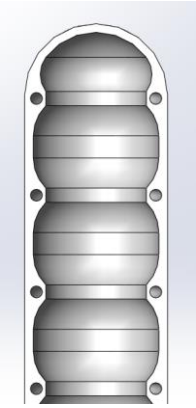

Figure 37: Bridge design

Figure 39 **(a) Bridge supported by two arches (Moore)**
(b) Aqueduct supported by many arches (Gaul)

This situation can be compared to that of arch bridges such as those seen in Figure 39. The arches can then be compared to ring stiffeners. According to Table 3, a design with ring stiffeners would be prone to shell buckling, general buckling, overall buckling and local stiffener buckling. However, instead of having separate bridges, and therefore separate contact points with the outer shell such as with lattices, the bridge shape was revolved around a central axis, providing support to the entire shell.

This design resulted in a buckling FOS of 23,2. Figure 40b displays how ring stiffeners in this case will be prone to overall buckling. The stress concentrates in the rings, however the stress seems to be more dispersed overall when compared to the other two designs (Figure 40c).

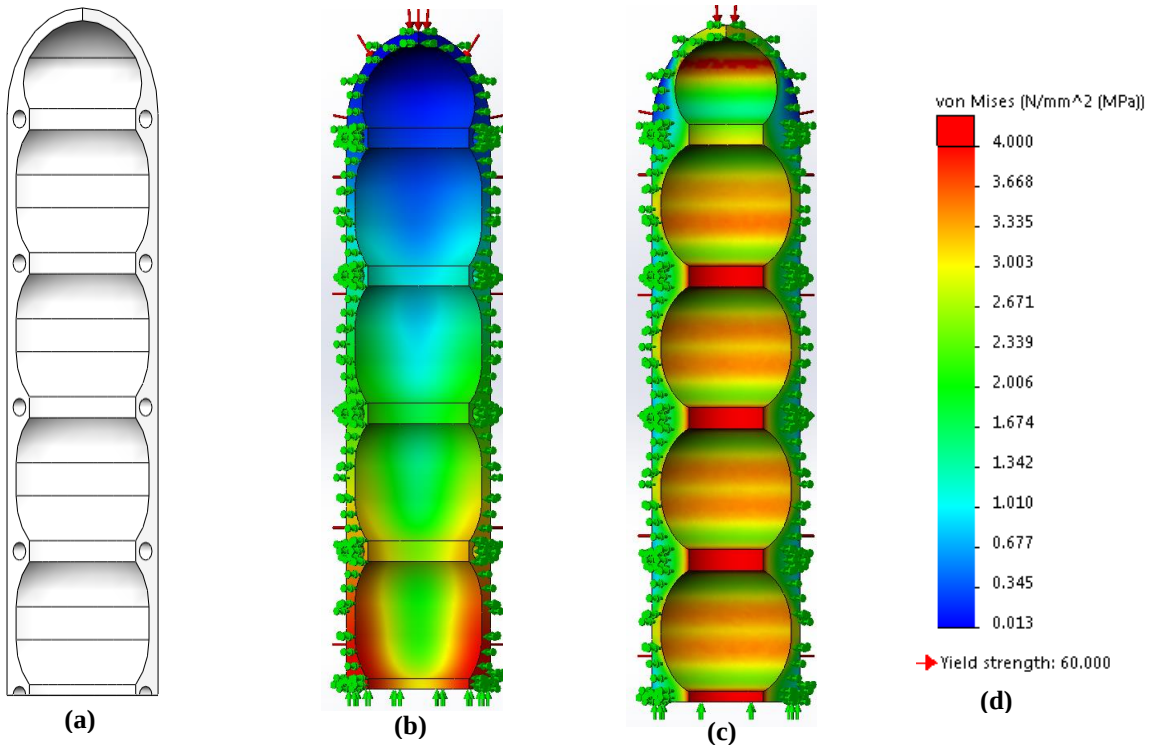

Figure 40 **(a) Bridge design, ¼ section view**
(b) Buckling results show overall buckling
(c) Stress concentrates in trusses
(d) Stress scale

Iterations of this design (as seen in Appendix F) explored shape of the arch, size of the arch feet and removal of material between the arches. Ultimately, the arches were designed as hemispheres and the tresses were left hollow. This increase the buckling FOS to 27 and caused the buckling mode to change to a shell buckling (Figure 41b). The stress became concentrated in the areas of the shell which were unsupported (Figure 41c).

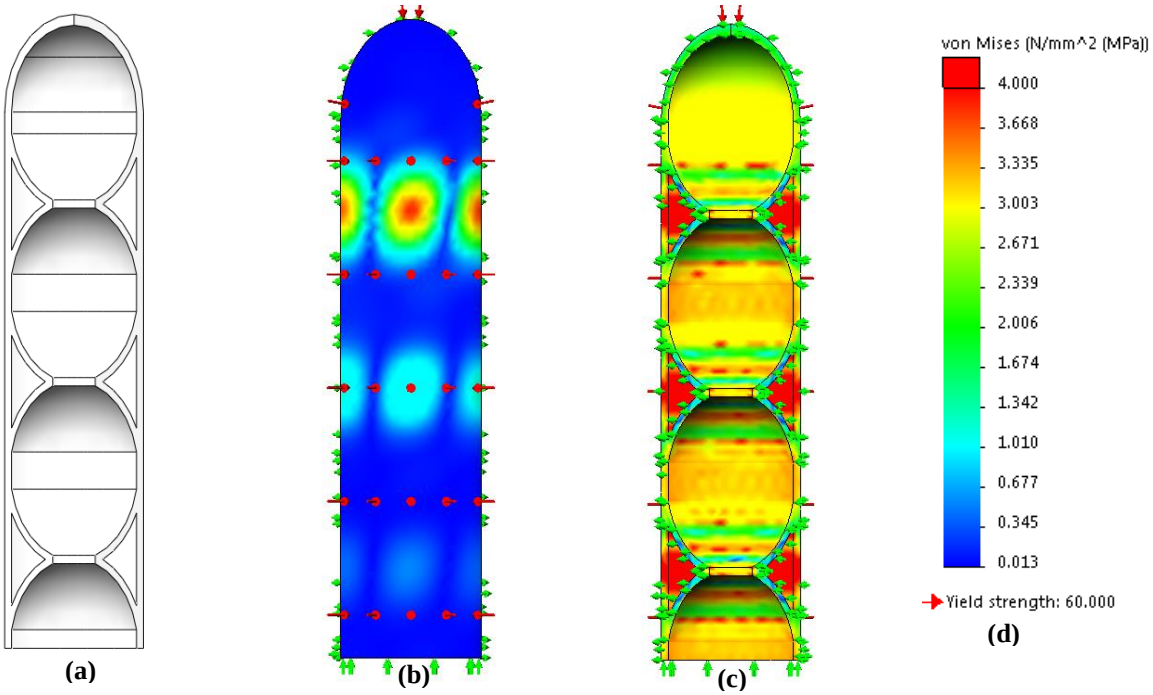

Figure 41 **(a) Updated bridge design, ¼ section view**
(b) Buckling results show panel buckling
(c) Stress concentrates in outer shell
(d) Stress scale

Step 2: Design Choice

The 3 designs were compared on certain criteria and rated in a decision-matrix. The results of the decision matrix are displayed in Table 9. Alternative designs were used when a superior one was found. The criteria are *CAD-ability, suitability for FDM AM, suitability for hardware embedding*, *buckling FEA FOS results* and *design optimization.* A further explanation of decision-matrix choices can be seen below.

CAD-ability refers to how easily the design can be built in the SolidWorks software. The speed and ease at which the design can be changed and optimized will depend on this, and therefore greatly influence the development process and end result.

The ability for the design to be produced via *FDM AM* is an important factor to take in to consideration even at this point because it will affect the end result. The final design will be optimized further later on for the manufacturing process, but starting with a design more suited for the process will allow for an even better result compared to a design which is relatively hard to produce.

One construction specification specifies that the inner assembly be embedded during the manufacturing process. This means that a section of the inner structure will be removed to make space for the inner assembly. Therefore, the inner structure should still maintain strength and ability to withstand buckling when this portion is removed without major re designs.

The results from the *buckling* FEA are taken in to consideration, as buckling is the main variable that the entire structure is seen to be vulnerable to. Foreseeable design optimization steps are taken in to consideration based on level of complexity.

Table 9: Decision-matrix for inner structure

Key: - = Disadvantage S = Satisfactory + = Advantage		*Baseline*	*Alternatives*		
	Weight Factor	Original Kynar Cannister (Baseline)	Rings and Ribs (2nd alternative)	Lattice	Bridge (2nd alternative)
			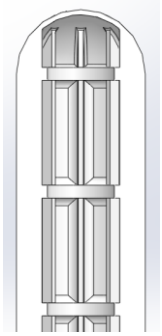	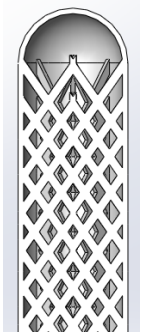	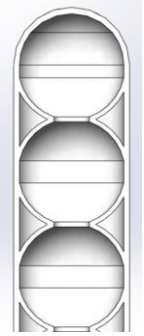
CAD-ability	2	0	**S**	-	**S**
FDM AM Suitability	1	0	+	-	+
Hardware Embedding	5	0	**S**	-	**S**
Buckling FOS	4	0	+	+	+
Design Optimization	3	0	-	-	+
Total +			5	4	8
Total -			3	11	0
Total			**2**	**-7**	**8**

Rings and Ribs was considered satisfactory for the SolidWorks environment due to its simple features such as the rings, ribs and fillets. It was seen as an advantage for FDM AM due to its minimum overhangs compared to the original. Hardware embedding was seen as satisfactory since the inner structure of Rings and Ribs provides an open cavity space that the inner assembly can fit in to. The buckling FEA resulted in a FOS of 11,6, higher than the original design at a FOS of 4. The literature suggests that several optimization tools within SolidWorks would need to be utilized to achieve an optimized result (see chapter *4.8.1: Designing for Buckling in Cylindrical Shells).* Although seen as feasible, the unpredictable buckling mode and future need for embedding are foreseen to complicate the delicately optimized design. This design came in second according to the decision matrix.

Lattice was considered to be at a disadvantage in relation to CAD-ability in the SolidWorks environment. SolidWorks simply does not provide the necessary tools for designing such structures and other tools which were tried specifically for designing lattices encountered problems. The length of time to design intricate lattices and delve deeper in to lattice structure was seen as un-manageable with the available software. The design also seems at a disadvantage for design optimization for the same reasons provided as non-CAD-ability. Numerous, small cross-sections of the branches in the lattice structure is also not suitable for FDM AM due to the nature of the process. This design does not seem suitable for hardware embedding either as the entire cavity is filled with the structure. A large re-design would be necessary to include this feature. The buckling FOS of Lattice was indeed higher than the original design, at 17,7 compared to 4. This design was seen as the worst compared to the baseline and other two designs.

The Bridge design was considered satisfactory in CAD-ability, due to how the design is sketched on one plane and then revolved to produce the structure. The design is seen as suitable for FDM AM due the continuous walls (because they are revolved) and the semi-acceptable overhangs. Similar to Rings and Ribs, Bridge is also seen as satisfactory for embedding hardware as it also contains a relatively open cavity space. This design resulted in the highest buckling FOS compared to all other designs at 27. This design is considered an advantage for optimization as the buckling load is consistent (a shell buckling in the different sections), suggesting that the design is modular and can be scaled if needed by adding or subtracting sections. Furthermore, the bridge design is based on the diameter of the cannister itself and is a full revolution. These variables are foreseen as being non-detrimental to the optimization process as compared to variables seen in the other two designs. This design received the highest score.

According to the decision matrix and the reasons stated above, the Bridge design is the optimal candidate to move forward with.

Step 3: Dimensioning for Function

This section is under intellectual property and is therefore explained further in Appendix G.

Step 4: Material and Strength

The construction specifications state that the design should withstand 20 MPa. Therefore, this step began with analyzing the Bridge design, and determining what could be strengthened. As can be seen in Figure 42a below, the sections of the outer wall which are unsupported by the bridge are susceptible to stress concentrations. Therefore, additional support was added in these areas. The support took the shape of hollow rings, which similarly to the rest of the design, are revolved around a central axis. This results in the stresses relocating to the inner sections of the rings.

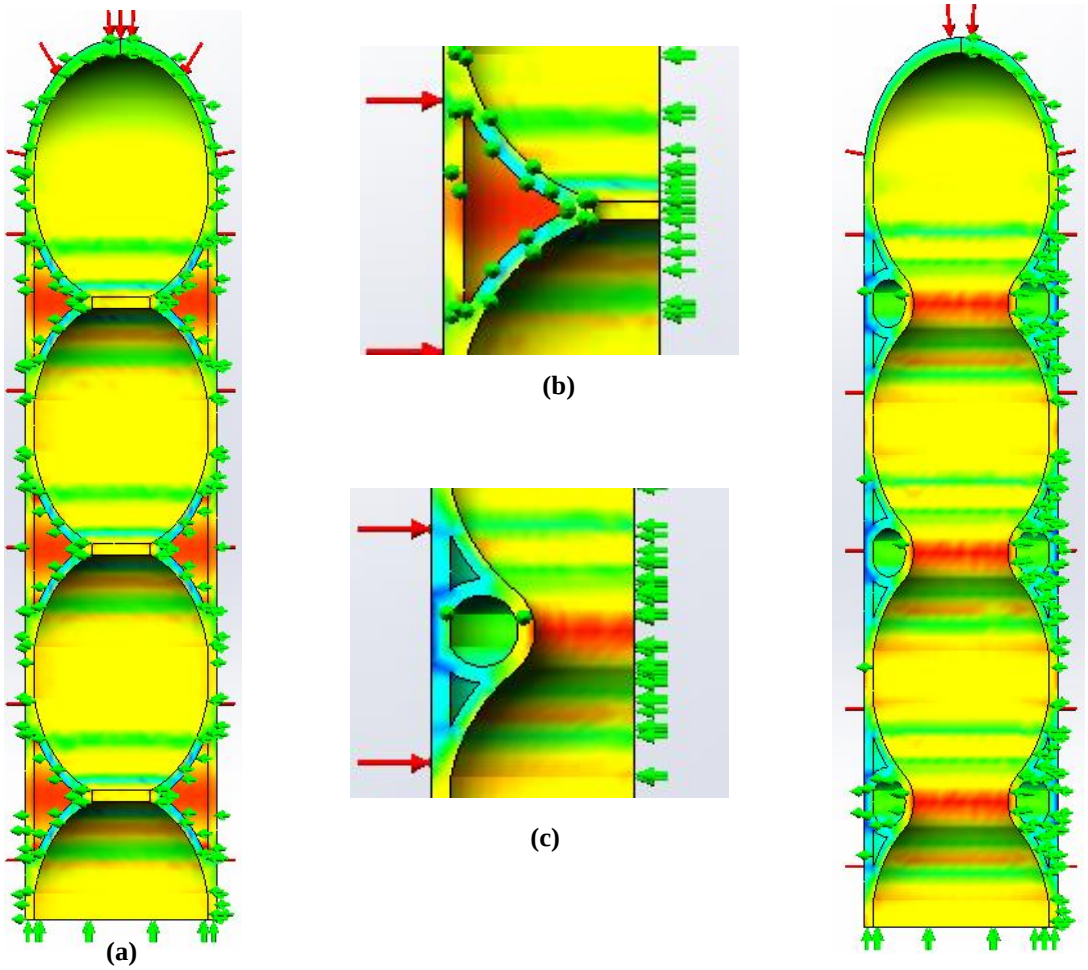

(a) **(b)** **(c)** **(d)**

Figure 42 **(a) Unsupported sections prone to stress concentrations**
(b) Close-up view
(c) Close-up view
(d) Support added in the form of hollow inner channels

This updated design was discussed with the company supervisors and manufacturers, and deemed a valid solution to move forward with.

The Ultem 1010 material data was incorporated to the CAD part. As FDM AM produces anisotropic parts the material was applied as a linear elastic orthotropic model type. Material data including flexural modulus, tensile strength and yield strength in Y and Z were procured from published data (see chapter *4.3: Polymer FDM Material Characteristics*).

Before applying the entire load, the Ultem material was first tested by comparing cannisters at different heights with a constant wall thickness (see Appendix X: Ultem Thick Wall). An increase in height lead to a larger overall volume, and therefore a necessity to weigh more to maintain functionality. This was resolved by thickening the walls. At a certain height (H=150), the structure seemed close enough to holding 20 MPa. This height was foreseen as being a height to start testing on the full structure with. This height would also suggest how many arches could fit within. Many iterations of wall thicknesses, including the outer wall, bridge tresses, size of arches and distance between arches were tested. Finally, a path to optimize the design was found and is described further in *Design Optimization* below.

Step 5: Inner Assembly

To construct the inner assembly holder as well as make room for it, a portion of the inner structure was cut out and formed in to a second piece (Figure 43). The cut was dimensioned to be the same outer diameter of the metal rings whereas the holder was cut to a diameter of 1mm less. This left a distance of 0,5mm between holder and wall and was included to allow for insertion during the embedding process. It was foreseen that this method would allow for the inner assembly to match with the inner structure and therefore continue to support the structure when embedded.

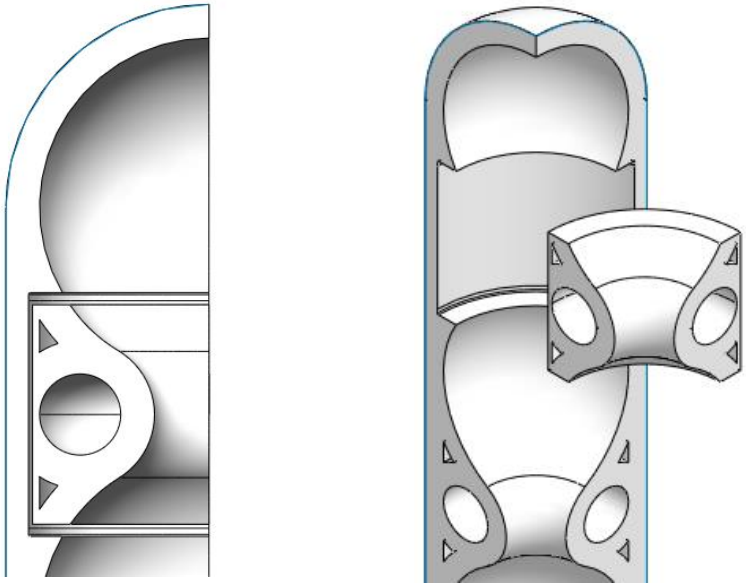

Figure 43: Cut section to form second piece

This cut piece was then transformed in to the inner assembly holder, allowing for the metal rods to fit within and adding placeholders for the metal rings. The holder can be seen in Figure 44.

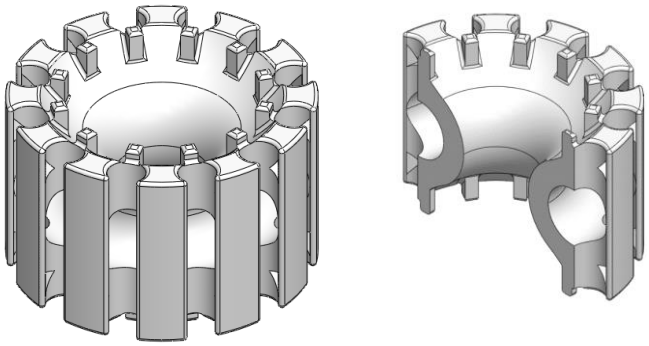

(a) (b)

Figure 44 **(a) Holder holds metal rod inserts and metal rings**
(b) Section view of holder

A base FEA analysis was carried out with the holder in place. As a simplifier, radial lines were placed on the wall where the metal rings should be and were limited to 0mm displacement in the radial direction, as the metal rings themselves are made of steel, and would displace relatively little compared to the rest of the structure. The holder was further simplified by removing additional metal ring place holders as well as spaces for the metal rods. The results can be seen in Figure 45, which shows that stress concentrates in the corners of the cut-out, directly where the radial lines were places, and therefore where the metal rings would meet the wall. Furthermore, the max amount that the wall displaces in this area is 0,6mm. This suggests that the initial 0,5mm gap between holder and wall is too large, and should be decreased so the holder can better support the wall and help negate the stress concentration. This will be investigated in *Design Optimization.*

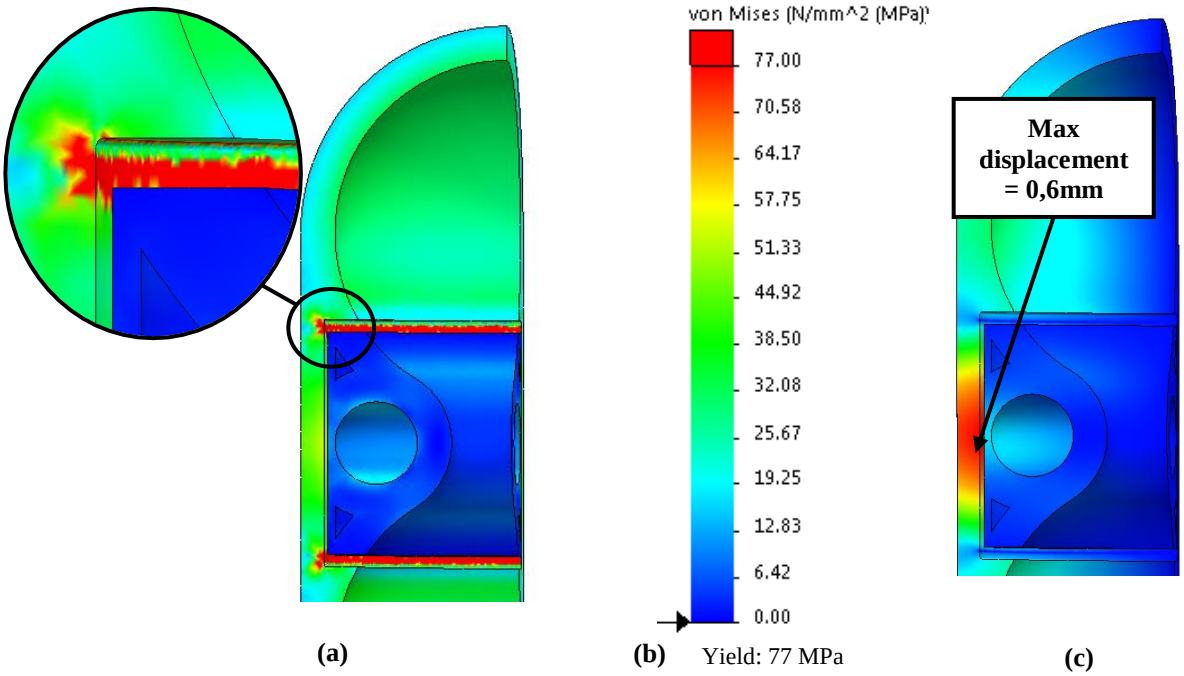

(a) (b) Yield: 77 MPa (c)

Figure 45: **(a) Stress concentrates in corners**
(b) Stress scale
(c) Max displacement forms in center section of wall

6.2.4 Design Optimization

Dimension Optimization

One aspect unique to this design is that the arch feet can be designed closer to each other or further away, which results in the hollow, revolved inner tubes to become smaller or larger. Due to the change in distance between the arches, the overall volume of the cannister changes as well, and ultimately the pressure that it can withstand. The larger the cannister, the thicker the walls, the stronger the cannister. Also, if a cannister had only two arches, then the optimum distance between the arches could be found. As seen by the chart in Appendix H, by increasing the height of the cylinder, the amount of pressure the cannister can withstand also increases. The buckling increases relatively little. Therefore, the limiting factor for this design becomes the revolved inner tubes. The tube's diameter is limited to what the FDM machine, in this case the Stratasys Fortus 450mc, can produce. For this moment, the diameter of the inner tube will be limited to 10,5 mm.

Once the inner tube dimension was set, and therefore the height of the cylinder, the excel sheet in Appendix D was used to find the weight that the cannister should be. Then the thickness of the cannister walls were altered until this weight was matched. Some dimensions can be seen in Figure 46 below. The design was then simulated to see if it would withstand a pressure of 20MPa in relation to flexure as well as buckling. The results can be seen in Figure 47.

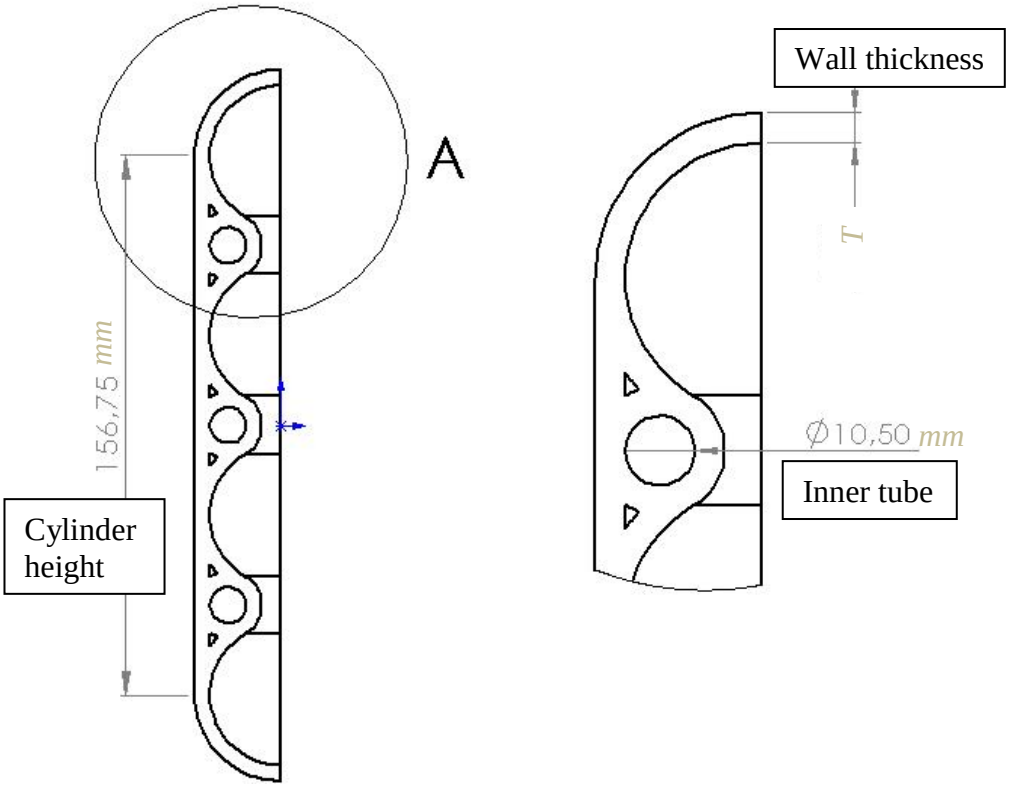

Figure 46: Variables of cannister and their dimensions

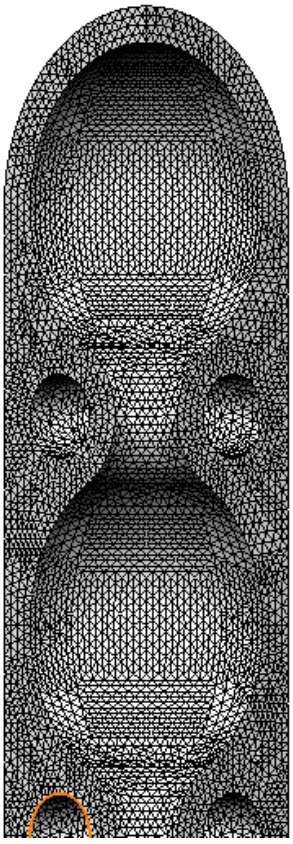

(a)

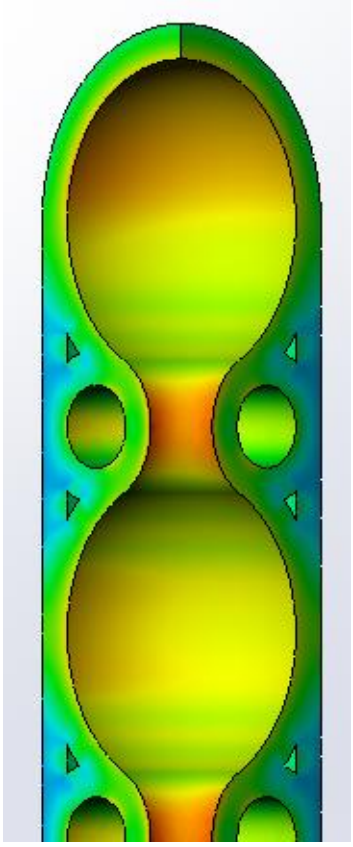

(b)

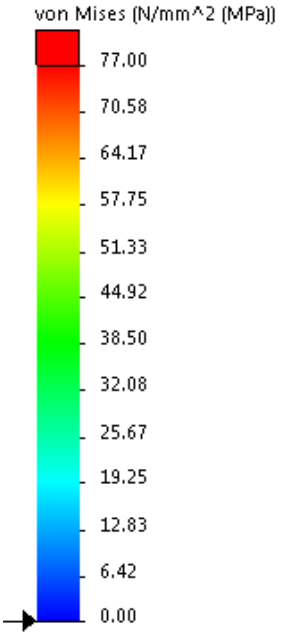

(c)

Study name:Buckling 1

Mode No.	Buckling Factor of Safety
1	3.2356

(d)

Figure 47: **(a) 1,2mm curvature-based mesh**
(b) Static analysis suggests that the design does not surpass its yield under 20MPa of pressure
(c) Stress scale
(d) Results of buckling analysis, shows design has buckling FOS of 3,2

Inner Assembly Optimization

As described in chapter *6.2.3: Functional Design, Step 5*, the inner assembly was cut from the initial shape and analyzed. The space between the inner assembly and inner wall of the tube was decreased to 0,25mm and reanalyzed. Figure 48 displays the results of the FEA static analysis with the embedded structure. To simplify the analysis, lines were drawn on the inner wall, representing the rigid metal rings which would go there in reality. The majority of the structure does not pass the yield strength, however the areas surrounding the additional fixed lines seem to surpass it.

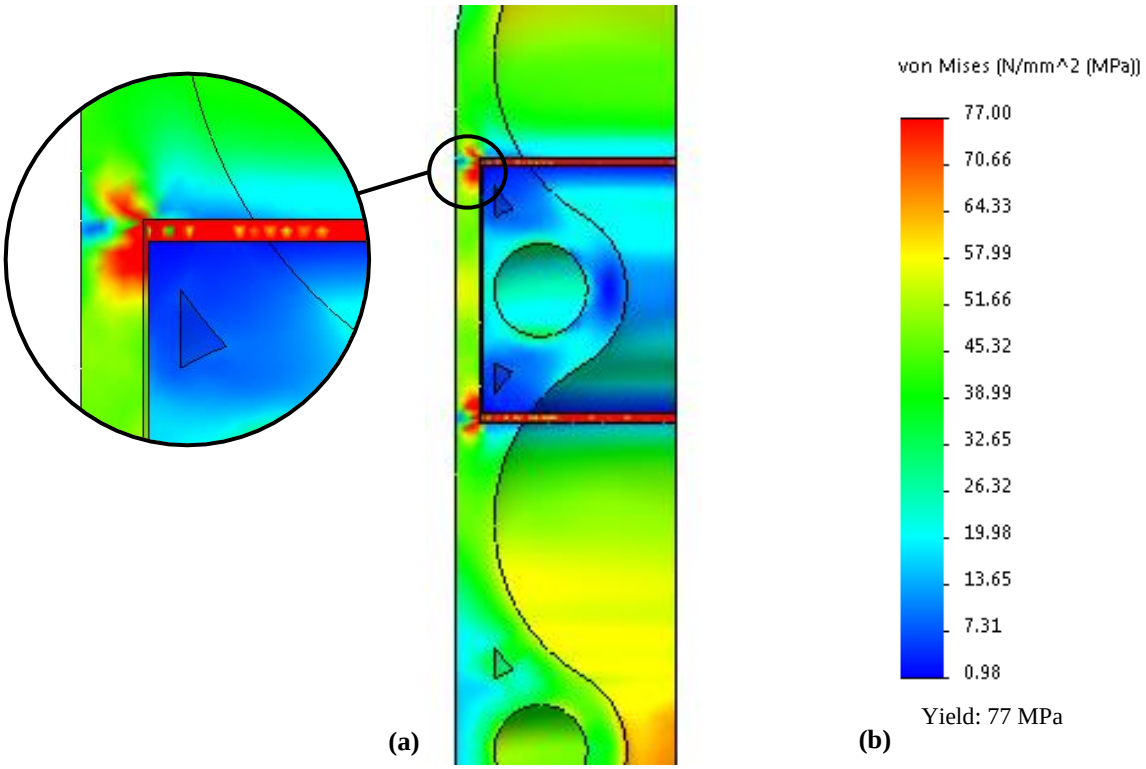

Figure 48 **(a) Stress concentrates at fixtures**
(b) Stress scale

The inner assembly was also analyzed for displacement. The wall just outside the inner assembly displaces a max of 0,42mm (Figure 49).

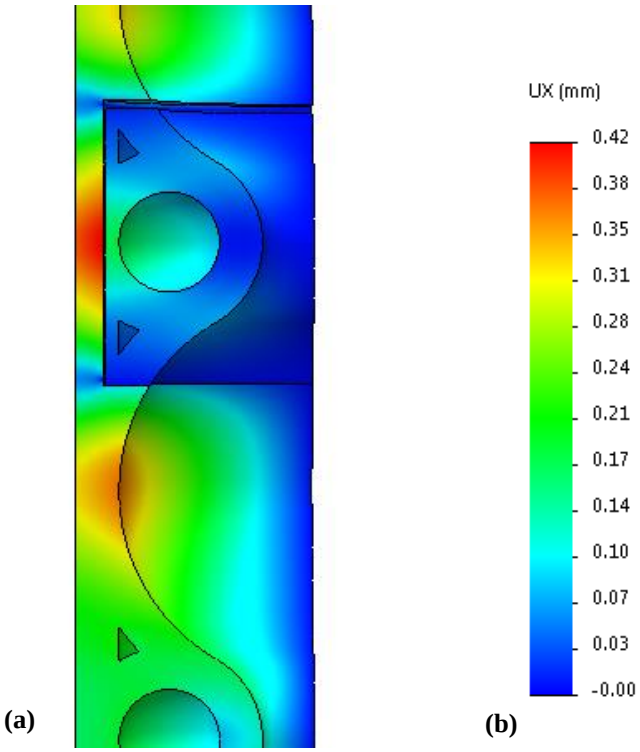

Figure 49 **(a) 0,42mm max displacement at center of section cut-out**
(b) Deplacement scale

6.2.5 Design Development

Development in Relation to FDM Process

The design displayed above is not optimal for the FDM process. See chapter *6.1.4: Design Development* for further explanation. The spherical end cap was replaced with a conical end cap. Table 10 below displays a chart comparing the FEA results of the spherical and conical end caps. As shown, the static analysis is similar. The buckling FOS decreases slightly with the conical end cap.

Table 10: FEA comparison between spherical and conical end caps

	Spherical end cap	*Conical end cap*	*Scale*
Max Stress (MPa)	77,5	85	
FEA Static Analysis	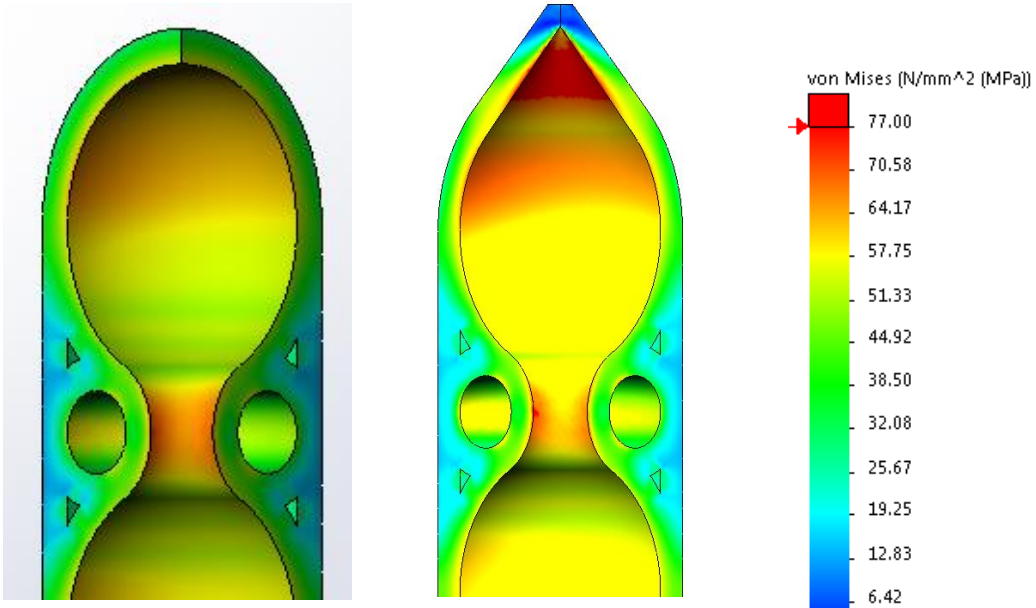		
Buckling FOS	Study name:Buckling 1 Mode No. 1 — Buckling Factor of Safety 3.2356	Study name:Buckling 1 Mode No. 1 — Buckling Factor of Safety 2.3053	
Weight (g)	249,4	251	

Development in Relation to Sealing Against Outside Environment

The entire structure, after manufacturing, needs to be sealed against its outside environment. This is accomplished by copper plating in post-processing. A copper plating of 0,06mm thickness will be added, as literature suggests that this thickness and above leads to a more ductile plating, and therefore less probability for fracture, leading to leakage (see chapter *4.6.2: Metal Plating*). With the additional plating, the entire structure weighs more. See Table 11 for weight comparison.

Table 11: Structural weight comparison

	Without plating	*With plating*
Weight (g)	251	254

FEA results suggest that the additional copper plating has also strengthened the inner structure. As seen in Figure 50 below, there are only slight stress concentrations located in the conical end caps at a max stress of 74,43 MPa.

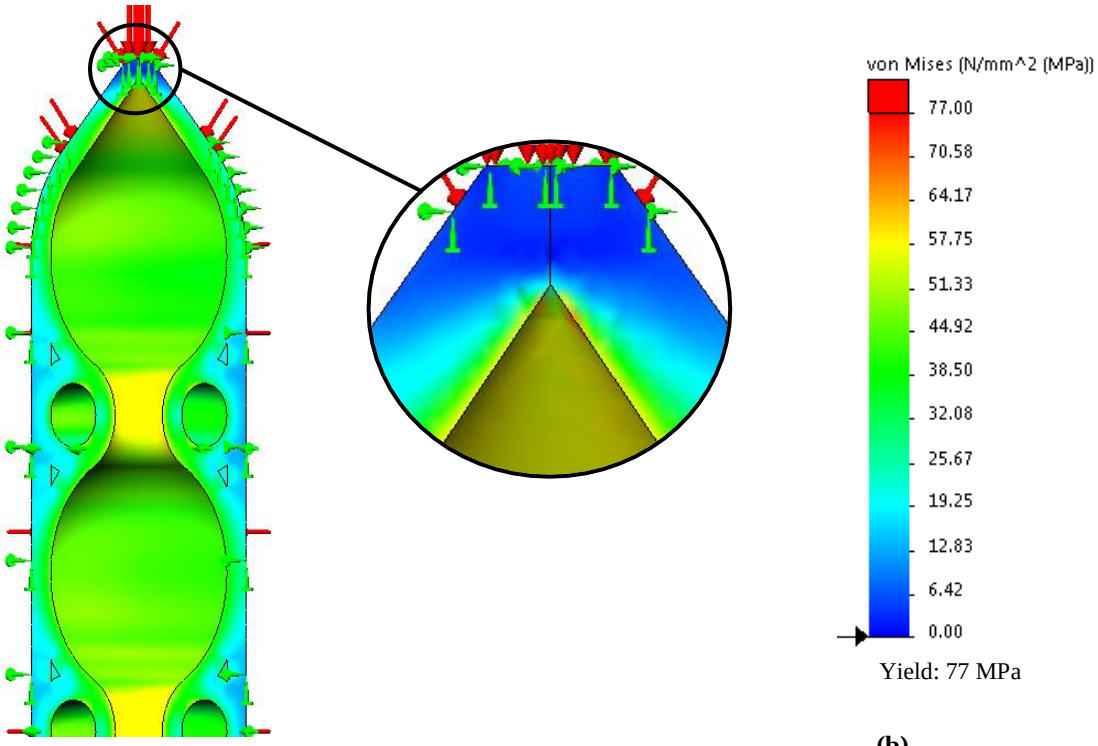

Figure 50 **(a) Stress concentrates at tip**
(b) Stress scale

Manufacturing Process Count

A sub-total of the part count (excluding metal rods and rings) and processes is seen below. The process 'holder insertion' is not counted as an additional process as it is carries out during the 'print cannister' process.

	Cannister	1
	Inner assembly holder	1
Total Part Count	=	2 Parts
	Print holder	1
	Print cannister	1
	Holder insertion	-
	Plate cannister	1
Total Process Count	=	3 Processes

7. RESULTS

This section describes the simulation results found in the study. Experimental results and analysis are found in chapter *5.4: Results of Material Tests* and *5.5: Analysis of Test Results.* Result sections are categorized under *ABSPlus-430* and *Ultem 1010*.

7.1. ABSPlus-430

The ABSPlus-430 resulting structure is seen below in Figure 51. The thickened wall allows the structure to withstand a hydrostatic pressure of 5,8 MPa, approximately 4x the pressure held by the original. The structure includes conical end-caps, an embedded inner structure and is sealed with HPA 200 H (Electrolube), a high performance acrylic coating. The structure is designed with the intention to be manufactured standing upright. Table 12 lists the results of the ABS product as well as comparative values from the original.

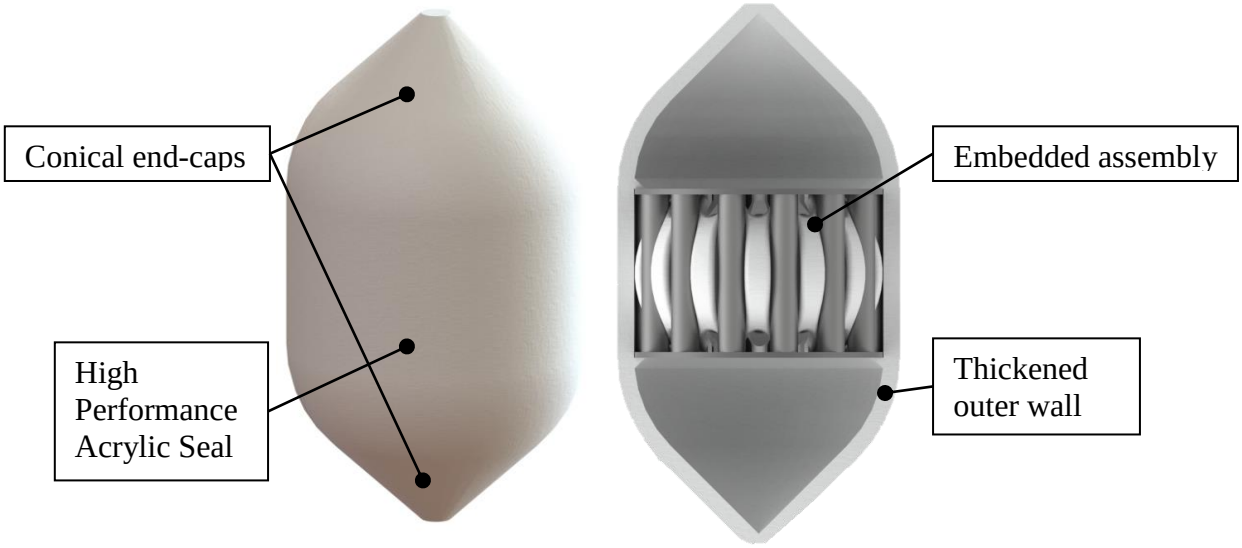

Figure 51: Full and sectioned view of ABSPlus-430 results

Table 12: Results of ABSPlus-430

***According to FEA**

	Original	New	Approximate % Increase/Decrease	Goal %	Fulfilled
Average Pressure Held* (MPa)	1,5	5,8	290	30	Yes
Buckling FOS	1	1,5	50	30	Yes
Component Count	4	2	-50	-20	Yes
Process Count	5	3	-40	-20	Yes
Total Mass (w/ inner assembly) (g)	532	111	-80		
Outer Dimensions (H x D) (mm)	324,6 x 50	95,7 x 50	-70		

7.2. Ultem 1010

The Ultem 1010 resulting structure is seen below in Figure 52. The 4 bridge shapes and 3 inner-tubes allow the structure to withstand a hydrostatic pressure of 20 MPa, approximately 13x the pressure held by the original. The structure includes conical end-caps, an embedded inner structure and is sealed with 60 μm of copper plating. The structure is designed with the intention to be manufactured standing upright. Table 13 lists the results of the Ultem product as well as comparative values from the original.

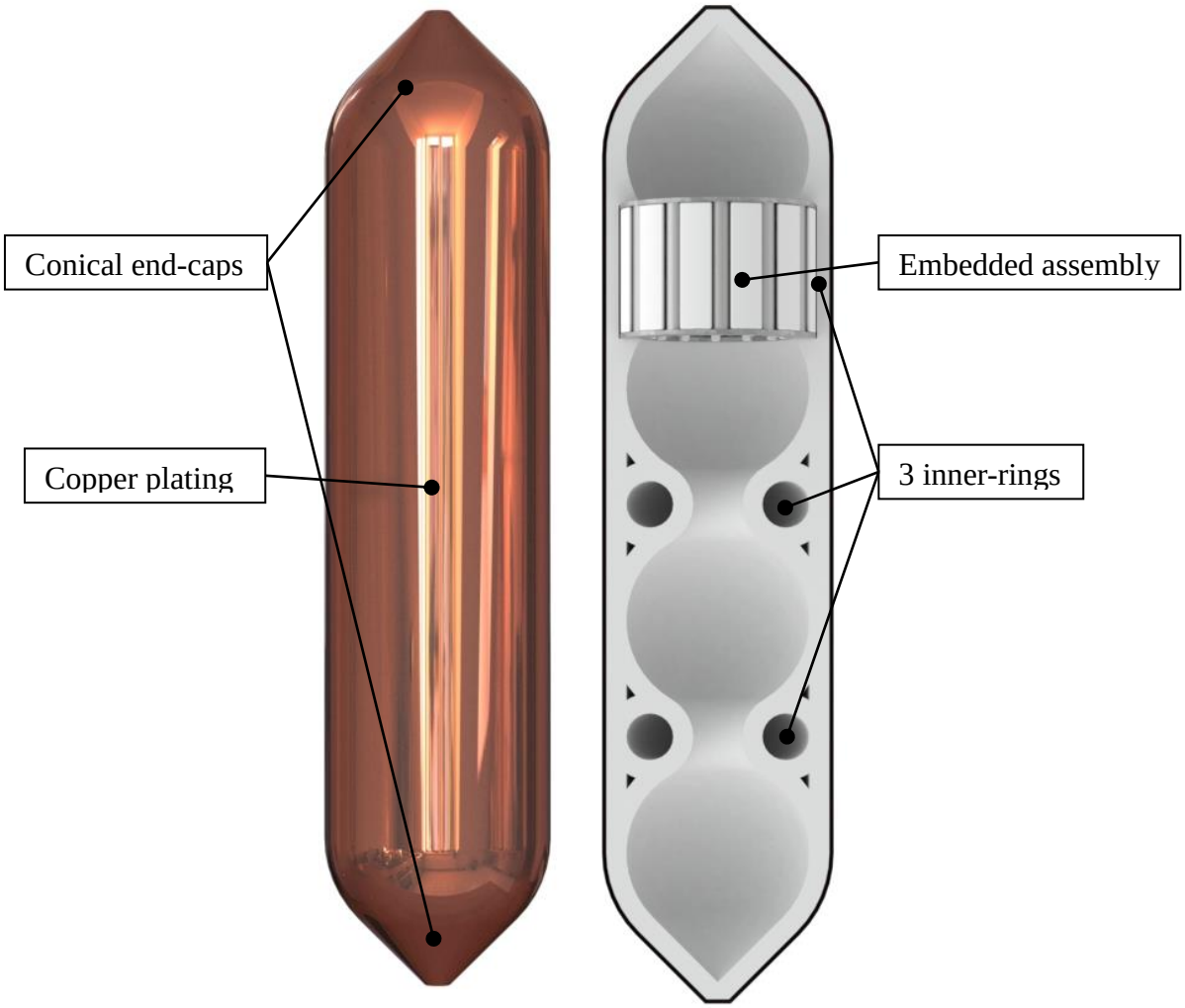

Figure 52: Full and sectioned front view of Ultem1010 results

Table 13: Results of Ultem 1010

***According to FEA**

	Original	New	Approximate % Increase/Decrease	Goal %	Fullfilled
Average Pressure Held* (MPa)	1,5	20	1200	30	Yes
Buckling FOS	1	1,9	90	30	Yes
Component Count	4	2	-50	-20	Yes
Process Count	5	3	-40	-20	Yes
Total Mass (w/ inner assembly) (g)	532	329	-40		
Outer Dimensions (H x D) (mm)	324,6x50	222,5x50	-30		

8. ANALYSIS

The following section analyzes the method, decisions and results of the study and answers the research questions.

8.1. Material tests

Material tests were conducted using ISO standards when available or followed methods used in literature that conducted similar studies. In one such material test (Performance of Sealants Under Pressure) the test was constructed as similarly to real life as possible to improve validity of results. However, this test was not able to be tested to the full pressure that the simulations suggest the design can withhold. Therefore, the Performance of Sealants Under Pressure is only proven up to 8 bar. The results of the Performance of Sealants are comparable to a similar study conducted by Mireles et al. (2011) in that the design of the part plays a role in the efficacy of the sealant, such as if the part has peaks in the form of points, the sealant may not form a seal. Therefore, this design aspect should be taken in to consideration when sealants are introduced. The results of the Flexural tests are also comparable to results shown in literature, such as by Neff et al. (2016), in that the post-processed specimens perform stronger than non-post-processed specimens. As the author points out, this is most likely due to that the post-process treatment is able to reduce the overall surface roughness of the specimen, which in turn makes the specimen more robust due to filling in weak and uneven points. This strength increase was not however included in the simulation study.

8.2. Additional tools and expertise

Certain tools were used to aid in decision making. A decision matrix was utilized to quantify several key factors and ultimately choose the base idea to move forward with. The basis of the chosen inner structure is based upon previous research regarding stabilizing structures under hydrostatic pressure. Published material data and simulation results were used in the development stage of the products and acted as a guide when adding or subtracting inner sub-structures.

Manufacturers including those who produced Ultem 1010 test specimens as well as those who performed the copper plating were consulted when necessary which contributes to the manufacturability of the products.

8.3. Structure simulation and structure test

Both products were simulated. In instances where the final results were simulated, fixtures were used to simplify the model. When conducting simulation studies using a simplified model (radially fixed lines along the inner wall instead of the stiff metal rings), stress concentrations form in these areas. This result is not regarded as accurate because the wall would have a larger area (from the ring) pushing against the wall and not a single point which the drawn line dictates. This was not investigated further due to time constraints, and the results display the values that the structures sustain without the additional line fixtures. In real life, the metal rings would most likely give additional strength and stiffness against compression and buckling due to their much stronger and stiffer material properties.

The simulations of the copper plated structures may behave differently to real life, due to how the copper plating permeates the substrate. If the plating permeates the substrate considerably, this would lead to an overall thicker plating, and as Saleh (2004) and Kannan (2014) point out, this would directly affect the maximum pressure the structure can hold. Furthermore, as Saleh (2004) concluded, the plating thickness does not relate accordingly to composite theory, and therefore the simulated results of the plated structures provided by CAD may not be true to real life depending on how this phenomenon is calculated by the program.

Due to the nature of the experiments and time constraints, no final tests were able to be done to compare with the simulations, including both structural and the copper plating post-processing.

8.4. Product design and manufacturing results

The ABSPlus-430 cannister results provided by the simulation suggests that it now holds three times the pressure and also has 1,5 buckling FOS at this pressure. This is in large part due to that the cannister was shortened significantly in design, and therefore is limited to the material yield strength. Like the Ultem 1010 design, several iterations of inner structures were analysed on the ABS product, however due to the failure being a material failure and not buckling failure, it was found that having a constant thickness in the outer wall provided the best design performance wise. The component count and process count are reduced by half with the AM design. This is seen as an accurate representation as due to the AM process and the ability to embed inner assemblies, the product would print as one complete component, automatically decreasing the number of components required. Similar to what Yuen (2016) concluded when embedding fluidic and optical devices into FDM parts, the ability to integrate and embed objects can be seen as a highly useful and unique aspect to FDM parts and allows for new functionalities and opportunities to become available for the product. The additional post-process treatment, a spray sealant, would be applied as a single extra step. The fact that this post-process can be added as a single step is also seen as advantageous, as Mireles et al. (2018) suggests, ease-of-use and working times should be taken in to consideration when used industrially when considering overall manufacturing process count and time. The resulting design also leads to 80% less mass, which would also lead to an overall decrease in material needed to create the part.

The Ultem 1010 cannister simulation results suggest that it can sustain an increase in pressure of approximately 12 times compared to the original design and maintains a buckling FOS of 2 at this pressure. The original cannister structure was a long, cylindrical column and therefore its failure mode was due to buckling. The new Ultem design is the result of testing a number of different structures, all taken from relevant theory on strengthening cylindrical shell structures under hydrostatic pressure. The simulation static analysis displays how the inner bridge structure does not encounter large stress concentrations, and instead the stress is relatively evenly distributed throughout. The bridge structure results in a similar mode of failure as ring stiffeners, in this case in the shell of the structure. However, due to the arches of the structure, the entirety of the separate shell areas is fully supported and even reinforced. Therefore, it can be seen that the increases in performance are a direct result of the inner structural design. The component count and process count are decreased by half from similar reasoning as the ABS product results described above. Furthermore, the overall mass of the Ultem 1010 cannister is 40% lighter than the original. The Ultem 1010 cannister is intended to be sealed by an additional copper plating, which as McCarthy (2012) notes, by incorporating metal plating on top of complex hollow structures produced by AM, a new hybrid approach is able to be reached. By taking this approach, it can further be reasoned that this post-processing choice is valid especially when taking the performance results in to consideration.

Additionally, the performance increase and decrease in processing steps and component count not only fulfilled the goals set out at the beginning of the study, but surpassed them. While most of the results compared generally better to the goals, the performance increase in regards to pressure held by the Ultem cannister far outweighed the goal, by 1200% as opposed to 30%. This further argues for utilizing and designing with AM specific design aspects.

8.5. Research Questions

RQ1: What AM specific design aspects are available to increase the performance of a structure when redeveloping a traditionally manufactured[3] product to one for AM?

Various AM specific design aspects were explored in this project, including lattice structures, inner hollow networks, hardware embedding, etc. The design aspects which were incorporated into the final results were inner hollow networks, hardware embedding, the ability to create the majority of the structure in one process and weight and volume management. These variables are seen as contributing factors to the final results of the study.

The use of inner hollow networks in the Ultem 1010 product greatly contributed to the performance of the structure. These inner hollow networks mimic ring stiffeners, which are regarded as common structures against buckling. More so, the incorporation of these circular structures also contributes in strengthening the structure against compression due to the hollow networks naturally forming arch-like structures along the entire column. It is unlikely that a product similar to that of the original Kynar cannister would be able to withstand higher pressures due to its tall cylindrical structure, whereas the structure seen in the results seems to be able to do so. These inner hollow structures would be very difficult or impossible to manufacture in traditional manufacturing processes, and therefore inner hollow networks are regards as unique design aspects to AM processes.

The ability to embed hardware indirectly leads to increase in performance in the structure. By embedding the hardware, the structure can be manufactured as a solid part. This decreases the part count, resulting in a decrease in connection points which would otherwise be prone to leaking and weak points. Therefore, the embedded hardware indirectly leads to a tighter seal on the product, allowing it to be sealed better and have higher overall strength and stability. Furthermore, although not necessarily performance based, but the ability to embed the hardware leads to fewer processing steps. Though not entirely unique to AM, the ability to form a single, enclosed structure with no additional seams or additional processes as seen as a great advantage to FDM AM.

The function of the product is directly affected by its volume and weight and therefore these two factors were important factors to be able to control. Due to the inner structure of the products, such as the inner hollow networks of the Ultem 1010, the use of FDM AM made it easier to control these variables due to the nature of the process and the ability to design for performance

[3] Traditional manufacturing refers to various subtractive manufacturing methods such as CNC milling and lathing or plastic injection molding. These processes are considered to be more limited when designing for, as one must take in to account uni-directional cutting possibilities as with the case of the CNC milling. Machinery required for injection molding becomes easily complicated and expensive especially when the design includes multi-directional through holes.

instead of being limited to traditional manufacturing factors, which as Hällgren (2017) notes, is an aspect unique to AM processes.

The above-mentioned design aspects are regarded as AM specific, and would not have been as easy to integrate through the use of traditional manufacturing methods. By incorporating these, the performance was increased such as amount of stress withheld, buckling FOS and maintenance of the specific mass to volume ratio required.

> *RQ2: What factors should be taken in to account when manufacturing an end-use part through FDM AM?*

When manufacturing an end-use part through FDM AM, several factors should be taken in to consideration as found by this study. These include the direction in which the product is manufactured, manufacturability of the product, the fit of embedded parts and necessary post-processing steps.

Due to the anisotropy of FDM parts, such as described by Bagsik et al. (2010) & (2012), manufacturing direction is crucial when dealing with end-use parts. During the design and analysis stage, the material properties for both ABSPlus-430 and Ultem 1010 were set for specific directions. The design of the entire structure was then based upon the planned build direction of the cannister. This led to decisions such as exchanging certain features for more "manufacturable" designs, such as the end caps. Instructions concerning build direction were always shared with the manufactures to ensure that the final parts were produced with the intended material properties. If either of the two final parts were printed in a different direction than what they were designed for, they would most likely fail to print at all due to steep overhangs.

Manufacturability is a factor that needs to be taken in to consideration when redeveloping a product from traditional manufacturing processes to AM. Even though FDM AM provides a higher degree of freedom in design, there are still some limiting factors due to the layer-by-layer deposition process. One feature in particular that needed to be redesigned was the spherical shaped end-caps. The large diameter of the end-caps resulted in large overhangs, which the FDM printer would most likely not have been able to produce. Therefore, a conical design was implemented instead. This new structure was reanalysed with FEA to make sure that the static and buckling results were not affected. This is described in detail in chapter *6.1.4: Design Development*. The flat surface on the end-cap (seen in chapter *5.1.2: Performance of Sealant Under Pressure Test Specimens, Specimen 2*) is also an advantage manufacturing wise, as the product is designed to be printed standing, and therefore the flat surface aids stability. The inner hollow tubes, although also a spherical shape, are deemed as having a small enough diameter to be printed successfully by FDM machine. This dimension choice was further supported by the manufacturers.

The fit of embedded parts is another factor that needed to be examined when manufacturing end-use parts. Due to the nature of the FDM process, the cavity in the printed part is most likely not the exact dimensions of the CAD model. Also, the type of fit that is wanted was taken in to consideration. During the optimization stage (see chapter *6.2.4: Design Optimization*), the distance between the embedded part and the wall seems to greatly affect how the load is carried in that area. This led to another optimization problem of finding the perfect distance in which the embedded part holds the most load (by being as close to the wall as possible) while also still being able to be inserted relatively easily during the printing process.

Post-processing on FDM parts is necessary for several reasons. The first being that the resulting products in this study will require partial support structures on the outside during printing, which will need to be removed by hand. The second reason is that the printed product is susceptible to leaking as it is housed in a pressurized, fluid environment, and therefore needs to be sealed in some way. To counteract leaking, both the ABSPlus-430 and Ultem 1010 products are sealed in an additional process, one by a spray acrylic sealant and the other by copper plating. The sealants even seem to provide a double function, the first being as a sealant and the second as an additional strengthening layer to the underlying structure. As seen in the Ultem 1010 product, the additional copper coating leads to an increase in buckling FOS, 1 to 2, under 20 MPa hydrostatic pressure. As buckling is the foreseen main mode of failure, this increase is substantial. Testing was carried out on several sealing methods at 0,8 MPa, the max pressure available. The test mimicked the real-life situation as closely as possible, which adds to the validity of the test. Also, similar to literature, the sealants resulted in a slight increase in yield strength. While the spray acrylic sealant and end cap design did prove successful at the 0,8 MPa pressure, the actual product may be pressurized at a higher value, which leads to the necessity of testing at those pressures as well. The Ultem 1010 copper plating sealant was not tested due to time constraints and wait times of manufactured and post-processed test specimens.

The above listed factors (build direction, manufacturability, fit and post-processing) are seen as not only being important for the products in the study, but in all end-use parts manufactured through AM. It was found that by taking these factors in to consideration, the redeveloped products will be able to be manufactured with a higher success rate and retain an optimal function.

8.6. Implications

This work implicates that AM cannot be simply compared to traditional manufacturing methods on the same exact design. Additional effort should be made to utilize additive manufacturing to its fullest potential through unique design aspects. These aspects would benefit a product's performance greatly, thereby affecting the value of it. This is similar to what has been implied from other studies within AM. Even though a larger scale redevelopment is costlier at that moment, it would surely be more valuable in the long run, especially for a product which will continue to be produced.

In relation to the product redeveloped in this study, the substantial increase in performance and decrease in processing steps provide a strong argument for additional examination, if not wholly converting. Further investigation would include manufacturing prototypes and performing destructive testing as well as undertaking studies which take place over a longer time period for testing the products in their actual environments.

9. CONCLUSIONS

This study focused on redeveloping a product for AM. Structural design elements to strengthen against buckling were analysed in depth as well as various post-processing techniques with the aim to fully seal the AM parts. The product in question is cylindrically shaped, is housed in a fluid environment and is typically under high pressure loads (up to 20 MPa). By incorporating design aspects specific to AM, such as inner hollow networks, hardware embedding and creating the majority of the structure in one process while also managing the weight and volume of the product, the performance of the product was drastically increased.

Two redeveloped products were the results of this study, one constructed in ABS for low-pressure ranges (up to around 5 MPa), and one constructed in Ultem for high-pressure ranges (up to 20 MPa). Compared to the original, traditionally manufactured product, the redeveloped ABS product has decreased in total mass and volume and has increased in average pressure held by 287%. It also retains a 1,5 factor against failing due to buckling. The Ultem product has increased in average pressure held by approximately 1200%, while still maintaining a 1,9 FOS against buckling failure. The number of components needed to manufacture these results have been halved compared to the original counterpart and both products are manufactured with approximately half the number of processes.

These results strongly suggest that the performance of the product focused upon in this study is drastically increased after redevelopment for AM by incorporating AM specific design concepts. This suggests that when redeveloping any product to be manufactured via AM, one should consider incorporating AM unique design aspects in order to take advantage of AM, as they can lead to a dramatic increase in performance of the product, and not simply use the original design.

The study also finds certain factors that are important to keep in mind when manufacturing this product, and thereby any other product, via FDM AM for end-use, such as build direction, manufacturability, fit of embedded parts and post-processing. Some of these aspects are instructed to be considered in the DFAM method utilized in this study, such as manufacturability. However, other aspects such as build direction, fit of embedded parts and especially post-processing seem to be left out. This can be due to that there exists a multitude of AM processes, and the DFAM methodology cannot easily accommodate all manufacturing aspects which should be considered. However, if these aspects are researched during the product development process, and even optimized, then they can further aid in increasing the performance of the product. If these aspects are not regarded at all, it could lead to the product performing worse or could even lead to failure in the product.

10. FUTURE WORK

There is a variety of future work that is recommended. First, similar studies should be conducted on the copper plated sealant as were conducted on the spray sealants. This includes testing for performance as well as additional mechanical properties that the plating provides, all at different temperatures. This would give insight into how the copper plated specimens compare to the non-plated under different temperatures and may suggest if the copper plating is necessary. This work will be conducted during summer 2019, and a report will follow detailing the findings.

Additional work includes manufacturing prototypes of both the ABS and Ultem models, sealing them, and testing them in pressure tanks at the allotted pressures suggested by the simulations. This would be necessary to gauge the accuracy of the simulated results. Furthermore, the coated polymers should be tested in the actual liquids which they will be housed for longer spans of time to gauge if the material can resist corrosion. If the sealants are not corrosion resistant to those specific chemicals, then other solutions will need to be examined. Lastly, in-depth manufacturability analysis should be performed to optimize the fit of the embedded parts, including around its diameter as well as the next printed layer that sits right on top. The limitations of the Stratasys FDM printers should be explored further in terms of the maximum diameter of a hollow circular structure that it can print successfully as this is what the optimization of the product is based on.

11. Bibliography

Ajibola, O. O. “Evaluation of Electroless-Nickel Plated Polypropylene under Thermal Cycling and Mechanical Tests.” *Tribology in Industry* (2016): 412-424.

Amdahl, Jørgen. “Chapter 5: Buckling of Cylindrical Shells.” 19 January 2005. *TMR4205 Buckling and Ultimate strength of Marine Structures.* <http://www.ivt.ntnu.no/imt/courses/tmr4205/literature/>.

Bagsik, A., V. Schöppner and E. Klemp. “FDM Part Quality Manufactured with Ultem.” 2010.

—. “Long-Term Ageing Effects on Fused Depostion Modeling Parts Manufactured with Ultem.” 2012.

Bousquet, Anna. *Additiv tillverkning i metall och topologioptimering*. Eskilstuna: Mälardalens Högskola, 2017.

BU, ABB Business Unit. *Gathering of information from BU regarding cannister* Barrett Sauter. 4 Febuary 2019.

Cain, Perry. *Supports in 3D Printing: A technology overview*. 2019. <https://www.3dhubs.com/knowledge-base/supports-3d-printing-technology-overview>.

Center for Innovation in Research and Teaching. *Key Issures in Quantitative Research*. 2018. 10 June 2019.

Dawoud, Michael, Iman Taha and Samy J. Ebeid. “Mechanical behaviour of ABS: An experimental study using FDM and injection moulding techinques.” *Journal of Manufacturing Processes 21* (2016): 39-45.

Equbal, Azhar and Anoop Kumar Sood. “Investigations on metallization in FDM build ABS part using electroless deposition method.” *Journal of Manufacturing Processes* (2015): 22-31.

Gajdos, Ivan & Spišák, Emil & Kascak, Lubos & Krasins’kyi, V. “Surface Finish Techniques for FDM Parts.” *Materials Science Forum* (n.d.): 45-48.

Gaul, Agnieszka. “The Pont du Gard aqueduct.” iStockphoto, n.d.

GE Additive. *Additive Manufacturing Processes*. 2019. <https://www.ge.com/additive/additive-manufacturing/information/additive-manufacturing-processes>.

Hällgren, Sebastian. “Some aspects on designing for metal Powder Bed Fusion.” *PhD Thesis*. Örebro University, 2017.

Hajmohammad, Mohammad Hadi et al. “Studying Effect of Geometrical Parameters on the Buckling of Cylindrical Shells under Hydrostatic Pressure.” *Indian Journal of Science and Technology* (2013).

ISO. *Standards*. n.d. <https://www.iso.org/standards.html>.

Kannan, S. et al. “Investigating the Influence of Electroplating Layer hickness on the Tensile Strength for Fused Deposition Processed ABS Thermoplastics.” *International Journal of Engineering and Technology (IJET)* (2014): 1047-1052.

Kindersley, Dorling. *Illustration of Submarine, Cutaway*.

Kumke, Martin, Hagen Watschke and Thomas Vietor. “A new methodological framework for design for additive manufacturing.” *Virtual and Physical Prototyping, 11:1* (2016): 3-19.

Lambert, Phil. *Tensile properties of materials: FDM printer & SLS printer*. 14 May 2014. <https://www.sculpteo.com/blog/2014/05/14/material-considerations-choose-right-plastic-production-method-part-2/>.

Lemák, D and J. Studnička. “Influence of Ring Stiffeners on a Steel Cylindrical Shell.” *Acta Polytechnica* (2005).

Lopatin, A. V. and E. V. Morozov. “Buckling of composite cylindrical shells with rigid end disks under hydrostatic pressure.” *Composite Structures* (2017): 136-143.
McCarthy, D. L. & Williams, C. B. “Creating complex hollow metal geometries using additive manufacturing and electroforming.” *23rd Annual International Solid Freeform Fabrication Symposium- An Additive Manufacturing Conference*. 2012. 108-120.
Miguel, M, et al. “Failure Analysis of Additive Manufacturing Nylon Parts Coated with Protective Products.” 2018.
Mireles, Jorge, et al. “Analysis of Sealing Methods for FDM-fabricated Parts.” *22nd Annual International Solid Freeform Fabrication Symposium- An Additive Manufacturing Conference*. SFF, 2011. 185-196.
Mittal, K. L. *Metallized Plastics 2: Fundamental and Applied Aspects*. New York: Springer Science and Business Media, 1991.
Moore, J. Paul. “The Natchez Trace Parkway Bridge.” iStockphoto, n.d.
Nam, Vu Hoai et al. “Nonlinear thermo-mechanical buckling and post-buckling of multilayer FGM cylindrical shell reinforced by spiral stiffenders surrounded by elastic foundation subjected to torsional loads.” *European Journal of Mechanics / A Solids* (2018): 393-406.
Neff, Clayton, Matthew Trapuzzano and Nathan B. Crane. “Imapact of Vapor Polishing on Surface Roughness and Mechanical Properties for 3D Printed ABS.” *Solid Freeform Fabrication 2016: Proceedings of the 27th Annual International Solid Freeform Fabrication Symposium- An Additive Manufacturing Conference Reviewed Paper*. Solid Freeform Fabrication , 2016. 2295-2304.
Olivera, Sharon et al. “Plating on acrylonitrile-butadiene-styrene (ABS) plastic: a review.” *Journal of Materials Science* (2016).
Quadrant Engineering Plastic Products. “Symalit PVDF 1000.” n.d. *Piedmont Plastics.* <https://www.piedmontplastics.com/resources/literatures/view/quadrant-symalitR-pvdf-1000>.
Rama Krishna, L. Siva and Ashok Gundeti. “A Comparative Study on the Components Fabricated by Injection Moulding and FDM 3D Printing Process.” *International Journal of Mechanical AND Production Engineering* (2017): 116-121.
Saleh, N. et al. “Effects of electroplating on the mechanical properties of stereolithography and laser sintered parts.” *Rapid prototyping journal* (2004): 305-315.
Stark, B., et al. “Embedded sensors for the health monitoring of 3D printed unmanned aerial systems.” *2014 International Conference on Unmanned Aircraft Systems (ICUAS)*. Orlando, FL, USA: IEEE, 2014.
Stratasys Direct Manufacturing. *Electroplating Goes Beyond Making FDM and PolyJet Parts Shine*. n.d. <https://www.stratasysdirect.com/manufacturing-services/finishing-assembly/electroplating-making-fdm-polyjet-parts-shine>.
—. *Stratasys Direct Manufactruing Selected by Airbus to 3D Print Polymer Serial Flying A350 XWB Parts* . 18 July 2017. <https://www.stratasysdirect.com/company/announcements/airbus-3d-print-polymer-a350-xwb-parts>.
Stratasys. “FDM Best Practice: Embedding Hardware.” 2014. *Stratasys.* 12 April 2019.
—. *Fortus 380MC and Fortus 450MC*. 2019. <https://www.stratasys.com/3d-printers/fortus-380mc-450mc>.
—. “Fortus ABS-M30: Characterization of Material Properties.” 2013.
—. “Reddot Ultem 9085 Resin 3D Printing Case Study.” n.d. *Stratasys.* <https://www.stratasys.com/resources/search/case-studies/reddot-ultem-9085?phrase=ultem%209085>.
—. “Stratasys F900.” 2019. *Stratasys.* 11 April 2019.

—. “Ultem 1010 resin.” 2019. *Stratasys.* <https://www.stratasys.com/materials/search/ultem1010>.
T., Tomiyama, et al. “Design methodologies: Industrial and educational applications.” *CIRP Anna Manuf Technol 58(2)* (n.d.): 543-565.
Varotsis, Alkaios B. *Introduction to FDM 3D printing*. 2019. <https://www.3dhubs.com/knowledge-base/introduction-fdm-3d-printing>.
Waters, Mike. *Basics of Stress, Loads, Strength of Materials & how they relate*. 2018. <https://smalltridesign.com/Trimaran-Articles/Stress-calcs.html>.
Wohlers, T. T., T. Caffrey and R. I. Campbell. “Wohlers Report 2017: 3D Printing and Additive Manufacturing State of the Industry: Annual Worldwide Progress Report.” 2017.
Yang, S. and Y. Zhao. “Additive manufacturing-enabled design theory and methodology: a critical review.” *The International Journal of Advanced Manufacturing Technology* (2015): 327-342.
Yuen, Po Ki. “Embedding objects during 3D printing to add new funtionalities.” *Biomicrofluidics* (2016).

12. APPENDICES

LIST OF APPENDICES

Appendix A- Kynar Cannister Drawing

This section has been removed due to company ownership

Appendix B- Function of cannister & *P*

This section has been removed due to company ownership

Appendix C- ABSPlus-M430 Flexural test results, unsealed and sealed, and result curves

Specimen		Flexural Modulus (MPa)	Average	$\sigma_{0.2}$ (MPa)	Average (MPa)
Y, unsealed	1	1560	1650	39,2	39,12
	2	1730		37,8	
	3	1750		38,6	
	4	1600		40,3	
	5	1610		39,7	
Z, unsealed	6	1600	1668	33,5	35,16
	7	1740		30,2	
	8	1680		38,1	
	9	1660		36,4	
	10	1660		37,6	
Y, sealed	11	1770	1678	35,4	38,18
	12	1620		37,0	
	13	1680		41,3	
	14	1590		37,5	
	15	1730		39,7	
Z, sealed	16	1750	1692	42,6	37,06
	17	1690		40,1	
	18	1610		30,8	
	19	1680		33,4	
	20	1730		38,4	

Results from software

No.	Specimen ID	Notes	Date/Clock time	E_f MPa	$\sigma_{0.2}$ MPa	σ_{fY} MPa	ε_{fY} %	σ_{fM} MPa	ε_{fM} %	σ_{fB} MPa	ε_{fB} %	h mm	b mm	A_0 mm²	Comment
~~1.1~~	Pretest-1	Pretest	~~2019-05-02 10:38:12~~	~~332~~	-	-	-	~~6,82~~	~~1,9~~	-	-	~~4~~	~~40~~	~~40,00~~	
1.3	UX	Compliance Test	2019-05-02 14:43:17	14600	-	-	-	57,5	0,4	-	-	4,289	9,991	42,85	spänn 31
1.5	UX	Compliance Test	2019-05-02 14:53:19	-	-	-	-	63,2	0,2	-	-	4,07	10,1	41,10	span 23
1.4	UX	Compliance Test	2019-05-02 14:47:09	-	-	-	-	57,5	0,2	-	-	4,289	9,991	42,85	Span 23
1.5	SX	Compliance Test	2019-05-02 14:50:43	-	-	-	-	57,3	0,2	-	-	4,3	9,981	42,92	Span 23
1.6	SZ	Compliance Test	2019-05-02 14:55:31	-	-	-	-	57,3	0,2	-	-	4,3	9,981	42,92	span 23
2.1	UX-1	Unsealed X	2019-05-02 10:45:28	1560	39,2	-	-	45,2	5,1	14,4	6,0	4,289	9,991	42,85	Didn't fully snap, still slightly attached
2.2	UX-2	Unsealed X	2019-05-02 10:54:31	1730	37,8	-	-	45,8	4,8	12,9	5,5	4,267	9,999	42,67	same
2.3	UX-3	Unsealed X	2019-05-02 11:03:21	1750	38,6	-	-	46,8	5,1	13,4	5,9	4,258	9,971	42,46	same
2.4	UX-4	Unsealed X	2019-05-02 11:09:48	1600	40,3	-	-	46,3	5,1	13,7	5,9	4,3	9,949	42,78	same
2.5	UX-5	Unsealed X	2019-05-02 11:16:06	1610	39,7	-	-	45,9	5,0	18,7	5,8	4,274	9,98	42,65	same
3.1	UZ-6	Unsealed Z	2019-05-02 11:23:59	1600	33,5	-	-	36,9	2,2	13,2	2,3	4,041	10,07	40,70	Less ductile behavior
3.2	UZ-7	Unsealed Z	2019-05-02 11:29:14	1740	30,2	-	-	33,8	1,9	13,2	1,9	4,017	10,06	40,39	snapped in half
3.3	UZ-8	Unsealed Z	2019-05-02 11:34:44	1680	38,1	-	-	39,7	2,4	15,0	2,5	4,036	10,05	40,56	snapped in half
3.4	UZ-9	Unsealed Z	2019-05-02 11:40:34	1660	36,4	-	-	38,6	2,3	14,2	2,4	4,04	10,08	40,73	snapped in half
3.5	UZ-10	Unsealed Z	2019-05-02 11:44:59	1660	37,6	-	-	39,4	2,4	15,0	2,5	4,027	10,06	40,50	snapped in half
4.4	SX-11	Sealed X	2019-05-02 13:40:23	1770	35,4	-	-	44,8	4,8	13,2	5,6	4,3	9,981	42,92	Didn't fully snap, still attached
4.5	SX-12	Sealed X	2019-05-02 13:48:15	1620	37,0	-	-	44,4	4,8	13,3	5,7	4,306	9,989	43,01	same
4.6	SX-13	Sealed X	2019-05-02 13:55:58	1680	41,3	-	-	48,0	5,2	14,0	6,1	4,24	10,02	42,48	same
4.7	SX-14	Sealed X	2019-05-02 14:04:07	1590	37,5	-	-	44,2	4,8	11,8	5,4	4,312	9,976	43,02	same
4.8	SX-15	Sealed X	2019-05-02 14:10:17	1730	39,7	-	-	47,2	4,7	13,6	5,4	4,231	9,967	42,17	same
5.9	SX-16	Sealed Z	2019-05-02 14:16:31	1750	42,6	-	-	44,9	3,1	16,9	3,2	4,044	10,05	40,64	Fully snapped
5.1	SZ-17	Sealed Z	2019-05-02 14:22:12	1690	40,1	-	-	40,1	2,6	15,2	2,6	4,087	10,07	41,14	same
5.2	SZ-18	Sealed Z	2019-05-02 14:26:56	1610	30,8	-	-	36,7	2,1	14,0	2,1	4,072	10,08	41,05	Fully snapped
5.3	SZ-19	Sealed Z	2019-05-02 14:30:15	1680	33,4	-	-	37,1	2,2	14,4	2,2	4,05	10,07	40,76	Fully snapped
5.4	SZ-20	Sealed Z	2019-05-02 14:34:03	1730	38,4	-	-	39,0	2,4	14,7	2,4	4,07	10,1	41,10	Fully snapped

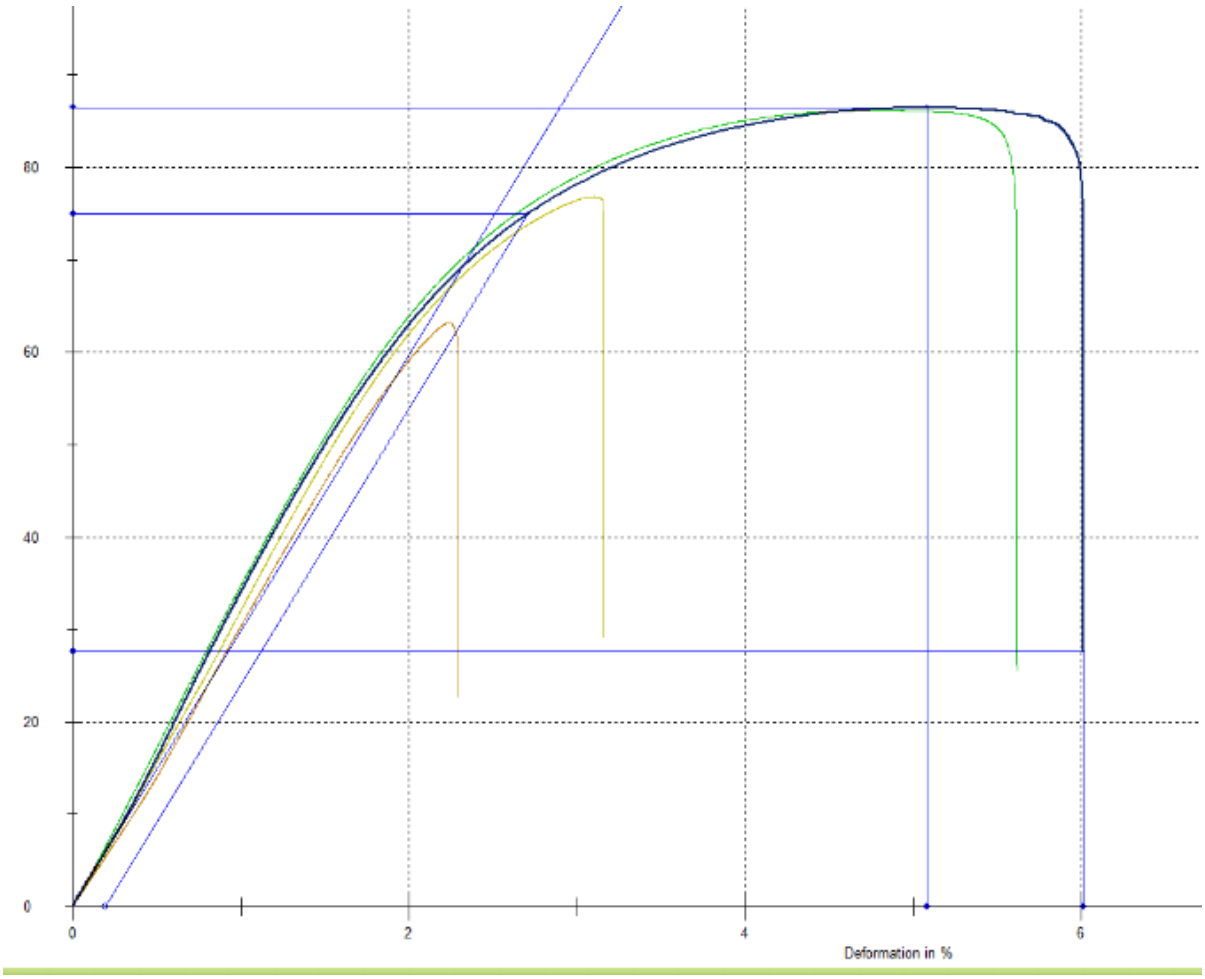

Figure: All curves Force (N) / Deformation %

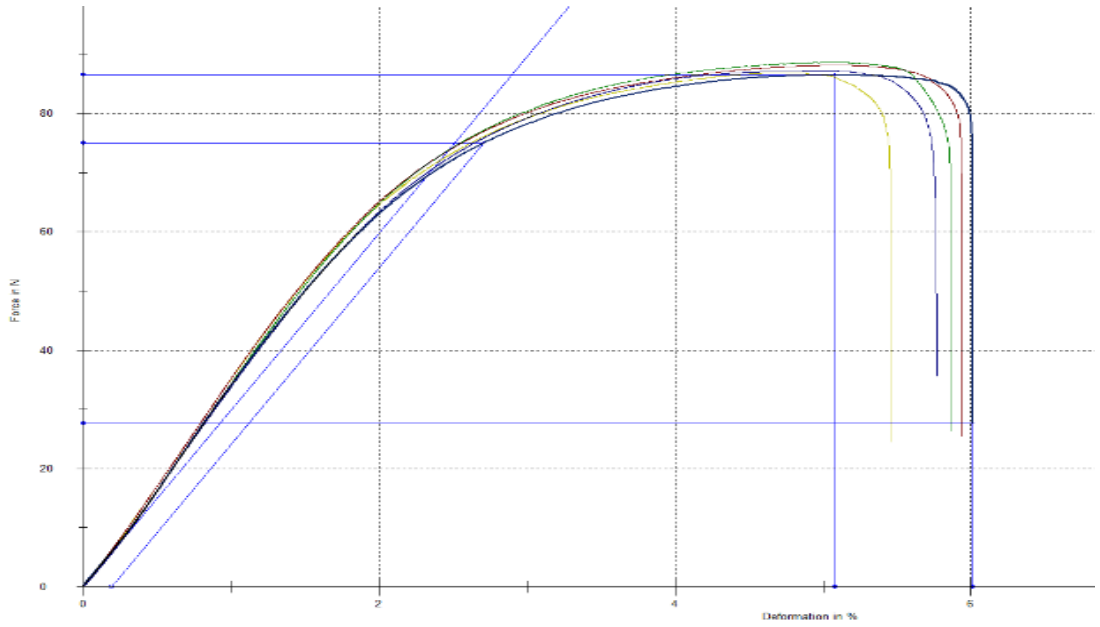

Figure: Y Unsealed Force (N) / Deformation %

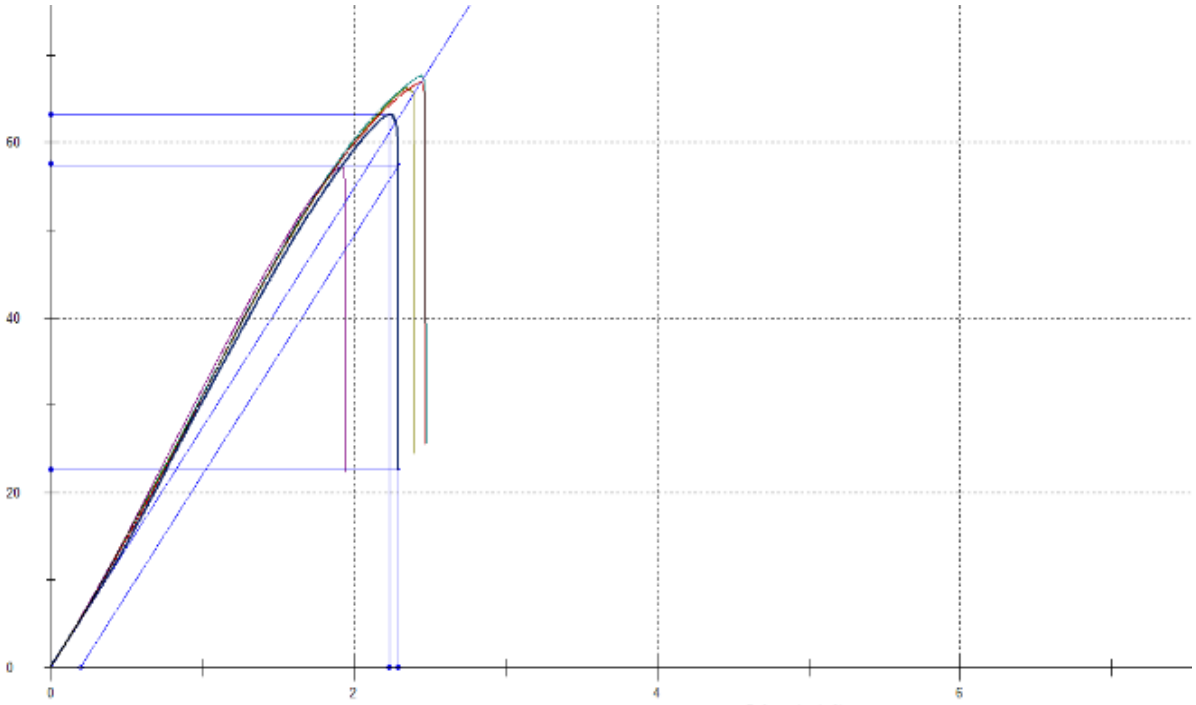

Figure: Z Unsealed Force (N) / Deformation %

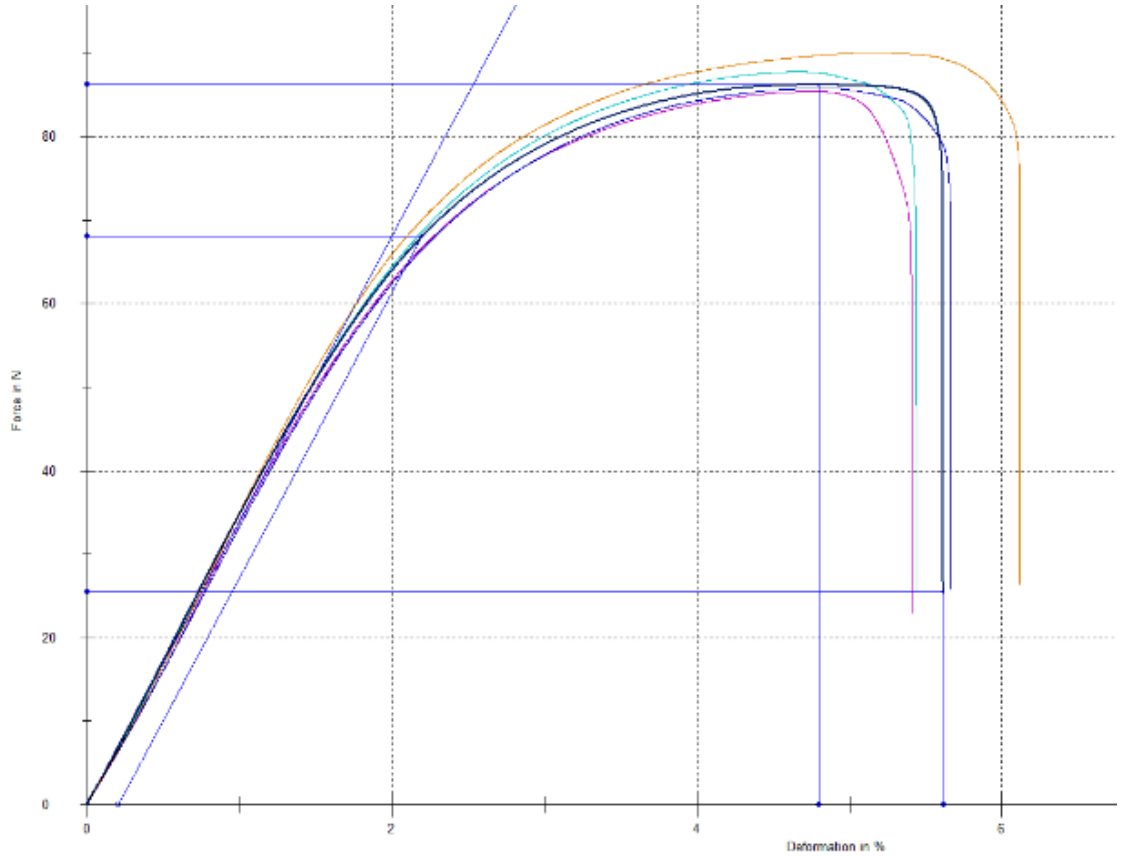

Figure: Y Sealed Force (N) / Deformation %

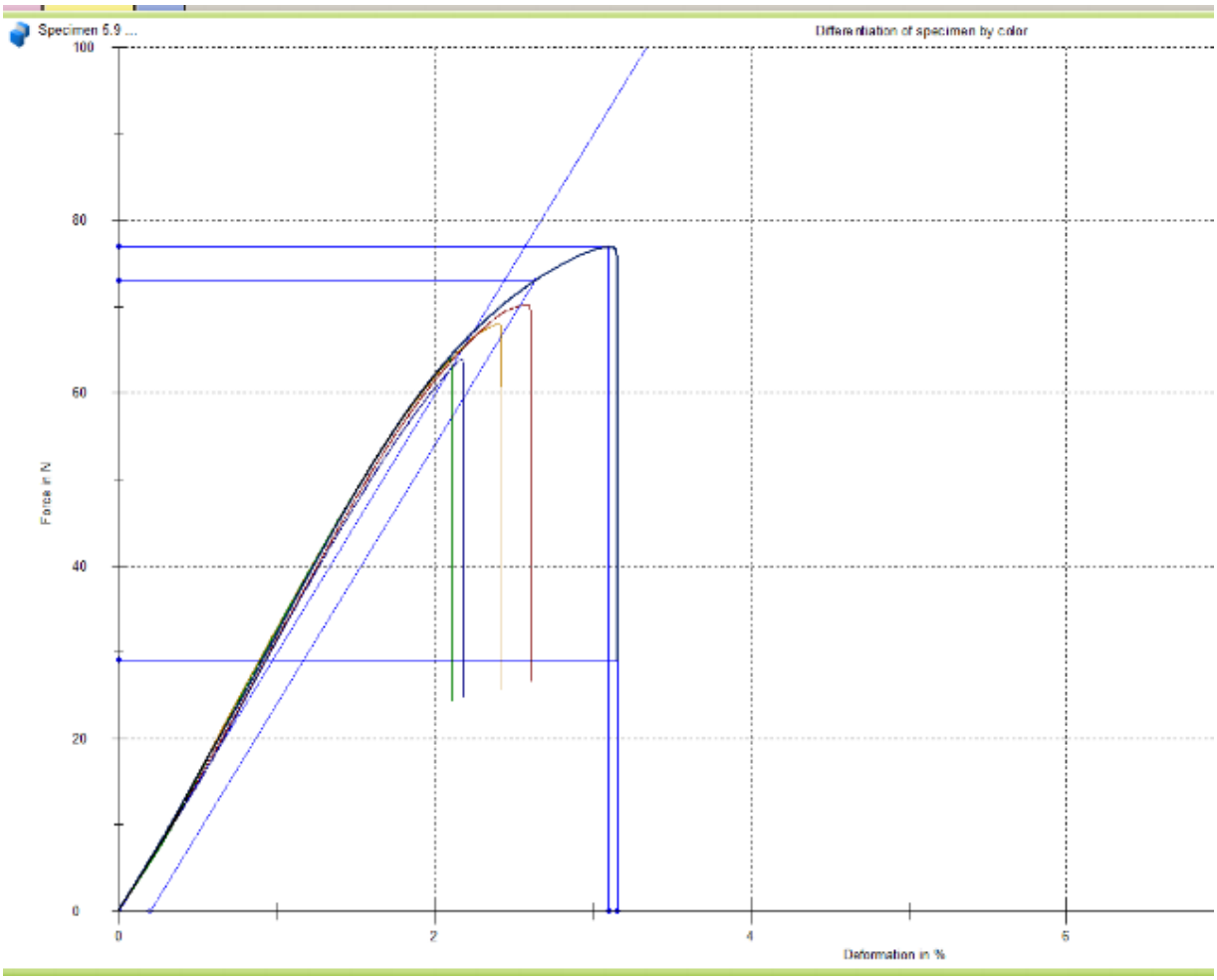

Figure: Z Sealed, Force (N) / Deformation %

Appendix D- Cannister comparison data

This section has been removed due to company ownership

Appendix E- Equations utilized in excel sheet to determine function of cannister

This section has been removed due to company ownership

Appendix F- Initial cannister design comparison data

This section has been removed due to company ownership

Appendix G- Dimensioning Ultem

This section has been removed due to company ownership

Appendix H- Arch Distance Optimization Investigation

This section has been removed due to company ownership